Genetic analysis of high malate-producing sake yeasts and its applications

Hiroaki Negoro

2021

CONTENTS

ABBREVIATIONS

ATP	adenosine 5'-triphosphate
DMS	dimethyl succinate
DOB	dropout base
5-FOA	5-fluoroorotic acid
GID	glucose induced degradation deficient
HPLC	high-performance liquid chromatography
LOH	loss of heterozygosity
MDH	malate dehydrogenase
MRM	multiple reaction monitoring
MS	mass spectrometry
NAD	nicotinamide adenine dinucleotide
NADH	NAD reduced form
OD	optical density
ORF	open reading frame
PCA	principal components analysis
PEX	peroxin
SD	synthetic defined
SDH	succinate dehydrogenase
TCA	tricarboxylic acid
VID	vacuolar import and degradation
YM	yeast malt
YNB	yeast nitrogen base

GENERAL INTRODUCTION

Budding yeast *Saccharomyces cerevisiae* has been used to make alcoholic beverages, such as wine, beer, and sake (a traditional Japanese alcoholic beverage) since recorded history. In modern times, yeast has contributed to elucidation of life sciences as a model organism and applied to various organic chemical production.. The whole genome sequence of *S. cerevisiae* type strain S288C was determined in 1996 (1), and furthermore, that of representative strain Kyokai No.7 (K-7) for sake brewing was determined in 2011 (2). These database have facilitated genetic analysis of industrial yeast strains.

The yeast produces not just ethanol but ester (aroma compounds), amino acids (bitter and umami compounds), organic acids (sourness compounds), and so on during fermentation. The organic acids in alcoholic beverages play an important role in determining the taste of these drinks. The major components of organic acids in sake are succinate, malate, and lactate (3). Succinate and malate are produced by *S. cerevisiae* during fermentation. (4). Malate is synthesized from glucose via three pathways in yeast. One is the oxidative pathway in the mitochondrion for aerobic metabolism: the tricarboxylic acid (TCA) cycle. Another is an alternate oxidative pathway in the peroxisome: the glyoxylate cycle. The other is reductive pathway in the cytoplasm for anaerobic metabolism (5-7). The vast majority of malate in sake is generated via the reductive pathway due to the anaerobic condition in sake mash during alcoholic fermentation (4).

Most organic acids affect the taste of sake. Succinate has an umami and complex taste. On the other hand, malate has a fresh and sour taste (8). Since malate has a taste that contributes to the desirable sour flavor of sake, various methods have been developed for breeding high malate-producing yeast without genetic modifications (9-11). Many studies have reported the isolation of high-malate-producing yeast strains for sake production, and revealed the mechanisms resulting in the high malate phenotype using several mutants (12-15). For example, a decrease in the mitochondrial activity in yeast was observed to have an immense influence on the production of malate (4, 14, 15).

However, the gene mutations responsible for the phenotype of high malate production in these strains are yet to be determined.

In this study, the author isolated newly high malate-producing strains K-901H and F-701H on the basis of its sensitivity towards dimethyl succinate (DMS) from sake yeast strains K-901 and F-701, respectively. To elucidate the mechanisms underlying enhanced malate production in the industrial sake yeast strains, gene mutations present in the high-malate phenotypes were investigated in strains K-901H and F-701H.

The comparative genome sequencing analysis between K-901H and K-901 revealed that a point mutation in the vacuolar import and degradation protein (*VID*) 24 gene caused a high acid phenotype in the K-901H. Vid24 is a component of the glucose induced degradation deficient (GID) complex that stimulate the catabolic degradation of gluconeogenic enzymes , such as fructose 1,6-bisphosphatase (Fbp1), isocitratelyase (Icl1), phosphoenolpyruvate carboxykinase (Pck1), and cytoplasmic malate dehydrogenase (Mdh2), in *S. cerevisiae* (16-18). It has been suggested that a high malate production was attributed to the accumulation of gluconeogenesis enzymes in *VID24* mutants. As a result of investigating the cause of high malate production in *VID24* mutant, a subcellular abnormal accumulation of Mdh2 in the *VID24* mutant enhanced the reduction of oxaloacetate to malate in the cytoplasm, resulting in increased malate levels.

K-901H was a diploid strain that was a heterozygous carrier of a *VID24* mutation, which was presumed to be semi- or fully dominant. Homozygous integrants of mutated *VID24* generated by genetic engineering showed higher malate productivity than the heterozygous mutants, suggesting that the mutation was semi-dominant in diploid yeast. Since genetically modified foods and beverages were not always acceptable to the public (19), a method was developed for selecting a homozygous *VID24* mutant from heterozygotes without employing a genetic engineering approach. The obtained sake yeast with a homozygous *VID24* mutation exhibited a higher level of malate productivity in sake brewing than the parent heterozygous mutant (K-901H).

Vid24 is a component of the glucose-induced degradation-deficient (GID) complex, a multisubunit E3 ubiquitin ligase that consists of seven proteins (Vid30/Gid1, Rmd5/Gid2, Vid24/Gid4, Vid28/Gid5, Gid7, Gid8, Fyv10/Gid9) in yeast (17, 20-22). The

GID complex specifically degrades gluconeogenic enzymes in the presence of glucose with the E2-conjugating enzyme Ubc8/Gid3 (17). The disruptants of *vid30*, *rmd5*, *ubc8*, *vid24*, *vid28*, *gid8*, and *fyv10* were found to produce higher levels of malate than their parent strain. To evaluate the impact of GID gene disruption on the intracellular metabolism, target proteome analysis was performed. The analysis exhibited that the expression of several glycolytic enzymes was enhanced, whereas the expression of enzymes involved in ethanol fermentation (from pyruvate to ethanol) was downregulated in the high-malate-producing strains compared with the low-malate-producing strains. The changes in the enzymes involved in glycolysis and ethanol fermentation were predicted to result from the adjustment of the cellular metabolism, such as regulation of ATP levels and modulation of the NAD^+ (nicotinamide adenine dinucleotide) and NADH (NAD reduced form) levels, to increased levels of organic acid and intracellular changes in pH.

High-malate-producing yeast strain No. 28 and No. 77 were developed based on their resistance to cycloheximide and mating strategies of haploid yeast cells (10). These strains have been bred in the "Brewing Society of Japan," a public interest incorporated foundation. The mechanism for high malate production in strain No. 28 and No. 77 was investigated by the genome sequencing analysis. Several mutations in GID protein-coding genes were detected in each strain, and one of them led to high malate production. A mutation in the *GID4* gene resulted in high malate production by strain No. 28, while a mutation in the *GID2* gene led to high malate production by strain No. 77.

The mechanisms contributing to the high acidity phenotype of the strain F-701H were investigated. A mutation in the peroxin-coding gene *PEX22* involved in the regulation of peroxisomal homeostasis was observed in F-701H, resulting in high malate production. Some peroxins including Pex22 play an important role in the transportation of peroxisomal matrix proteins (23, 24). The deficiency of Pex22 prevented Mdh3 from localizing to the peroxisomes, thereby promoting the production of malate in the yeast cytoplasm.

These results provide a useful indication to control the ability of malate production in yeasts. Because of a pleasant taste of malate in sake, the regulation of malate

level would improve the quality of sake possessing a characteristic taste. Additionally, since identification of the mutated gene responsible for malate production leads to suggestions for the brewing characteristics in high malate-producing strains, these findings will be useful for the process of sake brewing using these industrial strains.

Chapter I

Enhancement of malate-production and increase in sensitivity to dimethyl succinate by mutation of the *VID24* gene in *Saccharomyces cerevisiae*

The ability of producing organic acids varies with yeast strains. To date, some methods for breeding high-malate-producing strains from mutagenized sake yeasts have been developed in order to control the organic acids content in sake. Aikawa *et al*. obtained a high-malate-producing strain by isolating a mutant sensitive to dimethyl succinate (DMS), a specific inhibitor of succinate dehydrogenase (SDH) (9). Yoshida *et al*. acquired a high-malate-producing strain from cycloheximide tolerant strains (10). Asano *et al*. bred a high-malate-producing strain by isolating sake yeast with low-maltose-assimilation ability (12). The cycloheximide tolerant strains and the low-maltose-assimilating strain exhibited an increase in expression of genes coding malate dehydrogenase (MDH) during sake fermentation (12, 13). In addition, Oba *et al*. isolated a high-malate-producing strain from sake mashes (25), and they indicated that the enhancement of malate-production was correlated with a decrease in mitochondrial electron potential (14). The notion that mitochondrial activity in yeast has a great influence on malate-production is now accepted (4, 14, 15). In these several high-malate-producing strains mentioned above, there have been a number of reports of the mechanisms contributing to the high-acidity phenotype.

The variations in malate-productivity of these yeast strains are estimated to be charactarized by respective differences of mutations in some genes. In previous studies, it was investigated how yeast genes related to TCA cycle, such as α-ketoglutarate dehydrogenase, fumarate reductase, and SDH, regulated organic acid metabolism during sake fermentation (26-30). Furthermore, it was showed that the mitochondrial fission gene involved in the production of organic acids during alcohol fermentation (31). Thus, many genes associated with organic acid metabolism have been reported. Nevertheless, little has been reported on the determination of mutated genes which characterize distinction in the ability of producing malate among various industrial yeast strains.

In the present study, the author identified the gene mutation involved in the high-

acidity phenotype in an industrial strain isolated using the sensitivity to DMS. A point mutation in the *VID24* (alias *GID4*) gene, which plays an important role in the degradation of gluconeogenic enzymes, resulted in high-malate-productivity. The author suggested that Vid24p deficiency affected TCA cycle and glycolytic metabolism, and consequently increased the production of organic acids in yeast cells.

MATERIALS AND METHODS

Media and Strains Yeast cells were cultivated aerobically at 30°C in YPD medium containing 10 g/L yeast extract, 20 g/L polypepton, and 20 g/L glucose; YM10 medium containing 3 g/L yeast extract, 3 g/L malt extract, 5 g/L polypepton, and 100 g/L glucose; SD - ura medium containing 6.7 g/L yeast nitrogen base without amino acids (YNB w/o AA) (Becton Dickinson and Company, Franklin Lakes, NJ, USA), 20 g/L glucose, and 0.77 g/L complete supplement mixture - ura (MP Biomedicals, Solon, OH, USA); or glycerol-YNB medium containing 6.7 g/L YNB w/o AA and 20 g/L glycerol.

The media used for the evaluation of DMS sensitivity were DOB medium containing 6.7 g/L YNB w/o AA and 20 g/L glucose; DMS medium containing 6.7 g/L YNB w/o AA, 20 g/L glucose, and 15 g/L DMS; DOB + ura medium containing 6.7 g/L YNB w/o AA, 20 g/L glucose, and 20 mg/L uracil; or DMS + ura medium containing 6.7 g/L YNB w/o AA, 20 g/L glucose, 20 mg/L uracil, and 15 g/L DMS.

The sake yeast strain K-901H was obtained by ethyl methane sulphonate mutagenesis of wild-type sake yeast Kyokai No. 901 (K-901) (Brewing Society of Japan, Tokyo, Japan) and selected using sensitivity to DMS as previously described (9).

Disruptants derived from BY4743 were obtained from Yeast Knock Out Homozygous Diploid Collection YSC1056 (Thermo Fisher Scientific Inc., Waltham, MA, USA) (Table 1-1).

The *MAT***a** haploid yeast strain 4011a was isolated from spores of the *MAT***a**/*MAT*α diploid yeast strain 4011 (32, 33). GX-11 is the uracil auxotroph strain (*ura3*) of 4011a. Uracil auxotrophic yeast strains were selected for growth on 5- fluoroorotic acid (5-FOA) medium containing 6.7 g/L YNB w/o AA, 20 g/L glucose, 1

g/L 5-FOA, and 20 mg/L uracil (34).

Disruption of the *VID24*, *MDH1*, *MDH2*, *MDH3*, *HXT7*, *FBP1* or *PCK1* genes in 4011a-derived strains was performed using a PCR-based method with the primers listed in Table 1-2 and KanMX4 module-incorporated plasmid (35). Yeast transformations were performed by the lithium acetate method (36). The disruptants derived from 4011a are listed in Table 1-1.

Table 1-1 Genotypes and references of *S. cerevisiae* strains used in this study

Strain	Genotype	Reference
Kyoukai No.901 (K-901)	*MAT***a**/*MAT*α	Brewing Society of Japan
K-901H	K-901 *VID24* 391G>A/*VID24*	This study
BY4743	*MAT***a**/*MAT*α *his3Δ1/his3Δ1 leu2Δ0/leu2Δ0 LYS2/lys2Δ0 met15Δ0/MET15 ura3Δ0/ura3Δ0*	Thermo Fisher Scientific Inc.
BY4743Δadr1	BY4743 *adr1*::*kanMX4*/*adr1*::*kanMX4*	Thermo Fisher Scientific Inc.
BY4743Δmdh3	BY4743 *mdh3*::*kanMX4*/*mdh3*::*kanMX4*	Thermo Fisher Scientific Inc.
BY4743Δpdc5	BY4743 *pdc5*::*kanMX4*/*pdc5*::*kanMX4*	Thermo Fisher Scientific Inc.
BY4743Δvid24	BY4743 *vid24*::*kanMX4*/*vid24*::*kanMX4*	Thermo Fisher Scientific Inc.
4011	*MAT***a**/*MAT*α	(20)
4011a	4011 haploid strain *MAT***a**	This study
GX-11	4011a *ura3*	This study
GX-11Δvid24	GX-11 *vid24*::*kanMX4*	This study
GX-11Δmdh1	GX-11 *mdh1*::*kanMX4*	This study
GX-11Δmdh2	GX-11 *mdh2*::*kanMX4*	This study
GX-11Δmdh3	GX-11 *mdh3*::*kanMX4*	This study
GX-11Δhxt7	GX-11 *hxt7*::*kanMX4*	This study
GX-11Δfbp1	GX-11 *fbp1*::*kanMX4*	This study
GX-11Δpck1	GX-11 *pck1*::*kanMX4*	This study
GX-VID24	GX-11 *VID24* 391G>A	This study
GX-VID24Δmdh1	GX-VID24 *mdh1*::*kanMX4*	This study
GX-VID24Δmdh2	GX-VID24 *mdh2*::*kanMX4*	This study
GX-VID24Δmdh3	GX-VID24 *mdh3*::*kanMX4*	This study
GX-VID24Δhxt7	GX-VID24 *hxt7*::*kanMX4*	This study
GX-VID24Δfbp1	GX-VID24 *fbp1*::*kanMX4*	This study
GX-VID24Δpck1	GX-VID24 *pck1*::*kanMX4*	This study

Whole genome sequencing analysis Genomic DNA was extracted using the NucleoBond Buffer Set III and the NucleoBond AXG 20 Columns (MACHEREY-NAGEL GmbH & Co. KG, Düren, Germany) from K-901 and K-901H cells. Approximately 10 μg of genomic DNA from each sample were used for the analysis. Whole genome sequence was determined by the Takara-bio comparative genome analysis service (Takara Bio Inc., Otsu, Japan), using HiSeq2000 (Illumina Inc., San Diego, CA, USA). Sequence reads were assembled using the Burrows–Wheeler Aligner (BWA) ver0.5.9. software. The analysis identified variant positions relative to genome sequence of the sake yeast K-7 (Brewing Society of Japan) as a reference genotype (2). Comparison of K-901 or K-901H genome with K-7 genome was performed using SAMtools mpileup and varFilter software.

Construction of the point mutant The *VID24* mutation was introduced into GX-11 using a two-step gene replacement method (37). Using primers VID24(102)XbaI-F and VID24(787)HindIII-R (Table 1-2) with K-901H chromosomal DNA as the template, DNA fragments corresponding to the mutated regions of *VID24* of K-901H were amplified using PCR, digested with *Xba*I and *Hin*dIII, and cloned into pRS406 (Stratagene, La Jolla, CA, USA). After the plasmid DNA pRS406-VID24 containing

Table 1-2 Primers used in this study

Primer name	Primer sequence (5'-3')
VID24_KanMX4-up	GCGTCTTGTGCATGACACCAACACATATCGCAAGCTTGAGTCCGTACGCTGCAGGTCGACGG
VID24_KanMX4-down	GAAGAGAAAAGGGTATGCAGGTAAAAACGAATATATCACACATCATTAGAAAAACTCATCGAGCA
MDH1_KanMX4-up	GGAAGAAAAAAAACAAAAGGAAAAGGAAGGATACCATATACACGTACGCTGCAGGTCGACGG
MDH1_KanMX4-down	TTTTTTTCCCTATTTTTCACTCTATTTCTGATCTTGAACAATCTATTAGAAAAACTCATCGAGCA
MDH2_KanMX4-up	TATAAAGATAAAGATTTATCGATATGAGATAAAGATTGCTGCCGTACGCTGCAGGTCGACGG
MDH2_KanMX4-down	ATTATCAATTTGCTGCATTCTTATGCTTCGGTCCGATGCTCATTATTAGAAAAACTCATCGAGCA
MDH3_KanMX4-up	GTCAGTGCAAAAGAAAATAAAAAGAGACAAACAATCATAAACCGTACGCTGCAGGTCGACGG
MDH3_KanMX4-down	AAAGGAGTATAGAGTTAAGAAAAATATAAAAATTGAAGTAGCTCATTAGAAAAACTCATCGAGCA
HXT7_KanMX4-up	GCCAATACTTCACAATGTTCGAATCTATTCTTCATTTGCAGCTATTGTAACGTACGCTGCAGGTCGACGG
HXT7_KanMX4-down	CTGTATTATTTTGTATATATTAAAAACGTATTTACTTTTCAAGATATTAGAAAAACTCATCGAGCA
FBP1_KanMX4-up	CAGTGCGAACATATAAGAAACATCCCTCATACTACCACACATCGTACGCTGCAGGTCGACGG
FBP1_KanMX4-down	AGTACAGAACAAAGAAAATAAGAAAAGAAGGCGATCATTGAACTATTAGAAAAACTCATCGAGCA
PCK1_KanMX4-up	ACCAAACTCACGCAACTAATTATTCCATAATAAAATAACAACCGTACGCTGCAGGTCGACGG
PCK1_KanMX4-down	TTTTTTTTTTTGGATTGAACATATCGAACGAACATGTTTCGTTTATTAGAAAAACTCATCGAGCA
VID24(102)XbaI-F	CCCTGTTTCTAGAAATCAGTATCCGAT
VID24(787)HindIII-R	TTGGTGTAGTAGGAAGCTTCTGTGGAG

URA3 and mutated *VID24* was digested with *Eco*RI (the open reading frame of *VID24* contains *Eco*RI restriction site originally), the straight-chain DNA fragment was used to transform GX-11. The transformant was obtained by selection on SD - ura medium and was then cultivated in YPD for 24 h and then plated onto 5-FOA medium. Colonies appearing on 5-FOA medium resulting from loss of extraneous plasmid sequences containing *URA3* were candidates to be *VID24* mutants, GX-VID24. The *VID24* genotypes of individual clones were determined by DNA sequencing.

Comparison of the growth in DMS medium Yeast strains were cultivated in YPD medium at 30°C for 24 h. For comparison of K-901 with K-901H, the cells were collected and resuspended in DOB medium or DMS medium, to an optical density of 0.01 at 600 nm. For comparison of GX-11 with GX-VID24, the cells were collected and resuspended in DOB + ura medium or DMS + ura medium. Cell suspension cultures were incubated aerobically at 30°C, and their cell densities were automatically measured with a Bio-photorecorder (Advantec Toyo Co. Ltd., Tokyo, Japan).

One-step sake brewing test Yeast cells were cultivated in YPD medium at 30°C for 48 h, harvested by centrifugation, and resuspended in water. Koji is a culture of *Aspergillus oryzae* that is grown on steamed rice. Polished rice was preliminarily pulverized, gelatinized, and digested with thermostable α-amylase TU20 (Amano Enzyme Co. Ltd., Nagoya, Japan) (38), because enzyme activity of α-amylase derived from koji is known to decline in high acidity sake mash (39). Sake mash consisted of 40 g of polished rice with a polishing ratio of 70%, 10 g of koji, 20 μl of 90% lactic acid, 80 ml of water, and 1.3×10^8 yeast cells. Fermentation was carried out at 15°C. The loss of weight of the mash was correlated with carbon dioxide emission levels to monitor the fermentation progress. After 18 days, the mash was centrifuged and the supernatant was analyzed. The ethanol concentration was measured using Density/Specific Gravity Meter DA-650 (Kyoto Electronics Manufacturing Co. Ltd., Kyoto, Japan), after the supernatant was distilled. Acid and amino acid levels were measured with an electric potential difference autotitration apparatus (Kyoto Electronics Manufacturing Co. Ltd., Kyoto,

Japan) by the National Tax Administration Agency method (40). The levels of organic acids were quantified using high performance liquid chromatography Organic Acid Analysis System (Shimadzu Co. Ltd., Kyoto, Japan).

Assay of MDH activity Yeast cells were statically cultivated in YM10 medium at 30°C for 6 days, and shifted to YPD for 2 h to induce degradation of gluconeogenic enzymes. Cells were harvested by centrifugation, washed with distilled water, and resuspended in 50 mM sodium acetate (pH 5.0). The cells were disrupted in a microtube containing 0.4 mm glass beads by using Micro Smash MS-100R (TOMY SEIKO Co. LTD., Tokyo, Japan) at 500 rpm for 150 sec. The homogenates were centrifuged, and the supernatants were used as the crude enzyme solution. MDH activity in the supernatants was measured according to previously reported methods (41), using a microplate spectrophotometer xMark (Bio-Rad Laboratories Inc., Hercules, CA, USA). One unit of specific activity was defined as 1 μmol of substrate conversion per min per mg of protein. Protein contents were determined by Bradford method using Bio-Rad Protein Assay (Bio-Rad Laboratories Inc., Hercules, CA, USA) with bovine serum albumin as the standard protein.

Measurement of NADH/NAD$^+$ ratio The NADH/NAD$^+$ ratio was measured using EnzyChrom NAD$^+$/NADH Assay Kit E2ND-100 (BioAssay Systems, Hayward, CA, USA). Yeast cells were statically cultivated in YM10 medium at 30°C for 3 days, harvested by centrifugation, and washed with PBS buffer. 1.0×10^7 yeast cells were used in the assay the according to manufacturer's instructions. The absorbance at 565 nm was measured on a microplate spectrophotometer.

RESULTS

The high-malate-producing strain was isolated using DMS The high-malate-producing strain K-901H was isolated from K-901 as a DMS-sensitive mutant. K-901H cells were separated by negative selection of DMS by use of the slower growth rate than

K-901 on DMS medium. First, 61 DMS-sensitive colonies were obtained. Among the 61 colonies, 35 colonies exhibited high acid level compared with the parental strain K-901 in a small scale sake brewing test. The highest-acid-producing strain of the 35 clones was selected as K-901H. K-901H showed almost equal ethanol level to K-901 (data not shown). Then, a one-step sake brewing test was performed using K-901 and K-901H. The concentration of ethanol was approximately 19% for both strains. The values of malate and succinate concentrations in K-901H were 2.2-fold and 1.3-fold higher than those in K-901, respectively (Table 1-3). Automatic measurement of cell densities showed a delay in the onset of the logarithmic phase of K-901H in DMS medium as compared with that of K-901 (Fig. 1-1).

Table 1-3 Sake brewing tests of K-901 and K-901H

Parameter		Value (mean ± SD)	
		K-901	K-901H
Ethanol (vol %)		19.28 ± 0.11	18.83 ± 0.06
Specific gravity (15°C/4°C)		0.9928 ± 0.0002	0.9953 ± 0.0003
Acid level		2.43 ± 0.00	3.26 ± 0.01
Amino acid level		2.19 ± 0.01	1.88 ± 0.02
Organic acid (mg/L)	Malate	310 ± 1	695 ± 10
	Succinate	599 ± 3	762 ± 14
	Lactate	408 ± 1	429 ± 2
	Citrate	108 ± 0	108 ± 1
	Pyruvate	0 ± 0	30 ± 0
	Acetate	119 ± 1	74 ± 5

These experiments were repeated twice. Plus or minus represents standard deviations.

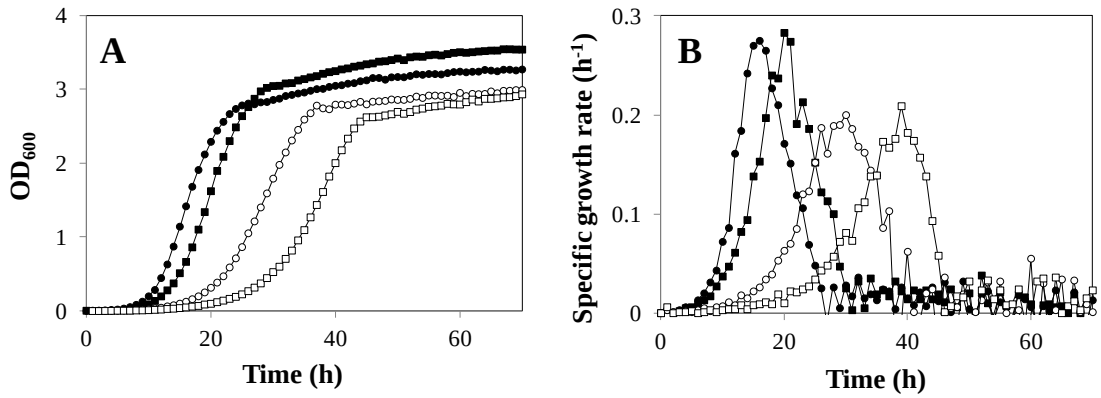

Fig. 1-1 Decrease in the growth rates of K-901H in DMS medium. Growth curves (A) and specific growth rates (B) of K-901 and K-901H in DOB medium or DMS medium.Symbols: closed circles, K-901 in DOB; closed squares, K-901H in DOB; opened circles, K-901 in DMS; opened squares, K-901H in DMS

Table 1-4 List of genes containing missense mutations between K-901 and K-901H

ADR1	*ALT2*	*ARG2*	*ASH1*	*ATX2*	*BNI1*	*BRE1*	*BRR2*
BSC2	*BYE1*	*CBF1*	*CDC48*	*CDC48*	*CFT1*	*CHS1*	*CKB1*
CKI1	*CMR2*	*COG7*	*COG8*	*CSE1*	*CWC22*	*DAK2*	*DAL4*
DAL5	*DAL81*	*DAT1*	*DCK1*	*DIA3*	*DPB11*	*DRE2*	*DSF2*
DUG1	*DUR1,2*	*ESF1*	*FAS1*	*FET5*	*FKS1*	*FOB1*	*FRE1*
FRM2	*FUN30*	*FUR4*	*GCV2*	*GIP4*	*GLN4*	*GMH1*	*HXT14*
INO80	*JEM1*	*KAR2*	*KEX1*	*KTR2*	*KTR3*	*LAG2*	*LAS21*
LEU9	*LIP2*	*LTE1*	*MDH3*	*MDN1*	*MKR1*	*MRM2*	*MSA1*
NGR1	*NOP13*	*NPP1*	*NPR3*	*NSP1*	*NUG1*	*NUP192*	*NUP60*
OAF3	*OCH1*	*PAN3*	*PBP1*	*PBP2*	*PCL2*	*PCL6*	*PCL8*
PDC5	*PDR11*	*PET127*	*PEX28*	*POL12*	*PPG1*	*PPS1*	*PSP2*
PTK2	*PTM1*	*PTP3*	*PUT4*	*RAD23*	*RAD30*	*RAX2*	*RFC1*
RFC5	*RIF1*	*RIM4*	*RLI1*	*RPA135*	*RPS22B*	*RRN11*	*RTG2*
RTT103	*SAP185*	*SBE22*	*SEC1*	*SEC8*	*SEC23*	*SGS1*	*SIR2*
SLP1	*SNR37*	*SPB1*	*SPT23*	*SSD1*	*SSF2*	*STE24*	*SWI4*
TAF1	*TAF2*	*TAT2*	*TCB3*	*TFC1*	*TIM23*	*TOM1*	*TPK3*
TPS2	*TRS33*	*UTP21*	*VAC17*	*VID24*	*YMD8*	*YOR1*	*YSP1*
ZRG8	*YDL129W*	*YDL158C*	*YDR444W*	*YER077C*	*YER184C*	*YGL101W*	*YHR049C-A*
YJL055W	*YLR177W*	*YLR334C*	*YOR022C*	*YPL025C*			

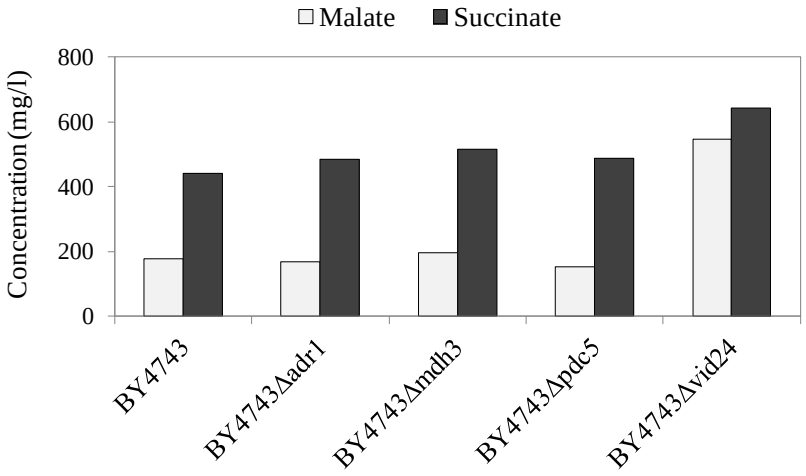

Fig. 1-2 Malate and succinate in sake brewing tests with BY4743, BY4743Δadr1, BY4743Δmdh3, BY4743Δpdc5, and BY4743Δvid24.

A mutation of the *VID24* gene resulted in high-malate-productivity To determine the gene responsible for high-malate-productivity in K-901H strain, genomic DNA extracted from K-901 and K-901H cells was subjected to whole-genome-sequencing analysis. In the analysis, 150 missense mutations (146 non-synonymous substitutions and 4 indel mutations), 65 synonymous substitutions, and 138 intergenic mutations were identified between K-901 and K-901H genome sequences. Among the 150 missense mutations (Table 1-4), the author focused on genes involved in glycolysis, gluconeogenesis, TCA cycle, or glyoxylate cycle, and then selected four genes; *ADR1*, *MDH3*, *PDC5* and *VID24*, as candidates for the responsible genes. Four disruptants derived from BY4743 were used for one-step sake brewing test, and the concentrations of organic acids were quantified. BY4743Δvid24 produced higher level of malate than the parental strain BY4743 (Fig. 1-2).

The author decided to investigate whether the non-synonymous substitutions in *VID24* increased the level of malate. The heterozygous mutation of a G to A substitution at nucleotide 391 (an amino acid replacement of arginine with glycine at residue 131) of the *VID24* open reading frame was detected in K-901H. Vid24 is a component of glucose induced degradation deficient (GID) complex, a multisubunit ubiquitin ligase that consists of GID proteins (Vid30, Rmd5, Vid24, Vid28, Gid7, Gid8, and Fyv10) (21). GID

complex is involved in the degradation of gluconeogenesis enzymes (20).

The *VID24-391A* mutant strain GX-VID24 was obtained as described in the *MATERIALS AND METHODS* section. A one-step sake brewing test was performed using GX-11 and GX-VID24. The concentration of ethanol was the same in the two strains, whereas the levels of organic acids were different. The values of malate and succinate in GX-VID24 were 3.6-fold and 2.0-fold higher than those in GX-11, respectively (Fig. 1-3). In addition, high levels of malate in GX-VID24 were also observed in YM10 cultivation. These data indicate that the point mutation *VID24-391A* increases the malate-productivity of *S. cerevisiae* during sake brewing.

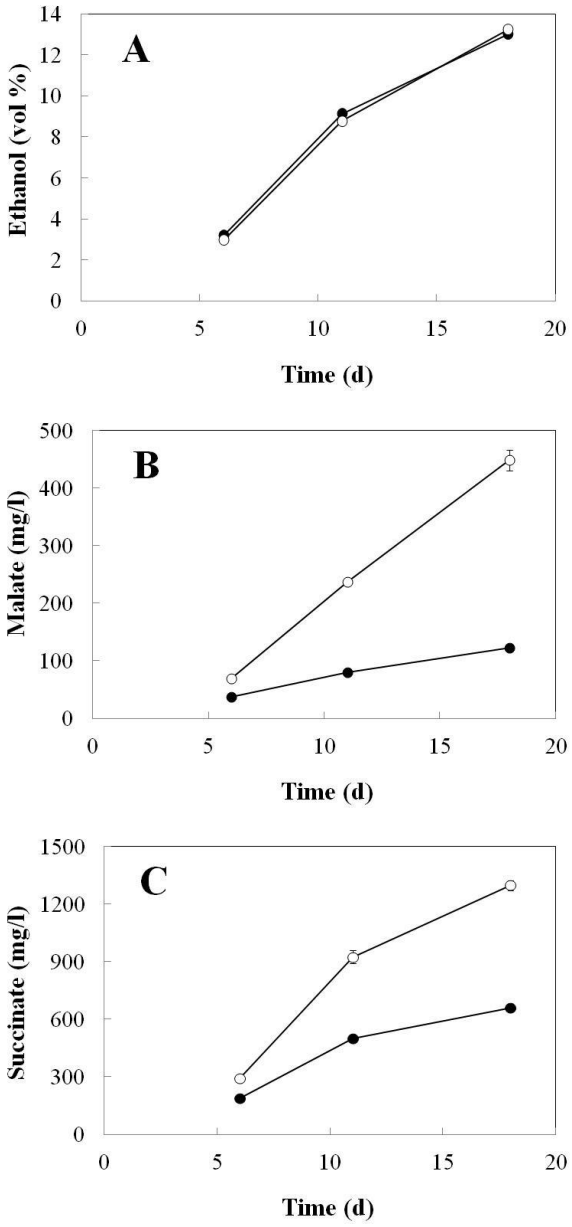

Fig. 1-3 Sake brewing tests of GX-11 and GX-VID24. Concentration of ethanol (A), malate (B), and succinate (C) were determined. The brewing tests were repeated twice. Error bar represents standard deviations. Symbols: closed circles, GX-11; open circles, GX-VID24.

The *VID24-391A* mutant exhibited phenotypes similar to the loss-of-function mutant of *VID24* in acid production Vid24 contains no remarkable protein-protein interaction domains, such as a Lissencephaly type-1-like homology motif (LisH), a C-terminal to LisH motif, and a degenerated RING finger domain, which are present in other GID proteins (21). Little is known about the relationship between the amino acid sequence and the function of Vid24p. To examine the effect of *VID24-391A* mutation on the function of Vid24, the author constructed the *vid24* disruptant strain, GX-11Δvid24. GX-11, GX-VID24, and GX-11Δvid24 were used for one-step sake brewing, and then organic acid levels were measured. As a result, GX-VID24 and GX-11Δvid24 were almost equal in malate-producing ability (Fig. 1-4), suggesting that *VID24-391A* mutation led to a deficiency in Vid24 function.

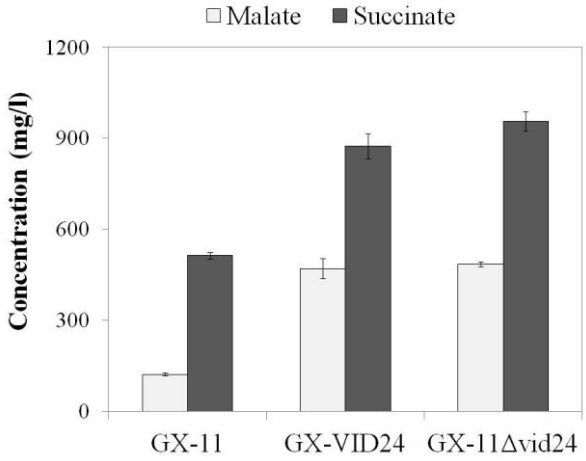

Fig. 1-4 Malate and succinate in sake brewing tests with GX-11, GX-VID24, and GX-11Δvid24. These brewing tests were repeated twice. Error bar represents standard deviations.

The increase in organic acid production in *VID24* mutants arose from participation of cytoplasmic malate dehydrogenase gene (*MDH2*) Disruption of *VID24* results in an intracellular accumulation of gluconeogenic enzymes such as fructose-1,6-bisphosphatase (Fbp1), phosphoenolpyruvate carboxykinase (Pck1), and Mdh2 (16, 17). Furthermore, the disruption of other GID genes (*VID30*, *RMD5*, and *VID28*) leads to an accumulation of Hxt7 (42). To investigate the possibility of the effects of these enzymes on acid production, disruption of *MDH2*, *HXT7*, *FBP1*, and *PCK1* in GX-11 and GX-VID24 were performed. In addition to these disruptants of the

gluconeogenic genes, the disruptants of mitochondrial malate dehydrogenase gene (*MDH1*) and peroxisomal malate dehydrogenase gene (*MDH3*), encoding isozymes of Mdh2, were also obtained. Mdh2 is required for growth on minimal medium with ethanol or acetate as a carbon source (41). The disruption of *MDH1* or *MDH3* results in an inability to grow with acetate or oleate, respectively (43, 44), resembling the utilization of carbon source in *MDH2* deficient cells. Hence, these isozymes of Mdh2 were suspected to be related to acid production. A one-step sake brewing test was carried out using disruptants with *MDH1*, *MDH2*, *MDH3*, *HXT7*, *FBP1* and *PCK1* in GX-11 and GX-VID24 strains (Table 1-1). The profiles of organic acids in GX-VID24Δmdh2 were almost equal to those in GX-11Δmdh2 but lower than those in GX-VID24 (Table 1-5). The same change in acid levels was observed in YM10 cultivation (data not shown). These data imply that the accumulation of Mdh2 in Vid24 deficient strain yields an increase of malate production.

Table 1-5 Sake brewing tests of disruptants derived from GX-11 and GX-VID24 genome

	Ethanol (vol %)	Specific gravity (15°C/4°C)	Acid level	Amino acid level	Organic acid (mg/l)				
					Malate	Succinate	Citrate	Pyruvate	Acetate
GX-11	16.27	1.0048	3.83	3.05	152	793	70	53	461
GX-11Δmdh1	16.12	1.0070	4.38	2.97	285	556	66	208	491
GX-11Δmdh2	16.21	1.0059	3.84	3.12	77	541	76	n.d.	463
GX-11Δmdh3	16.47	1.0045	4.20	2.98	175	830	70	29	431
GX-11Δhxt7	16.34	1.0040	4.14	3.04	144	780	69	47	520
GX-11Δfbp1	16.08	1.0069	4.20	3.03	136	748	67	198	472
GX-11Δpck1	16.21	1.0070	3.89	3.07	153	730	66	165	322
GX-VID24	15.85	1.0081	6.44	2.63	731	2154	75	175	139
GX-VID24Δmdh1	15.63	1.0107	5.44	3.06	1383	648	65	233	435
GX-VID24Δmdh2	16.27	1.0050	3.43	3.30	79	564	79	n.d.	571
GX-VID24Δmdh3	15.91	1.0083	6.54	2.66	844	2235	76	158	109
GX-VID24Δhxt7	15.86	1.0080	6.35	2.70	719	2162	77	179	162
GX-VID24Δfbp1	15.78	1.0099	6.15	2.77	758	2048	75	194	116
GX-VID24Δpck1	15.76	1.0104	6.13	2.85	858	2090	74	165	70

n.d. means Not Detected.

To address this hypothesis, the enzyme activity of MDH in disruptants with *MDH1*, *MDH2*, and *MDH3* was measured. The approach was based on the assumption that MDH activity in GX-VID24, GX-VID24Δmdh1, and GX-VID24Δmdh3 cells ought to be higher than that in GX-11, GX-11Δmdh1, and GX-11Δmdh3 cells, respectively, due to accumulation of Mdh2 in Vid24 deficient strain. The total cellular MDH activity consists of three isozymes: Mdh1, Mdh2, and Mdh3. As shown in Table 1-6, MDH activity showed marginally significant difference between GX-11Δmdh1 and GX-VID24Δmdh1, as well as between GX-11Δmdh3 and GX-VID24Δmdh3. The expression of *MDH2* is very low in yeast cells (45), and Mdh2 is subject to glucose catabolite inactivation (46). Hence, subtle changes in Mdh2 appeared to result in the enhancement of malate production. Due to Mdh1 accounting for most of total MDH activity (41), it was considered to be difficult to definitively detect the difference in MDH activity attributed to Mdh2.

Table 1-6 MDH activities of disruptants derived from GX-11 and GX-VID24

	MDH activity (unit/mg)	Malate (mg/l)	Succinate (mg/l)
GX-11	0.261 ± 0.017	42 ± 1	265 ± 2
GX-11Δmdh1	0.014 ± 0.003	82 ± 4	230 ± 22
GX-11Δmdh2	0.234 ± 0.023	22 ± 1	183 ± 16
GX-11Δmdh3	0.249 ± 0.022	44 ± 2	294 ± 16
GX-VID24	0.289 ± 0.077	153 ± 13[b]	533 ± 53[b]
GX-VID24Δmdh1	0.024 ± 0.006[a]	341 ± 17[b]	286 ± 18[b]
GX-VID24Δmdh2	0.225 ± 0.017	25 ± 3	177 ± 15
GX-VID24Δmdh3	0.291 ± 0.024[a]	170 ± 6[b]	490 ± 31[b]

These cultures were repeated three times. Plus or minus represents standard deviations.

[a] Marginally significantly higher than the GX-11-derived strain (*t* test; $0.05 < P < 0.1$)

[b] Significantly higher than the GX-11-derived strain (*t* test; $P < 0.05$)

Recent studies have proposed that low mitochondrial activity was involved in high-malate-production in *S. cerevisiae* (4, 11, 14, 15). One study suggested that low mitochondrial activity caused the increase in NADH/NAD^+ ratio in yeast cytosol (11);

however, the NADH/NAD^+ ratio in GX-VID24 cells was almost identical to that in GX-11 cells (GX-VID24: 0.47, GX-11: 0.44, these values represent the mean of the two independent cultures). Furthermore, another study showed that mutants with decreased mitochondrial membrane potential grew slowly compared with the parental strain on minimal medium containing glycerol as the sole carbon source (14), whereas there was no significant difference in the growth in glycerol-YNB medium between GX-VID24 and GX-11 (data not shown). In addition, several studies revealed that the decrease in mitochondrial membrane potential led to a reduction in the production of succinate (4, 14), while the level of succinate in GX-VID24 was higher than that in GX-11 (Table 1-6). Taken together, these data indicated that the increase in malate production in *VID24* mutants did not result from the decrease in mitochondrial activity.

The *VID24* mutant induced DMS sensitivity In order to elucidate whether the *VID24-391A* mutation was implicated in sensitivity to DMS in yeasts, the growth characteristics of GX-11 and GX-VID24 strains were compared when they were incubated in DOB + ura medium or DMS + ura medium. The same method in DMS-sensitivity test of K-901 and K-901H was used to automatically measure their cell densities. It took a longer time for GX-VID24 to reach a maximum specific growth rate than for GX-11 in DMS + ura medium (Fig. 1-5). The lag time to reach a maximum specific growth rates in DMS + ura medium and DOB + ura medium were 16.5 h and 24.5 h for GX-11 and GX-VID24, respectively. This result suggests that *VID24-391A* mutation in yeasts leads to a reduction in tolerance to DMS.

DISCUSSION

A high-malate-producing sake yeast was isolated using DMS, and genome sequencing analysis revealed that *VID24* was at least one of the responsible genes for high-acid-productivity and DMS sensitivity. As shown in Fig. 1-5, *VID24-391A* mutation reduced the tolerance to DMS in yeast. However, the rates of DMS uptake and its metabolism are unknown. Therefore, it was unclear how the increase in organic acids

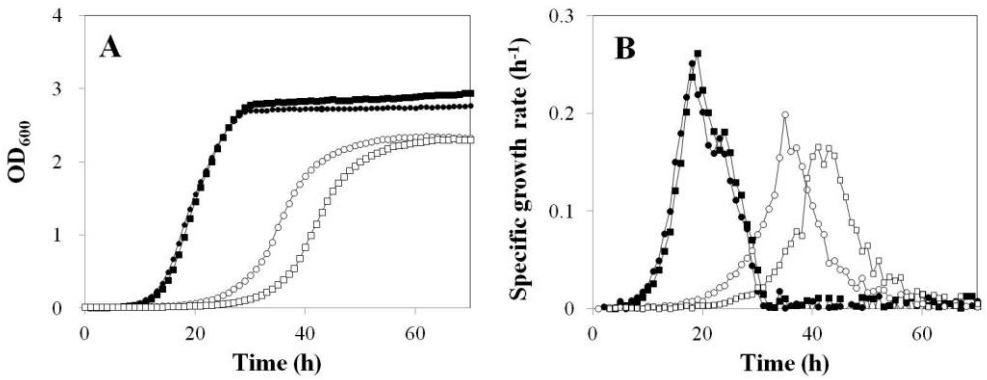

Fig. 1-5 Decrease in the growth rates of GX-VID24 in the medium containing DMS. Growth curves (A) and specific growth rates (B) of GX-11 and GX-VID24 in DOB + ura medium or DMS + ura medium. The values in two independent cultures showed similar results and the plots present averaged values.

resulted from the *VID24* mutation impacted sensitivity to DMS. Since a high-malate-producing strain No.28 (Brewing Society of Japan) does not have higher sensitivity to DMS than its paren

t strain (10), DMS sensitivity was apparently not brought about just by the accumulation of malate. It is possible that *VID24* mutant is susceptible to a growth inhibition by an excess accumulation of the intracellular succinate which could not be metabolized due to the presence of DMS, a specific inhibitor of SDH. This hypothetical mechanism would not be adapted to high-malate-producing strains with low mitochondrial activity, such as No.28 (15), because of a reduction in the conversion of malate to succinate in mitochondria. The correlations between DMS sensitivity and acid production remain a matter of debate.

Vid24, a component of GID complex, is known to be involved in catabolite degradation of Fbp1, Pck1, and Mdh2 in *S. cerevisiae*. These enzymes of gluconeogenesis are degraded via the ubiquitin proteasome and vacuole system by GID complex (16, 17, 20, 47-51). The *VID24-391A* point mutation caused enhancement in the ability of malate production in yeast (Fig. 1-3), and this mutation appeared to induce Vid24 loss of function (Fig. 1-4). Gluconeogenic enzymes such as Fbp1, Pck1, and Mdh2, normally be degraded

via the Vid24p-mediated ubiquitination pathway, were accumulated in *VID24* disruptant cells (16, 17). Among these enzymes, the abnormal accumulation of Mdh2 would enhance reduction of oxaloacetate to malate in the cytosol (Table 1-5, Table 1-6). This assumption is supported by previous studies indicating that a large fraction of malate in sake mash is due to the reduction of oxaloacetate to malate by Mdh2 in cytosol during alcoholic fermentation (4), and that overexpression of cytosolic malate dehydrogenase increased malate level (6). Recent studies have showed that the decrease in mitochondrial electron potential elevated the ability of malate production in industrial yeast strains (4, 11, 14, 15). However, these data ($NADH/NAD^+$ ratio, growth in glycerol-medium, and succinate productivity) indicated that the increase of malate production in *VID24* mutant was attributed to a different mechanism from the mitochondrial activity-relevant model. Deletion of *VID30*, *RMD5*, *VID28,* or *GID8* (these are all GID proteins), in addition to *VID24*, results in the accumulation of Mdh2p in yeast cells (16). Therefore, it is likely that the deficiency of *VID30*, *RMD5*, *VID28,* or *GID8* enhances malate production.

The accumulated malate was presumed to be converted to succinate through a reductive anaerobic pathway in the cytosol, or to be transported into mitochondria and used aerobically in the oxidative TCA cycle, consequently, the level of succinate increased. In the experiments with sake brewing test using GX-VID24, the amount of succinate also increased concurrently with malate. It may be possible to change the ratio of malate to succinate by the regulation of dissolved oxygen levels (4, 26). Furthermore, the level of malate in GX-VID24Δmdh1 was higher than in GX-VID24, and the level of succinate in GX-VID24Δmdh1 was lower than in GX-VID24 (Table 1-5). Mdh1 catalyzes the interconversion of malate and oxaloacetate in the TCA cycle (52). The accumulation of malate could be facilitated in GX-VID24Δmdh1 cells due to loss of the conversion of mitochondrial malate translocated from cytosol to oxaloacetate.

K-901H is diploid yeast and the heterozygous *VID24-391A* mutant. To investigate *VID24* mutation, the author used the haploid yeast strain GX-11. Because of two phenotypes of both high acidity and DMS sensitivity in K-901H, the heterozygous mutation of the *VID24* gene was assumed to be semidominant or dominant. For instance, it is known that heterozygous *FAS2* mutation (*FAS2-3748A*), leading to elevation of

hexanoic acid levels, is semidominant (53). A homozygous mutant of *FAS2*, constructed from the heterozygous mutant by loss of heterozygosity method, produced much elevated levels of hexanoic acid compared with the heterozygous mutant (54). Thus, the levels of hexanoic acid change depending on the genotype of *FAS2* mutation, heterozygous or homozygous. Similarly to *FAS2* mutation, a homozygous mutant of *VID24* could generate higher level of malate than the heterozygous mutant of *VID24* on the assumption that *VID24-391A* mutation is semidominant.

In this study, the author identified *VID24* as the gene responsible for the high acidity phenotype in industrial sake yeast. Many researchers have exploited methods for breeding high-malate-producing yeasts (6, 9-12, 25, 45). This results provide a useful indication to control the ability of malate production in yeasts. Because of a pleasant taste of malate in sake (8), the regulation of malate level would improve the quality of sake possessing a characteristic taste.

SUMMARY

The author determined the mutated gene involved in high malate production in yeast, isolated as a sensitive mutant to DMS. In the comparative whole genome analysis between high-malate-producing strain and its parent strain, one of the non-synonymous substitutions was identified in the *VID24* gene. The mutation of *VID24* resulted in enhancement of malate-productivity and sensitivity to DMS. The mutation appeared to lead to a deficiency in Vid24 function. Furthermore, disruption of *MDH2* gene in the *VID24* mutant inhibited the high-malate-producing phenotype. Vid24 is known as a component of the multisubunit ubiquitin ligase and participates in the degradation of gluconeogenic enzymes such as Mdh2. The author suggest that the enhancement of malate-productivity results from an accumulation of Mdh2 due to the loss of Vid24 function. These findings propose a novel mechanism for the regulation of organic acid production in yeast cells by the component of ubiquitin ligase, Vid24.

Chapter II

Breeding of high malate-producing diploid sake yeast with a homozygous mutation in the *VID24* gene

The author reported that a point mutation in the *VID 24* gene caused a high acid phenotype in the K-901H sake yeast strain. K-901H is a diploid strain that is a heterozygous carrier of a *VID24* mutation, which is presumed to be semi- or fully dominant. Homozygous genotypes are generally more useful than heterozygous genotypes because homozygous mutants have higher activity than their heterozygous counterparts. For example, the *fatty acid synthase* (*FAS*) *2* mutation causing elevated hexanoic acid levels is semidominant, and higher levels of hexanoic acid were produced by homozygous as compared to heterozygous mutants of *FAS2* (54). If it is assumed that the *VID24* mutation is semidominant, then it is possible that higher levels of malate are generated by homozygous than heterozygous mutants.

Sporulation and mating are widely used in diploid yeast to obtain homozygous mutants. However, such mutants are not readily obtained for diploid sake yeast without genetic modification, since they rarely sporulate (33). The author therefore hypothesized that the loss of heterozygosity (LOH) method based on phenotypic differences between heterozygous and homozygous mutants would be effective for isolating homozygous from heterozygous *VID24* mutants of sake yeast (55).

In the present study, the author generated heterozygous and homozygous integrants of mutated *VID24* (GRI-VID24 and GRI-VID24×2, respectively) by genetic engineering, and compared these in terms of malate productivity. Acid productivity was higher in the homozygous than in the heterozygous integrants. the author then developed a method for selecting a homozygous *VID24* mutant (K-901H×2) from heterozygotes (K-901H) without employing a genetic engineering approach.

MATERIALS AND METHODS

Media and S and yeast strains Yeast cells were cultured aerobically at 30°C in

YPD medium containing 10 g/L yeast extract, 20 g/L polypepton, and 20 g/L glucose; YM10 medium containing 3 g/L yeast extract, 3 g/L malt extract, 5 g/L polypepton, and 100 g/L glucose; or SD - ura medium containing 6.7 g/L yeast nitrogen base without amino acids (YNB w/o AA) (Becton Dickinson and Company, Franklin Lakes, NJ, USA), 20 g/L glucose, and 0.77 g/L complete supplement mixture - ura (MP Biomedicals, Solon, OH, USA).

The following media were used to evaluate DMS sensitivity: DOB medium containing 6.7 g/L YNB w/o AA and 20 g/L glucose; DMS medium containing 6.7 g/L YNB w/o AA, 20 g/L glucose, and 15 g/L DMS; or DMS-2 medium containing 6.7 g/L YNB w/o AA, 20 g/L glucose, and 20 g/L DMS.

The GRI-117-U sake yeast strain (*MAT***a**/*MATα ura3*/*ura3*) was obtained as previously described (55). Uracil auxotrophic yeast strains were selected for growth on 5-fluoroorotic acid (5-FOA) medium containing 6.7 g/L YNB w/o AA, 20 g/L glucose, 1 g/L 5-FOA, and 20 mg/L uracil (34).

The K-901H sake yeast strain was obtained by ethyl methane sulfonate mutagenesis of Kyokai No. 901 (K-901) (Brewing Society of Japan, Tokyo, Japan) as described in Chapter I (Table 2-1).

Table 2-1 Genotypes and references of *S. cerevisiae* strains used in this study

Strain	Genotype	Reference
K-901	*MAT***a**/*MATα*	Brewing Society of Japan
K-901H	*MAT***a**/*MATα VID24* 391G>A/*VID24*	Chapter I
K-901H×2	*MAT***a**/*MATα VID24* 391G>A/*VID24* 391G>A	This study
GRI-117-U	*MAT***a**/*MATα ura3*/*ura3*	(55)
GRI-VID24-U	*MAT***a**/*MATα ura3*/*ura3 VID24* 391G>A/*VID24*	This study
GRI-VID24×2-U	*MAT***a**/*MATα ura3*/*ura3 VID24* 391G>A/*VID24* 391G>A	This study
GRI-117	*MAT***a**/*MATα URA3*/*ura3*	This study
GRI-VID24	*MAT***a**/*MATα URA3*/*ura3 VID24* 391G>A/*VID24*	This study
GRI-VID24×2	*MAT***a**/*MATα URA3*/*ura3 VID24* 391G>A/*VID24* 391G>A	This study

Table 2-2 Primers used in this study

Primer name	Primer sequence (5'-3')
VID24(102)XbaI-F	CCCTGTTTCTAGAAATCAGTATCCGAT
VID24(787)HindIII-R	TTGGTGTAGTAGGAAGCTTCTGTGGAG
URA3-F	ATGTCGAAAGCTACATATAAGGAACGTGCT
URA3-R	TTAGTTTTGCTGGCCGCATCTTCTCAAATA

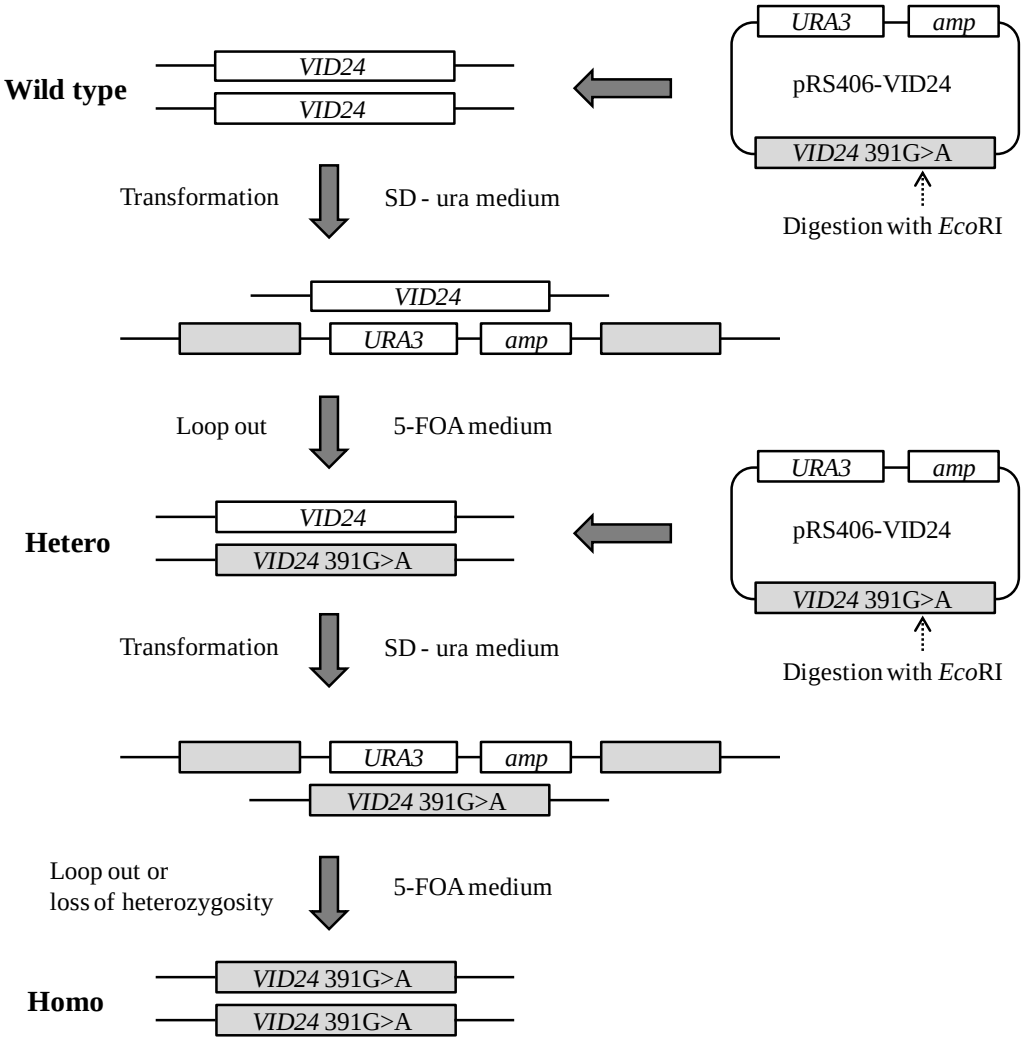

Fig. 2-1 Strategy for construction of homozygous *VID24* mutants by genetic engineering.

Construction of heterozygous and homozygous point mutants The *VID24* 391G>A mutation (Gly131Arg) was introduced in homozygous form into GRI-117-U using a two-step gene replacement method (Fig. 2-1) (37). The author first isolated a heterozygous integrant (GRI-VID24-U). Using primers VID24(102)XbaI-F and VID24(787)HindIII-R (Table 2-2) with K-901H chromosomal DNA as the template, DNA fragments corresponding to the mutated *VID24* regions of K-901H were amplified by PCR, digested with *Xba*I and *Hin*dIII, and cloned into the pRS406 vector (Stratagene, La Jolla, CA, USA). The pRS406-VID24 plasmid containing *URA3* and mutated *VID24*

was digested with *Eco*RI, and the fragment was used to transform GRI-117-U. Yeast transformations were performed by the lithium acetate method (36). Transformants were obtained by selection on SD - ura medium and then cultured in YPD for 24 h before plating onto 5-FOA medium. Colonies resulting from the loss of extraneous *URA3*-containing sequences were selected as candidate heterozygous *VID24* integrants (GRI-VID24-U). *VID24* genotypes of individual clones were verified by DNA sequencing. GRI-VID24×2-U homozygous integrants were selected by the same procedure to obtain GRI-VID24-U. The digested fragment from pRS406-VID24 was used to transform GRI-VID24-U. A transformant with a mutated *VID24* open reading frame integrated into the genome was obtained by selection on SD - ura medium, and candidate homozygous integrants (GRI-VID24×2-U) were isolated with 5-FOA medium. *VID24* genotypes were confirmed by DNA sequencing. Finally, DNA fragments containing *URA3* amplified from K-901 using the primers listed in Table 2-2 were transferred into GRI-117-U, GRI-VID24-U, and GRI-VID24×2-U to complement uracil auxotrophy, yielding GRI-117, GRI-VID24, and GRI-VID24×2, respectively (Table 2-1).

Comparison of growth in DMS medium Growth in DMS medium was evaluated as described in Chapter I. Cells were resuspended in DOB or DMS medium to an optical density of 0.01 at 660 nm.

One-step sake brewing test The sake brewing test and analysis of the supernatant from the sake mash were carried out as described in Chapter I.

Small-scale cultivation test for evaluation of malate production Yeast cells were statically cultured in 0.2 ml of YM10 medium at 30°C for 3 days. The culture was centrifuged, and the concentration of malate in the supernatant was measured using the Enzymatic Bio Analysis L-Malic Acid kit (DiaSys Diagnostic Systems GmbH, Holzheim, Germany)

RESULTS

Acid production is higher in homozygous than in heterozygous *VID24* mutants

To evaluate whether the genotype of the *VID24* mutation alters the levels of malate produced, heterozygous and homozygous *VID24* 391G>A integrants were generated. The author introduced the *VID24* mutation into the GRI-117-U strain, and obtained the heterozygous and homozygous integrants GRI-VID24-U and GRI-VID24×2-U, respectively (Fig. 2-1).

A one-step sake brewing test was carried out using GRI-117, GRI-VID24, and GRI-VID24×2. The malate concentration in GRI-VID24×2 was 4.5- and 3.1-fold higher than in GRI-117 and GRI-VID24, respectively (Table 2-3). A high level of malate productivity in GRI-VID24×2 was also observed in YM10 (data not shown). These results suggest that the heterozygous *VID24* mutation is semidominant, but that the homozygous *VID24* mutants generate higher levels of malate.

The ethanol concentration is generally reduced in high malate-producing strains due to increased consumption of available carbon sources for the production of malate (9, 12, 25, 56); however GRI-VID24 generated higher levels of ethanol than GRI-117 (Table 2-3). The *VID24* mutation may cause changes in the ability to assimilate carbon, and lead to high ethanol production.

Table 2-3 Sake brewing tests of GRI-117, GRI-VID24, and GRI-VID24×2

Parameter		Value (mean ± SD)		
		GRI-117	GRI-VID24	GRI-VID24×2
Ethanol (vol %)		16.85 ± 0.12	17.52 ± 0.09	16.35 ± 0.07 [a]
Specific gravity (15°C/4°C)		1.0040 ± 0.0008	0.9991 ± 0.0003	1.0081 ± 0.0004 [b]
Organic acid (mg/l)	Malate	314 ± 20	456 ± 44	1413 ± 84 [b]
	Succinate	326 ± 19	426 ± 40	515 ± 32
	Acetate	102 ± 12	143 ± 9	103 ± 12

The brewing tests were repeated thrice. Plus or minus represents standard deviations.

[a] Significantly lower than GRI-VID24 (*t* test; $P < 0.01$)

[b] Significantly higher than GRI-VID24 (*t* test; $P < 0.01$)

Homozygous *VID24* integrants increased DMS sensitivity The *VID24* 391G>A mutation in haploid yeast strains reduces tolerance to DMS. To determine whether the genotype of the *VID24* mutation plays a role in sensitivity to DMS in yeast, the growth characteristics of GRI-117, GRI-VID24, and GRI-VID24×2 strains grown in DOB or DMS medium were compared. Cell density measurements revealed a slight delay in the onset of the logarithmic phase in GRI-VID24 as compared to GRI-117 in DMS medium. In addition, GRI-VID24×2 took longer to reach a maximum specific growth rate than GRI-VID24 in DMS medium (Fig. 2-2). These results indicate that sensitivity to DMS is regulated by the genotype of the *VID24* mutation.

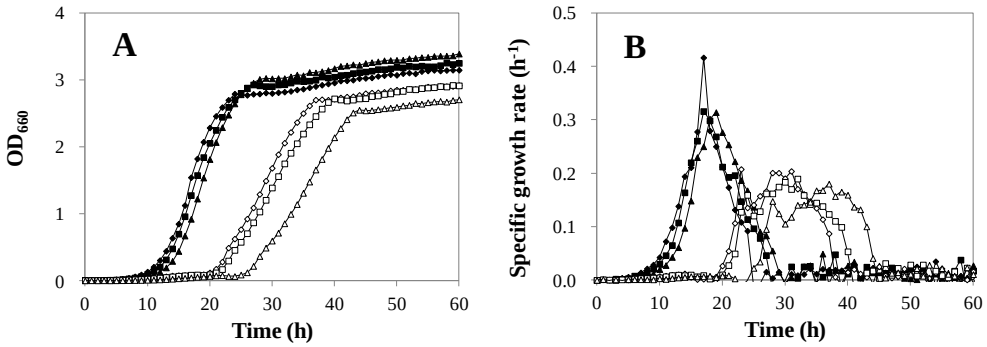

Fig. 2-2 Growth rates of mutated *VID24* integrants derived from GRI-117-U in medium containing DMS. (A) Growth curves and (B) specific growth rates of GRI-117, GRI-VID24, and GRI-VID24×2 in DOB or DMS medium. Plots represent mean values of four independent cultures.

Symbols: closed diamonds, GRI-117 in DOB; closed squares, GRI-VID24 in DOB; closed triangles, GRI-VID24×2 in DOB; open diamonds, GRI-117 in DMS; open squares, GRI-VID24 in DMS; open triangles, GRI-VID24×2 in DMS.

A homozygous *VID24* mutant was isolated from K-901H without genetic modification The author took advantage of the greater DMS sensitivity of the homozygous as compared to the heterozygous *VID24* mutant to select a homozygous *VID24* mutant without genetic modification. The author first examined whether the survival rate for heterozygous and homozygous *VID24* integrants differed under nystatin

enrichment in DMS medium (22). GRI-VID24 and GRI-VID24×2 were cultured in YPD medium for 24 h, and harvested by centrifugation. Cells were resuspended in DMS medium to an optical density of 0.1 at 660 nm. After culturing for 18 h, cells were cultured for 2 in 5 mg/L nystatin with shaking before they were harvested and resuspended in water. Approximately 5×10^5 cells (including dead cells) were spread onto a YPD plate and incubated at 30°C for 30 h. Compared to control cells that were not exposed to nystatin, the survival rates of GRI-VID24 and GRI-VID24×2 cells were 0.0029% and 0.0084%, respectively. These data demonstrate that nystatin enrichment of DMS medium allowed homozygous mutants of *VID24* to be concentrated more efficiently by a factor of 2.9.

The author isolated homozygous *VID24* mutants from K-901H cells carrying a heterozygous mutation. K-901H were cultured in YPD medium for 24 h, harvested by centrifugation, and resuspended in water. Cells were exposed to ultraviolet irradiation to induce LOH (57-59), and then resuspended in DMS medium to an optical density of 0.1 at 660 nm. After culturing, cells were exposed to nystatin as described above and spread onto a YPD plate. Homozygous *VID24* mutants generated from K-901H were expected to survive in the presence of nystatin owing to a delay in the onset of the logarithmic phase. About 100 colonies appeared on each YPD plate, and a total of 921 colonies were replicated on DMS-2 plates. Of these, 61 colonies that grew more slowly than K-901H or did not grow on DMS-2 were selected as candidate homozygous *VID24* mutants. Of the 61 colonies, three produced >1.5 times more malate than the parental K-901H strain in a small-scale cultivation test in YM10 (Fig. 2-3). The *VID24* genotype of individual colonies was determined by DNA sequencing; one identified clone was homozygous for the *VID24* mutation (K-901H×2), and the others were heterozygous mutants.

Sake brewing and DMS sensitivity tests were carried out with the homozygous *VID24* mutant isolated from K-901H A one-step sake brewing test was carried out using K-901, K-901H, and K-901H×2. The concentration of ethanol was around 16%-17% for each strain. Malate concentration was 3.7- and 1.7-fold higher in K-901H×2 than in K-901 and K-901H, respectively (Table 2-4). In addition, cell density measurements

revealed a delay in the onset of the logarithmic phase in K-901H×2 as compared to K-901H in DMS medium (Fig. 2-4).

Of the three colonies exhibiting high malate productivity in the small-scale cultivation test, heterozygous *VID24* mutants exhibited lower malate levels than K-901H×2 in the sake brewing test (data not shown). Since the initial cell densities were not uniform in the cultivation test, it was presumed that the growth phases of these strains differed.

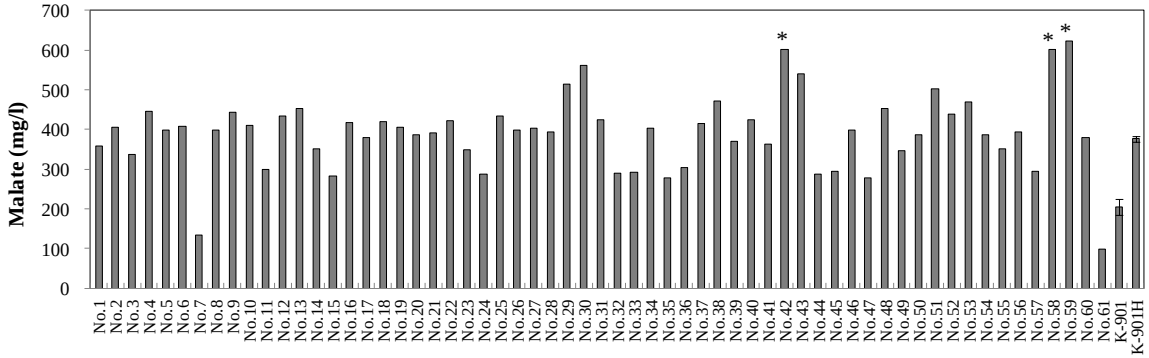

Fig. 2-3 Malate production in the K-901H parental strain and DMS-sensitive strains in a small-scale cultivation test. The test was repeated twice for K-901 and K901H; error bars represent standard deviations. Asterisks denote strains that exhibited > 1.5 times the amount of malate in strain K-901H. Of the 61 strains, no.59 was identical to K-901H×2.

Table 2-4 Sake brewing tests of K-901, K-901H, and K-901H×2

Parameter		Value (mean ± SD)		
		K-901	K-901H	K-901H×2
Ethanol (vol %)		17.04 ± 0.07	15.82 ± 0.09	16.68 ± 0.12 [b]
Specific gravity (15°C/4°C)		1.0027 ± 0.0001	1.0115 ± 0.0008	1.0050 ± 0.0007 [a]
Organic acid (mg/l)	Malate	383 ± 4	558 ± 20	1574 ± 38 [b]
	Succinate	355 ± 3	407 ± 13	547 ± 23 [b]
	Acetate	591 ± 7	582 ± 34	371 ± 16 [a]

The brewing tests were repeated thrice. Plus or minus represents standard deviations.

[a] Significantly lower than K-901H (*t* test; $P < 0.01$)

[b] Significantly higher than K-901H (*t* test; $P < 0.01$)

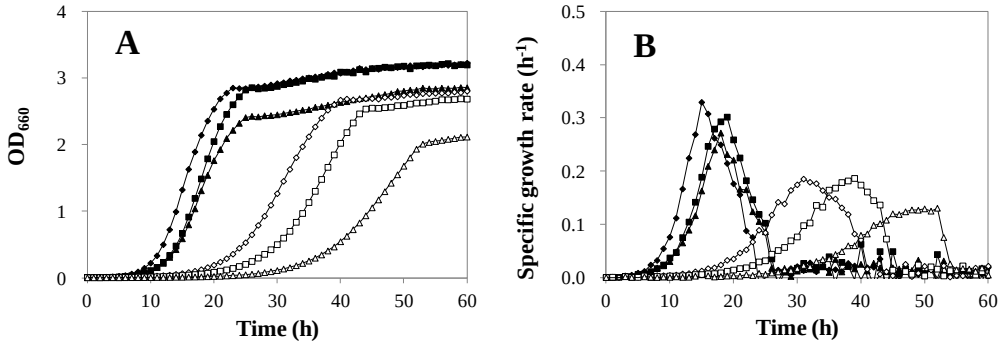

Fig. 2-4 Growth rates of *VID24* mutants of sake yeast in medium containing DMS. (A) Growth curves and (B) specific growth rates of K-901, K-901H, and K-901H×2 in DOB or DMS medium. Plots represent mean values of four independent cultures.

Symbols: closed diamonds, K-901 in DOB; closed squares, K-901H in DOB; closed triangles, K-901H×2 in DOB; open diamonds, K-901 in DMS; open squares, K-901H in DMS; open triangles, K-901H×2 in DMS.

DISCUSSION

The *VID24* 391G>A mutation enhances malate production and reduces DMS tolerance in *S. cerevisiae*. This mutation appears to induce loss of Vid24p function. Vid24 is a component of the glucose-induced-degradation-deficient (GID) complex that stimulates the catabolic degradation of gluconeogenic enzymes (17, 20, 21). *VID24* deletion reduced the function of the GID complex, resulting in intracellular accumulation of Mdh2 (16). These findings indicate that abnormal accumulation of Mdh2 enhances the reduction of oxaloacetate to malate in the cytosol. In the present study, the homozygous *VID24* mutant K-901H×2 generated higher levels of malate than the heterozygous mutant K-901H, suggesting that the mutation is semidominant in diploid yeast. The amount of succinate increased concurrently with malate concentration in the homozygous mutant, which was attributed to the conversion of mitochondrial malate translocated from the cytosol to succinate through the tricarboxylic acid cycle. In contrast, the amount of acetate was decreased in the homozygous mutant, which was presumed to result from changes in

the ratio of oxaloacetate to acetate converted from pyruvate. Alterations in organic acid composition have been observed in another strain carrying the *VID24* mutation in Chapter I. Mdh2 was predicted to accumulate to a greater extent in homozygous as compared to heterozygous mutant cells based on the assumption that the heterozygote retained some functional Vid24 molecules in which the normal GID complex degraded Mdh2 to some extent, whereas the homozygote had only dysfunctional Vid24. The GID complex is involved in the degradation of gluconeogenic enzymes such as Fbp1, Pck1, and Icl1 (16, 17, 60), which would tend to accumulate in the homozygous *VID24* mutant in addition to Mdh2. It is possible that these mutants differ in terms of growth on non-fermentable carbon sources.

Many high malate-producing strains have been isolated from mutagenized sake yeast (9, 11, 12, 25, 56). These methods depend on incidental mutations and selection markers such as DMS, cycloheximide, or maltose-assimilation ability (9, 12, 56). The author identified *VID24* as a candidate gene responsible for high malate productivity in a DMS sensitive mutant in Chapter I. The present study demonstrated that the genotype of the *VID24* mutation influenced the level of malate production in diploid yeasts, which were amenable to selection of a high malate-producing yeast strain.

The rate of spontaneous LOH in yeast is around 10^{-5} to 10^{-4} (55, 61). On the other hand, the frequency of *VID24* homozygous mutation based on LOH was approximately 1×10^{-3} (1/921) using the method developed in this study. Thus, the method was 10- to 100-fold more effective for generating *VID24* homozygous mutants. The increase in efficiency was likely due to ultraviolet irradiation and nystatin enrichment in DMS medium, which exploited the difference in DMS sensitivity between homo- and heterozygous mutants of *VID24*. Nystatin enrichment was estimated to increase the number of homozygous mutants by 2.9-fold. Furthermore, this method involving comparisons of growth on DMS-2 and small-scale cultivation tests is suitable for high-throughput screening.

The features of the high malate-producing sake yeast (K-901H×2) differed from those of the high malate-producing transformant with *VID24* mutation (GRI-VID24×2) in several respects. For instance, the homozygous *VID24* mutant K-901H×2 showed

higher levels of ethanol than the heterozygous mutant K-901H (Table 2-4). Conversely, GRI-VID24×2 exhibited lower levels of ethanol than GRI-VID24 (Table 2-3). Furthermore, the optical density values in the stationary phase of K-901H×2 were lower than those of K-901H in both DOB and DMS media (Fig. 2-4), which was not the case for GRI-VID24×2 (Fig. 2-2). This is thought to result from as-yet unidentified mutations in the K-901H×2 genome. K-901H×2 is expected to have several mutations relative to K-901H in addition to the *VID24* mutation due to mutagenesis induced by ultraviolet irradiation.

Genetically modified foods and beverages are not always acceptable to the public (19). GRI-VID24×2 had no foreign DNA sequences and should therefore be classified as a self-cloning rather than a genetically modified yeast. To date, one self-cloning sake yeast strain has been approved for industrial sake brewing by the Japanese government (62); however, self-cloning organisms are seldom used in industrial applications in Japan, even though they are not genetic recombinants (63). In addition, constructing a self-cloning homozygous point mutant is time-consuming and laborious. In contrast, the method generated a homozygous *VID24* mutant based on high sensitivity to DMS without genetic modifications. K-901H×2 is not a genetically modified strain and produced more malate than K-901H. Given the pleasant taste of malate in sake (8), these findings will enable the full control of malate content in sake, thereby improving its quality and appeal.

SUMMARY

The author examined the relationship between heterozygous and homozygous mutants of *VID24* and malate productivity in diploid sake yeast and developed a method for breeding a higher malate-producing strain. The author first generated diploid yeast with a homozygous *VID24* mutation by genetic engineering. The homozygous integrants produced more malate during sake brewing and grew more slowly in DMS medium than wild-type and heterozygous integrants. Thus, the genotype of the *VID24* mutation influenced the level of malate production and sensitivity to DMS in diploid yeast. The author then obtained a homozygous from a heterozygous mutant without genetic

engineering, by ultraviolet irradiation and culturing in DMS with nystatin enrichment. The non-genetically modified sake yeast with a homozygous *VID24* mutation exhibited a higher level of malate productivity than the parent heterozygous mutant strain. These findings provide a basis for controlling malate production in yeast, and thereby regulating malate levels in sake.

Chapter III

Effects of mutations of GID protein-coding genes on malate production and enzyme expression profiles in *Saccharomyces cerevisiae*

The author isolated a high malate-producing strain based on its sensitivity towards dimethyl succinate without genetic modifications as described in Chapter I. A missense mutation in the *VID24* (alias *GID4*) gene of this strain was found to be responsible for the high malate phenotype. The mutation *VID24* 391 G>A was considered to lead to deficiency in Vid24 function since the mutant strain exhibited phenotypes similar to the *vid24* disruptant.

In yeast, Vid24 is a component of GID complex, a multisubunit E3 ubiquitin ligase that consists of seven proteins (Vid30/Gid30, Rmd5/Gid2, Vid24/Gid4, Vid28/Gid5, Gid7, Gid8, Fyv10/Gid9) (17, 20-22). The GID complex specifically degrades gluconeogenic enzymes, such as Fbp1, Icl1, Mdh2, and Pck1, in the presence of glucose with the E2 conjugating enzyme, Ubc8/Gid3 (16, 17). The disruption of GID protein-coding genes induces the accumulation of these gluconeogenic enzymes in yeast cells. Recently, it was demonstrated that Vid24 is a recognition protein that recognizes the gluconeogenic enzymes by their proline residue at position 1 or 2 of the N-terminus (18). Furthermore, the gene expression and protein stability of Vid24 were found to be tightly regulated by the presence of glucose to control proper function of the GID E3 ubiquitin ligase (64). Although previous study in Chapter I suggested that Mdh2 is involved in the high malate production observed in *VID24* mutants, the precise mechanism for this phenotype remains unclear. Furthermore, it is not known whether the component proteins of the GID complex, except for Vid24, participate in the production of metabolites, such as organic acids, during fermentation. It is possible that the deletion of GID protein-coding genes also causes an increase in malate production, as well as *vid24* disruption.

In this study, the author investigated the mechanism for the increased malate production of the *gid4* disruptant. Additionally, the author examined whether the deletion of GID protein alters the productivity of organic acids. Target proteome analysis was performed to evaluate the central carbon metabolism in yeast cells, as well as the organic

acid production. These results indicate that the accumulation of Mdh2 contributes to a high malate production in the disruptant of *vid24*, and that not only Vid24, but the component proteins of the GID complex, were involved in organic acid production, simultaneously changing the profiles of numerous proteins involved in glycolysis and ethanol fermentation.

Table 3-1 Genotypes and references of *S. cerevisiae* strains used in this study

Strain	Genotype	Reference
BY4743	*MAT***a**/*MATα his3Δ1/his3Δ1 leu2Δ0/leu2Δ0 LYS2/lys2Δ0 met15Δ0/MET15 ura3Δ0/ura3Δ0*	Thermo Fisher Scientific Inc.
BY4743 *vid30*Δ	BY4743 *vid30*::*kanMX4*/*vid30*::*kanMX4*	Thermo Fisher Scientific Inc.
BY4743 *rmd5*Δ	BY4743 *rmd5*::*kanMX4*/*rmd5*::*kanMX4*	Thermo Fisher Scientific Inc.
BY4743 *ubc8*Δ	BY4743 *ubc8*::*kanMX4*/*ubc8*::*kanMX4*	Thermo Fisher Scientific Inc.
BY4743 *vid24*Δ	BY4743 *vid24*::*kanMX4*/*vid24*::*kanMX4*	Thermo Fisher Scientific Inc.
BY4743 *vid28*Δ	BY4743 *vid28*::*kanMX4*/*vid28*::*kanMX4*	Thermo Fisher Scientific Inc.
BY4743 *ubp14*Δ	BY4743 *ubp14*::*kanMX4*/*ubp14*::*kanMX4*	Thermo Fisher Scientific Inc.
BY4743 *gid7*Δ	BY4743 *gid7*::*kanMX4*/*gid7*::*kanMX4*	Thermo Fisher Scientific Inc.
BY4743 *gid8*Δ	BY4743 *gid8*::*kanMX4*/*gid8*::*kanMX4*	Thermo Fisher Scientific Inc.
BY4743 *fyv10*Δ	BY4743 *fyv10*::*kanMX4*/*fyv10*::*kanMX4*	Thermo Fisher Scientific Inc.
GX-11	*MAT***a** *ura3*	Chapter I
GX-11 *fbp1*Δ	GX-11 *fbp1*::*kanMX4*	Chapter I
GX-11 *icl1*Δ	GX-11 *icl1*::*kanMX4*	This study
GX-11 *mdh2*Δ	GX-11 *mdh2*::*kanMX4*	Chapter I
GX-11 *pck1*Δ	GX-11 *pck1*::*kanMX4*	Chapter I
GX-VID24	GX-11 *VID24* 391G>A	Chapter I
GX-VID24 *fbp1*Δ	GX-VID24 *fbp1*::*kanMX4*	Chapter I
GX-VID24 *icl1*Δ	GX-VID24 *icl1*::*kanMX4*	This study
GX-VID24 *mdh2*Δ	GX-VID24 *mdh2*::*kanMX4*	Chapter I
GX-VID24 *pck1*Δ	GX-VID24 *pck1*::*kanMX4*	Chapter I
GX-mMDH2	GX-11 *MDH2* 4C>T	This study
GX-VID24-mMDH2	GX-VID24 *MDH2* 4C>T	This study

MATERIALS AND METHODS

Media and yeast strains Yeast cells were cultured in yeast extract peptone dextrose (YPD) medium [yeast extract (10 g/L), polypeptone (20 g/L), and glucose (20 g/L)], yeast malt (YM) medium [YM10; yeast extract (3 g/L), malt extract (3 g/L), polypeptone (5 g/L), and glucose (100 g/L)], synthetic defined medium lacking uracil [SD –ura; yeast nitrogen base without amino acids (YNB w/o amino acids (AA).7 g/L; Becton Dickinson and Company, Franklin Lakes, NJ, USA), complete supplement mixture –ura (0.77 g/L; MP Biomedicals, Solon, OH, USA) and glucose (20 g/L)], or 5-fluoroorotic acid (5-FOA) medium [5-FOA (1 g/L), uracil (20 mg/L), YNB w/o AA (6.7 g/L), and glucose (20 g/L)].

For the preparation of the isotope-labeled standards of the S288C strain, ^{15}N-Dropout Base (DOB) medium [^{15}N –DOB; ^{15}N ammonium sulfate (5 g/L; Cambridge Isotope Laboratories, Andover, MA, USA), yeast nitrogen base without amino acids and ammonium sulfate (YNB w/o AA and AS, 1.7 g/L; Becton Dickinson and Company, Franklin Lakes, NJ, USA), and glucose (20 g/L)] was used for preculture. ^{15}N-YNB-ethanol medium [^{15}N ammonium sulfate (5 g/L), YNB w/o AA and AS (1.7 g/L) and ethanol (20 g/L)] was used for the main culture.

The *MAT***a** uracil auxotroph strain GX-11 and the *VID24* 391G>A mutant GX-VID24 were obtained as described in Chapter I. The disruption of the *FBP1*, *ICL1*, *MDH2*, *PCK1*, or *CIT2* genes in GX-11 and GX-VID24 was performed using a PCR-based method with the primers listed in Table 3-2 in combination with a *kanMX4* module-carrying plasmid (35), and PrimeSTAR Max DNA Polymerase (Takara Bio Inc., Otsu, Japan). Yeast transformants were obtained using the lithium acetate method (36). The disruptants used are listed in Table 3-1.

The disruptants derived from the strain BY4743 (ATCC 4040005) were obtained from the Yeast Knock Out Homozygous Diploid Collection (YSC1056; Thermo Fisher Scientific Inc., Waltham, MA, USA) (Table 3-1).

Table 3-2 Primers used in this study

Primer name	Primer sequence (5'-3')
ICL1-KanMX4-F	CTAACAATTGAGAGAAAACTCTTAGCATAACATAACA AAAAGTCAACGAAAACGTACGCTGCAGGTCGACGG
ICL1-KanMX4-R-3	CTATTTCTTTACGCCATTTTCTTTGAATTGATCTTCTGT GACACCGGTTCTTAGAAAAACTCATCGAGCA
MDH2(-794)InFusion-F	CTATAGGGCGAATTGCTTTCTTTTTCACTATTGCTCGA ACCGCCTGCGATGAGCTAAG
MDH2(29)C4T-R	CTATGGATGGTGTAACTGAGTGAGACATG
MDH2(-21)C4T-F	TATCATAAAAGTTATAGTAACATGTCTCAC
MDH2(727)InFusion-R	AGGGAACAAAAGCTGGTATTAAATATTTCAATTTGTCC TCATTTAATCTCGATAGGAAGTTTGACTGTG
pRS406_InFusion-F	CAGCTTTTGTTCCCTTTAGTGAGGG
pRS406_InFusion-R	CAATTCGCCCTATAGTGAGTCGTATTAC

Construction of the *MDH2* point mutants, GX-mMDH2, and GX-VID24-mMDH2 The *MDH2* 4C>T mutation was introduced in GX-11 and GX-VID24 using a two-step gene replacement method (37). The plasmid pRS406-mMDH2 was constructed using an In-Fusion HD Cloning Kit (Takara Bio Inc., Otsu, Japan) with pRS406 and the mutated *MDH2* fragments. The pRS406 fragment was amplified from the pRS406 plasmid (Stratagene, La Jolla, CA, USA) using the pRS406_InFusion-F and pRS406_InFusion-R primers (Table 3-2). The mutated *MDH2* fragment was obtained by performing fusion PCR with mMDH2-1 and mMDH2-2 fragments. The mMDH2-1 fragment was amplified using the primers MDH2(-794)InFusion-F and MDH2(29)C4T-R and using the GX-11 genomic DNA as the template. The mMDH2-2 fragment was amplified using the primers MDH2(-21)C4T-F and MDH2(727)InFusion-R and the GX-11 genomic DNA as the template (Table 3-2). After the plasmid pRS406-mMDH2 (containing *URA3* and mutated *MDH2*) was digested with *Xba*I (the open reading frame (ORF) of *MDH2*, containing the *Xba*I restriction enzyme site endogenously), the linearized DNA was used to transform GX-11 and GX-VID24. The transformants were selected by growing the cells on SD –ura medium. Next, they were cultivated in YPD

medium for 24 h and plated onto 5-FOA medium. The colonies appearing on the 5-FOA medium, resulting from the loss of extraneous plasmid sequences containing *URA3*, were selected as the *MDH2* 4C>T mutant progeny, namely GX-mMDH2 and GX-VID24-mMDH2, respectively. The genotype of the *MDH2* clones was determined by DNA sequencing.

YM10 cultivation test Yeast cells were cultivated aerobically in YPD medium at 30°C for 24 h and harvested by centrifugation (5000 × *g*, 5 min, 4°C). The cells were resuspended in YM10 medium to an optical density at 600 nm (OD_{600}) of 0.1. The culture was incubated at 30°C without shaking. Cell density at OD_{600} was determined using a UV spectrometer (UV-2550; Shimadzu Co., Ltd., Kyoto, Japan). Cell viability in the culture was measured using an automated cell counter (Cellometer X2; Nexcelom Bioscience, Lawrence, MA, USA). The amount of organic acids in the supernatant was measured using a high-performance liquid chromatography (HPLC)-based Organic Acid Analysis System (Shimadzu Co., Ltd., Kyoto, Japan). The glucose concentration was measured using a glucose measuring instrument, GA-1103 (Arkray Co., Ltd., Kyoto, Japan). The ethanol concentration was measured using an alcohol measuring instrument, AL-3 (Riken Keiki Co., Ltd., Tokyo, Japan).

Target proteome analysis Crude proteins were extracted from *S. cerevisiae* cells as previously described (65-67). The YM10 cultivation test was followed by the centrifugation of 40 mL of culture at 5000 × *g* at 4 °C for 5 min. The resulting cell pellet was resuspended in 1 mL of lysis buffer, which was then transferred to a 2 mL screwcap tube (Watson Co., Ltd., Tokyo, Japan) containing zirconia beads and crushed using Micro Smash MS-100R (Tomy Medico. Ltd., Tokyo, Japan). Following centrifugation at 20000 × *g* at 4 °C for 5 min, the supernatant was transferred to a low protein adsorption tube (Sumitomo Bakelite Co., Ltd., Tokyo, Japan) to determine the protein concentrations using the Bradford Method (68). Trypsin digestion was performed as described previously (68, 69). To accurately compare the protein levels, the peptide samples were mixed with fully ^{15}N labeled peptide sample from S288C strain cultured in ^{15}N-YNB-

ethanol medium at 30°C for 96 h aerobically. The ^{15}N labeled peptide sample was used as an internal standard, and subsequently employed for all analyses in this study. Equal amounts of digested peptide derived from the target strain cultured using unlabeled nitrogen and S288C cultured in ^{15}N-YNB-ethanol medium were mixed. The peptide mixture was desalted using a stage-tip C18 (70). The desalted peptide samples were analyzed using a nano LC-mass spectrometry (MS) system (LC-20ADnano and LCMS-8060; Shimadzu Co., Ltd., Kyoto, Japan) as previously described (71, 72). The analytical conditions were as follows: HPLC column: L-column ODS (pore size: 5 μm, 0.1 × 150 mm; CERI, Tokyo, Japan); trap column: L-column ODS (pore size: 5 μm, 0.3 × 5 mm; CERI, Tokyo, Japan); solvent system: 0.1% formic acid and 5% acetonitrile in water: 0.1% formic acid and 95% acetonitrile in water; drying gas flow: off; collision induced dissociation gas pressure: 310 kPa; interface voltage: +1.6 keV; detection mode: multiple reaction monitoring (MRM) positive. The gradient program was as follows: 0:100, v/v at 0 min; 0:100 at 7 min; 35:65 at 45 min; 50:50 at 50 min; and 100:0 at 65 min. A flow rate of 400 nL/min was used. MS detection was performed at an interface temperature of 350°C. The desolvation line temperature was 150°C, while the heat block temperature was 200°C. The data were recorded using LabSolutions LCMS (version 5.6) (Shimadzu Co., Ltd., Kyoto, Japan). An MRM assay for 56 proteins responsible for glycolysis, TCA cycle, and ethanol production was used, as per previous studies with some modifications (65, 72). Several target peptides for gluconeogenic enzymes have been changed (Table 3-3).

Data analysis The chromatographic data was processed using Skyline (version 4.1) (73, 74). The relative peak areas were determined for all peptides using the ^{15}N-labeled peptides as the internal standards.

Principal component analysis (PCA) and hierarchical clustering analysis were performed using Clustvis (75). The distance value for hierarchical clustering analysis was calculated using the Pearson correlation coefficients of the *z*-scored data for each protein, defined as the correlation subtracted from 1. Hierarchical cluster trees were generated using the average linkage method.

Table 3-3 Target peptides in MRM assay

Protein	Peptide
Ach1	AFANWENFK
	NGQYLGWSGFTGVGTPK
	SQVVSNNPEMIR
Aco1	GYDAGENTYQAPPADR
	TIFTVTPGSEQIR
	TTTDHISMAGPWLK
Aco2	AGSAINYIGNIR
	IPFFVTPGSEQIR
Acs1	ILAGESDQLGDVSTLSNPGIVR
Adh1	ANELLINVK
	ATDGGAHGVINVSVSEAAIEASTR
	SIGGEVFIDFTK
	VVGLSTLPEIYEK
Adh2	ANGTVVLVGLPAGAK
Adh3	GVIFYENK
	SEVFSHVVK
Adh6	AMGAETYVISR
	IWVETLPVGEAGVHEAFER
Ald3	ESGDTGVDNYLQIK
	GYFIPPTIFTDVPETSK
	QDLAQIIELTR
Ald4	AFSNGSWNGIDPIDR
	GDVDLVINYLK
	IAPALVTGNTVVLK
	TAESTPLSALYVSK
	VAFTGSTATGR
Ald5	ALFNLADLVEK
	AMEDDVDEAVAAAK
Ald6	ANFQGAITNR
	IYVQEGIYDELLAAFK
	SVAVDSSESNLK
	VGIPAGVVNIVPGPGR
Fba1	GAIAAAHYIR
	GISNEGQNASIK
Cit1	AIGVLPQLIIDR
	ANQEVLEWLFK
	LVSTIYEVAPGVLTK
	YLWDTLNAGR
Cit2	AFGILAQLITDR
	FSEIYPIHAQDVR
	NVASYLQSNSSQEK
Sdh1	DVAAPVTLK
	TIIATGGYGR
Sdh2	DLVPDLTNFYQQYK
Sdh3	AAIAEEQILNK
Sdh4	LETENDGVVGLVK
Lpd1	LVIDDQFNSK
	RPYIAGLGAEK
Eno1	NVNDVIAPAFVK
	TAGIQIVADDLTVTNPK
	AVDDFLISLDGTANK
Eno2	AAQDSFAANWGVMVSHR
	AVDDFLLSLDGTANK
	TAGIQIVADDLTVTNPAR
Fbp1	DSTEGFDTDIITLPR
	SSIWLGSSGEIDK
	LLPDSSGTINDVLR
	NATGDFTLVLNALQFAFK
	AELVNLVGLAGASNFTGDQQK
Fum1	AIQQAADEVASGK
	LITDAAYSFR
	SAAIVNESLGGLDPK
Tdh1	LISWYDNEYGYSAR
	VVDLIEYVAK
	VVITAPSSSAPMFVVGVNHTK
	IDVAVDSTGVFK
Tdh2	IATFQER
	HIIVDGHK
Tdh3	DPANLPWGSSNVDIAIDSTGVFK
Gpm1	AIQTANIALEK
	SFDVPPPPIDASSPFSQK
	VYPDVLYTSK
Gcy1	AVGVSNFSINNLK

Protein	Peptide
Hxk1	ESGNYLAIDLGGTNLR
	IEDDPFENLEDTDDIFQK
	LVLLELNEK
Glk1	GVLLAADLGGTNFR
	HALALSPLGAEGER
	LGFTFSYPVDQTSLNSGTLIR
Idh1	DIGGSSSTTDFTNEIINK
	DYAVFEPGSR
Idh2	LADGLFVNVAK
	YTVSFIEGDGIGPEISK
Idp1	FANILESATLNTVQQDGIMTK
	SAYVTTEEFLDAVEK
Idp2	ATDVIVPEEGELR
Idp3	GEETSTNSIASIFAWTR
	LDNTDDVIK
Pfk1	AVLEFTPETPSPLIGILENK
Pfk2	AIDYVEATANSHSR
	GWSAEGGTNIGTAR
	NAVSTKPTPPPAPEASAESGLSSK
	SEWPSLIEELLK
Cdc19	EPVSDWTDDVEAR
	GVNLPGTDVDLPALSEK
	IENQQGVNNFDEILK
	TNNPETLVALR
Mls1	NQIDFDTPR
	STEITGPPLR
Mdh2	EINIESGLTPR
	GVSYVDYDIVNR
	VNSMPDVPVIGGHSGETIIPLFSQSNFLSR
Mdh1	FISEVENTDPTQER
	GVATDLSHIPTNSVVK
	SEGIEFFASPVTLGPDGIEK
	VTVLGAGGGIGQPLSLLLK
Mdh3	EEQLVNTAVK
	LSPYVSELALYDIR
	AQQLVGDNSIEYFSLPIVLR
Kgd1	FGLEGLESVVPGIK
	YVNLSLVANPSHLESQDPVVLGR
Kdg2	AQEPPVASNSFTPFPR
	NAESLSVLDIENEIVR
Pdb1	VTGADVPTPYAK
	YGVSAEVINLR
Pdc1	AQYNEIQGWDHLSLLPTFGAK
	LLTTIADAAK
	TPANAAVPASTPLK
	YGGVYVGTLSKPEVK
Pdc6	WAGNANELNAAYAADGYAR
	WGLKPYLFVLNNDGYTIEK
Pgk1	ASAPGSVILLENLR
	SSAAGNTVIIGGGDTATVAK
	TIVWNGPPGVFEFEK
	VLENTEIGDSIFDK
Pck1	FGSVLENVIYDEK
	GAVTNLANLFVQNFK
	SHVVDYDDSSITENTR
	ATPDVLAAGPQFE
Pyc1	LDGGNAYAGTIISPHYDSMLVK
	ETYGDLSVLPTR
Pgi1	LATELPAWSK
	TFTNYDGSK
	TFTTAETITNANTAK
	VVDPETTLFLIASK
Lsc1	SGTLTYEAVQQTTK
	VIFQGFTGK
Tpi1	ASGAFTGENSVDQIK
	KPQVTVGAQNAYLK
	TFFVGGNFK
Pyc2	VDFIHPGYGFLSENSEFADK
	TIAIYSHEDR
Icl1	EILGHEIFFDWELPR
	LDADAAEIEK
	TDSEAATLISSTIDTR

One-step sake brewing test The sake brewing test was carried out as described in chapter I. The glucose and organic acids in the supernatant of the sake mash were analyzed in the same manner as the YM10 cultivation test. After distilling the supernatant, the ethanol concentration and specific gravity were measured using a Density/Specific Gravity Meter DA-650 (Kyoto Electronics Manufacturing Co. Ltd., Kyoto, Japan).

RESULTS

Participation of *MDH2* in high malate production of *VID24* mutant The *VID24* 391G>A mutant exhibited a high-malate-producing phenotype. Vid24 is required for catabolite degradation of gluconeogenic enzymes, such as Fbp1, Icl1, Mdh2, and Pck1 (16, 18). The gluconeogenic enzymes appeared to affect the production of malate in the *VID24* mutant. To determine the role of gluconeogenic enzymes in malate production, *FBP1*, *ICL1*, *MDH2*, and *PCK1* disruptants were generated in the GX-11 and GX-VID24 strains and evaluated with the YM10 cultivation test (Fig. 3-1). The level of malate production observed in GX-VID24 *mdh2*Δ was lower than that in GX-VID24, while it was almost identical to that observed in GX-11 and GX-11 *mdh2*Δ. The disruption of *MDH2* inhibited high malate production in the *VID24* mutant. This result implied that the loss of Mdh2 degradation mediated by the GID complex in the *VID24* mutant facilitated the conversion of oxaloacetate to malate.

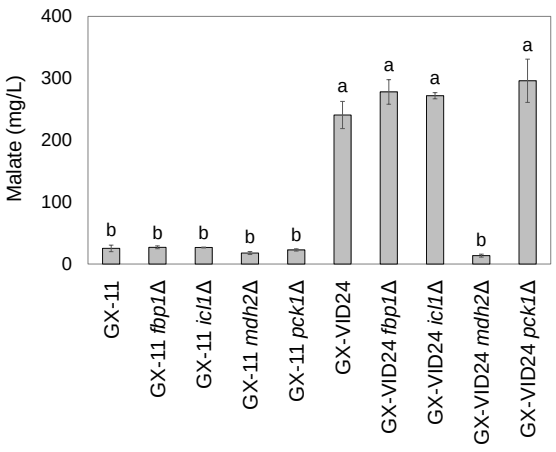

Fig. 3-1 Malate production by the disruptants of gluconeogenic enzyme-coding genes in YM10 cultivation test for four days. All the cultivation tests were repeated in triplicate. Each error bar represents the respective standard deviation. Data were analyzed using the Tukey-Kramer test. The same letters indicate that there was no statistically significant difference among the strains ($p < 0.05$).

The inhibition of Mdh2 degradation by N-terminal mutation is responsible for high malate production Vid24, a subunit of the GID ubiquitin ligase, recognizes the gluconeogenic enzymes by their proline residue at position 1 or 2 of the N-terminus, which is followed by the polyubiquitination and degradation of gluconeogenic enzymes by the GID complex (18, 76). Thus, the degradation of gluconeogenic enzymes requires N-terminal proline. The N-terminal proline residues substituted by other amino acids inhibit this degradation, resulting in the subcellular accumulation of mutated gluconeogenic enzymes (18). To determine whether the loss of Mdh2 degradation in *VID24* mutants leads to high malate production, Mdh2 mutants (substitution of proline at residue 2 with serine) were generated in the GX-11 and GX-VID24 strains, which were subsequently evaluated using the YM10 cultivation test (Fig. 3-2). The amount of malate produced by the Mdh2 P2S mutant (GX-mMDH2) was higher than that produced by the parent strain (GX-11), while it was equal to that produced by the Vid24 G131R mutant (GX-VID24). These results support the above-mentioned hypothesis.

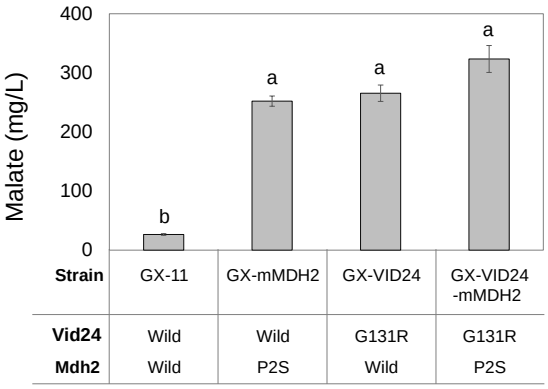

Fig. 3-2 Malate production by mutants of Mdh2 and/or Vid24 in YM10 cultivation test for four days. All the cultivation tests were repeated in triplicate. Each error bar represents the respective standard deviation. Data were analyzed using the Tukey-Kramer test. The same letters indicate that there was no statistically significant difference among the strains ($p < 0.05$).

Comparison of protein abundance profiles between *vid24* disruptant and its parent strain To determine whether intracellular Mdh2 protein accumulates in *VID24* mutants, the level of Mdh2 was measured directly. Since an increased in malate could affect the regulation of the central metabolism due to the change in intracellular pH, the levels of several proteins of the central metabolism, as well as Mdh2, were quantitated using target proteome analysis. Target proteome analysis is used to determine the levels

of target proteins via MRM assays using LC-MS (65, 67). In this study, MRM assay methods were used for the analysis of 56 proteins associated with glycolysis, the TCA cycle, and ethanol biosynthesis (65, 72).

The homozygous disruptant of *vid24* and its parent strain BY4743 were cultured in YM10. The concentrations of organic acids, glucose, and ethanol in the supernatant at 22, 40, 72, 136, 160, and 188 h were measured (Fig. 3-3). The concentration of ethanol in *vid24*Δ was lower than that in BY4743 only from 40 h to 136 h. The amount of malate, pyruvate, and succinate in *vid24*Δ was higher than that in BY4743. The levels of fumarate and acetate in *vid24*Δ were lower than those in BY4743. Cell viability in *vid24*Δ was lower than that in BY4743 from 136 h to 188 h.

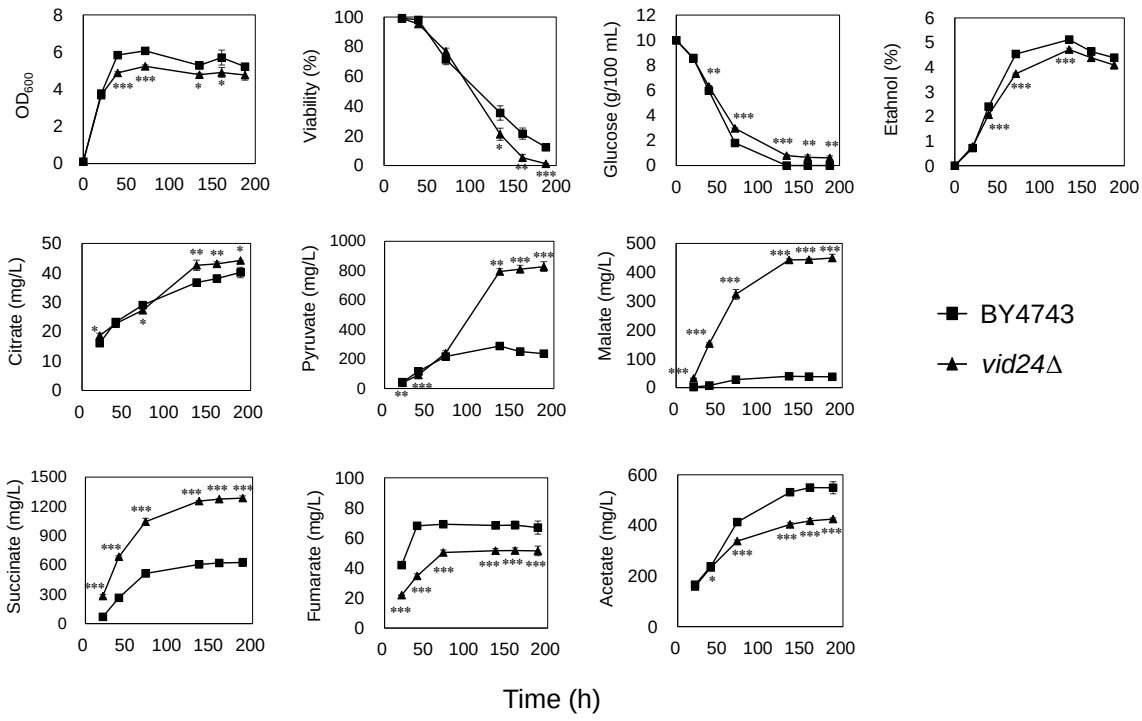

Fig. 3-3 Comparison of glucose, ethanol, and organic acids in the culture supernatants between disruptant of *vid24* and its parent strain in YM10 cultivation test. All the cultivation tests were repeated in triplicate. Each error bar represents the respective standard deviation. The significance of the difference between BY4743 and *vid24*Δ during the same culture period was analyzed using Student's *t*-test ($^{*}p < 0.05$, $^{**}p < 0.01$, $^{***}p < 0.001$)

The crude proteins were extracted from cells collected at 40, 72 136, and 188 h. The digested peptide samples were prepared by trypsin digestion before being subjected to target proteome analysis using the MRM assay methods with nano LC-MS. The MRM assays were used to determine the abundance of peptides derived from 41 proteins (Table 3-4). Fbp1 and Icl1, which were the targets of GID complex-mediated degradation (18), were undetectable in both strains. The relative expression levels of the enzymes in the central carbon metabolism, including glycolysis, the TCA cycle, and ethanol biosynthesis, were compared (Fig. 3-4a). The data showed that *vid24*Δ expressed higher amounts of Mdh2 than BY4743 at 136 and 188 h. Similarly, the amount of Pck1 in *vid24*Δ was higher than that in BY4743 at 188 h. The results indicated that at least some gluconeogenic enzymes, including Mdh2, were accumulated in *vid24*Δ strain, strongly supporting the hypothesis that the inhibition of Mdh2 degradation in *VID24* mutants results in high malate production.

In the *vid24*Δ strain, the expression profiles of some proteins differed from BY4743. For example, the amount of glycolysis enzymes, such as Pgi1, Tpi1, Tdh1, Tdh2, Tdh3, Gpm1, and Eno1, in *vid24*Δ were higher than that in BY4743 at 72 h, but lower at 136 h. To compare the abundance profiles of the 41 proteins, PCA was conducted (Figs. 3-4b, 3-4c). It was indicated that the experimental errors in the protein abundance data were lower than the expressional variations as the triplicate data of each strain, where each cultivation period formed clusters and 75.5% of the total variance was explained by principal components (PC) 1 and 2 (Fig. 3-4b). The score plot showed that PC2 score was different, while PC1 was almost the same between *vid24*Δ and BY4743 when comparing the samples of the same cultivation periods. On the other hand, the PC1 scores at 40 h and 72 h were distinct from those at 136 h and 188 h in both strains. The results suggested that the PC2 score characterized the differences between BY4743 and *vid24*Δ, whereas the PC1 score may reflect a phase of growth. Mdh2 and Pck1 had highly positive loading scores of PC1, which appeared to respond to glucose depletion in the culture medium at 136 and 188 h (Fig. 3-4c). Several enzymes involved in glycolysis (Tpi1, Tdh2, Tdh1, Pgi1, Gpm1, Tdh3, and Eno1) showed highly negative loading scores of PC2, while some enzymes responsible for the TCA cycle (Fum1, Kgd1, Pyc2, Pyc1, and Cit1) showed

highly positive loading scores (Fig. 3-4c). These data suggested that *vid24*Δ differed in the balance of protein expression in glycolysis and the TCA cycle from BY4743.

Table 3-4 The relative expression levels of intracellular proteins of BY4743 and *vid24*Δ in YM10 cultivation test were determined using the ^{15}N-labeled peptides as the internal standards. All cultivation tests were repeated in triplicate.

Protein	Quantification peptide	BY4743 40 h	BY4743 72 h	BY4743 136 h	BY4743 188 h	*vid24*Δ 40 h	*vid24*Δ 72 h	*vid24*Δ 136 h	*vid24*Δ 188 h
Ach1	AFANWENFK	0.03	0.06	0.02	0.01	0.02	0.05	0.00	0.00
Aco1	TIFTVTPGSEQIR	0.30	0.46	0.08	0.03	0.51	0.56	0.00	0.02
Adh1	ANELLINVK	3.06	3.56	0.08	0.27	3.92	3.01	0.09	0.41
Adh3	GVIFYENK	1.88	0.87	0.09	0.20	1.06	0.46	0.09	0.29
Adh6	AMGAETYVISR	1.34	1.73	1.10	0.09	2.73	3.78	0.04	0.07
Ald3	ESGDTGVDNYLQIK	0.27	0.23	0.12	0.00	0.02	0.00	0.00	0.00
Ald4	VAFTGSTATGR	0.09	0.15	0.00	0.02	0.05	0.04	0.00	0.01
Ald5	ALFNLADLVEK	0.23	0.22	0.07	0.02	0.49	0.21	0.01	0.02
Ald6	VGIPAGVVNIVPGPGR	0.16	0.14	0.01	0.01	0.22	0.11	0.00	0.01
Fba1	GISNEGQNASIK	2.05	0.27	0.14	0.49	0.80	0.32	0.16	0.65
Cit1	AIGVLPQLIIDR	0.11	0.07	0.01	0.02	0.06	0.03	0.00	0.01
Lpd1	LVIDDQFNSK	0.56	0.94	0.38	0.15	0.87	1.52	0.05	0.07
Eno1	NVNDVIAPAFVK	2.56	4.30	3.62	0.64	2.32	4.84	0.18	0.30
Eno2	TAGIQIVADDLTVTNPAR	60.89	55.25	2.78	6.65	32.19	10.38	3.25	8.35
Fum1	AIQQAADEVASGK	0.37	0.20	0.00	0.02	0.32	0.01	0.00	0.06
Tdh1	IDVAVDSTGVFK	9.14	21.33	29.25	18.52	5.62	20.29	3.02	1.21
Tdh2	IATFQER	4.53	7.20	10.24	6.37	6.47	12.18	2.11	0.72
Tdh3	DPANLPWGSSNVDIAIDSTGVFK	1.24	1.05	2.02	0.99	1.12	1.82	0.34	0.06
Gpm1	AIQTANIALEK	4.26	7.90	7.28	2.05	6.78	14.53	0.13	0.62
Gcy1	AVGVSNFSINNLK	2.68	2.47	0.05	0.22	2.33	0.77	0.05	0.17
Hxk1	IEDDPFENLEDTDDIFQK	1.77	2.75	0.46	0.10	0.87	1.73	0.06	0.12
Glk1	GVLLAADLGGTNFR	0.97	1.41	0.01	0.06	0.63	1.08	0.01	0.04
Idh1	DYAVFEPGSR	0.34	0.48	0.04	0.04	0.47	0.72	0.01	0.04
Idh2	LADGLFVNVAK	0.26	0.44	0.04	0.02	0.37	0.55	0.00	0.04
Idp1	FANILESATLNTVQQDGIMTK	1.20	2.39	0.25	0.09	2.45	2.46	0.05	0.06
Pfk1	AVLEFTPETPSPLIGILENK	4.58	3.91	0.12	0.12	4.00	3.15	0.03	0.36
Pfk2	GWSAEGGTNIGTAR	3.86	4.53	0.05	0.12	3.83	2.97	0.08	0.34
Cdc19	EPVSDWTDDVEAR	5.40	7.95	2.23	0.28	7.83	13.63	0.05	0.43
Mdh2	EINIESGLTPR	0.03	0.00	0.00	0.00	0.01	0.00	0.04	0.14
Mdh1	FISEVENTDPTQER	0.13	0.25	0.01	0.01	0.15	0.27	0.00	0.01
Kgd1	FGLEGLESVVPGIK	0.18	0.01	0.01	0.03	0.02	0.01	0.01	0.02
Pdb1	VTGADVPTPYAK	2.77	2.60	0.08	0.33	4.96	7.68	0.67	0.82
Pdc1	TPANAAVPASTPLK	1.33	0.67	0.58	0.35	1.25	1.96	0.32	0.26
Pdc6	WAGNANELNAAYAADGYAR	0.89	0.54	0.41	0.29	0.88	1.10	0.23	0.26
Pgk1	VLENTEIGDSIFDK	1.59	1.77	0.04	0.15	1.72	1.51	0.06	0.21
Pck1	FGSVLENVIYDEK	0.00	0.00	0.00	0.00	0.00	0.00	0.00	0.00
Pyc1	ETYGDLSVLPTR	0.11	0.05	0.01	0.00	0.10	0.02	0.02	0.01
Pgi1	VVDPETTLFLIASK	4.02	5.97	10.26	8.38	5.41	6.75	0.65	0.56
Lsc1	VIFQGFTGK	0.27	0.40	0.01	0.03	0.34	0.64	0.00	0.04
Tpi1	ASGAFTGENSVDQIK	6.02	9.94	18.56	11.39	7.70	15.83	12.47	0.87
Pyc2	VDFIHPGYGFLSENSEFADK	0.11	0.03	0.01	0.03	0.03	0.00	0.01	0.06

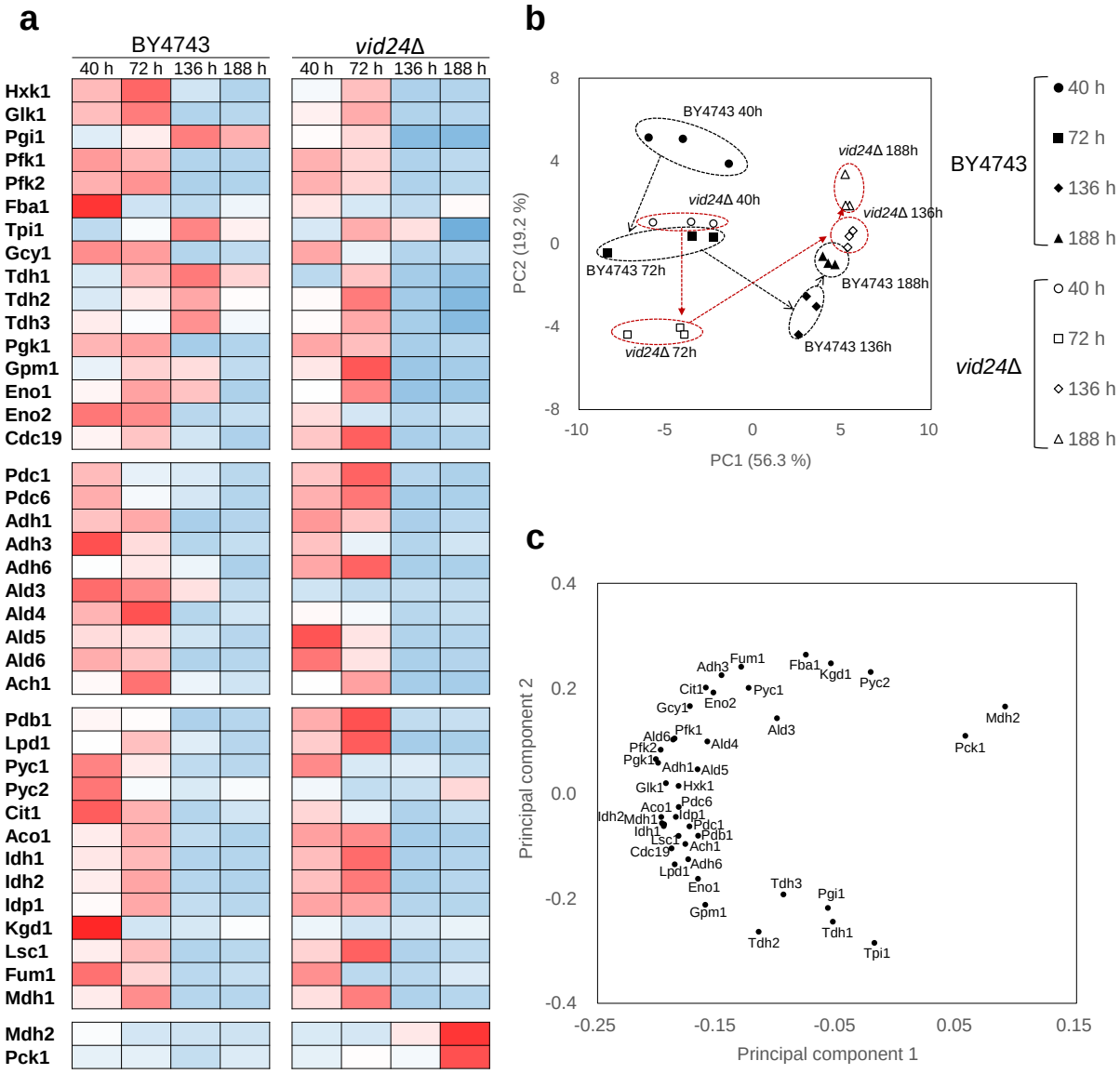

Fig. 3-4 Comparison of the expression levels of intracellular proteins between the disruptant of *vid24* and its parent strain in YM10 cultivation test. The *z*-scored protein abundance data was used for analysis. All cultivation tests were repeated in triplicate. (a) Heat map of the protein expression levels. The *z*-scored protein abundance represent the means of three independent cultivations. (b) Principal component analysis showing the fluctuations of the levels of intracellular protein in yeast. The score plots of principle component 1 and 2 are shown. (c) Loading plot of principle component 1 and 2. The protein names are represented in the figure.

Fermentation and organic acid productions of GID-protein coding gene disruptants To further understand the role of the GID complex in the production of malate in yeast cells, disruptants of GID-protein coding genes (*vid30*Δ, *rmd5*Δ, *ubc8*Δ, *vid24*Δ, *vid28*Δ, *ubp14*Δ, *gid7*Δ, *gid8*Δ, and *fyv10*Δ) were cultivated with YM10 for 72 h, during which the concentrations of organic acids and ethanol and the levels of glucose consumption were measured (Table 3-5). As a result, it was observed that the disruptants of *VID30*, *RMD5*, *UBC8*, *VID24*, *VID28*, *GID8*, and *FYV10* (high malate-producing strains) produced markedly higher levels of malate and succinate than those produced by the parent BY4743 strain, *ubp14*Δ, and *gid7*Δ (low malate-producing strains). In contrast, the levels of pyruvate, fumarate, and acetate produced by high malate-producing strains were lower than those in the low malate-producing strains. The glucose consumption of the high malate-producing strains was lower than that of BY4743 and *ubp14*Δ. In particular, the disruptants of *VID28* and *FYV10* showed considerably lower levels of glucose consumption than *vid30*Δ, *rmd5*Δ, *ubc8*Δ, *vid24*Δ, and *gid8*Δ. Furthermore, the same change in the levels of organic acid was observed in the one-step sake brewing test (Table 3-6). These data suggest that the functions of the GID proteins in the organic acid metabolism varied.

Table 3-5 The concentration of glucose, ethanol, and organic acids in the supernatants of the YM10 cultivation test. All cultivation tests were repeated in triplicate. "±" represents the standard deviations. Data were analyzed using the Tukey-Kramer test. The same letters indicated that there was no statistically. The same letters indicated that there was no statistically

Parameter		Glucose (g/dL)	Ethanol (vol %)	Organic acid (mg/L)					
				Citrate	Pyruvate	Malate	Succinate	Fumarate	Acetate
Value (mean ± SD)	BY4743	1.70 ± 0.10 ^{e}	4.57 ± 0.18 ^{ab}	28 ± 1 ^{d}	193 ± 8 ^{a}	18 ± 2 ^{e}	388 ± 15 ^{d}	63 ± 1 ^{b}	389 ± 4 ^{b}
	*vid30*Δ	3.03 ± 0.03 ^{c}	3.75 ± 0.10 ^{cde}	34 ± 0 ^{ab}	125 ± 1 ^{e}	245 ± 2 ^{a}	1046 ± 15 ^{a}	44 ± 1 ^{c}	231 ± 1 ^{de}
	*rmd5*Δ	2.90 ± 0.10 ^{cd}	3.75 ± 0.09 ^{cde}	33 ± 0 ^{abc}	126 ± 4 ^{de}	238 ± 7 ^{ab}	1023 ± 11 ^{ab}	43 ± 2 ^{cd}	226 ± 11 ^{e}
	*ubc8*Δ	3.00 ± 0.12 ^{c}	3.88 ± 0.20 ^{bcd}	34 ± 0 ^{ab}	126 ± 1 ^{de}	246 ± 6 ^{a}	1040 ± 13 ^{ab}	46 ± 2 ^{c}	225 ± 5 ^{e}
	*vid24*Δ	2.64 ± 0.07 ^{cd}	4.22 ± 0.08	33 ± 0 ^{abc}	128 ± 3 ^{de}	255 ± 11 ^{a}	1027 ± 24 ^{ab}	46 ± 1 ^{c}	228 ± 0 ^{e}
	*vid28*Δ	3.66 ± 0.03 ^{b}	3.45 ± 0.05 ^{de}	30 ± 0 ^{bcd}	151 ± 7 ^{cd}	201 ± 3 ^{c}	963 ± 7 ^{b}	34 ± 2 ^{d}	267 ± 0 ^{d}
	*ubp14*Δ	1.68 ± 0.02 ^{e}	4.75 ± 0.22 ^{a}	29 ± 2 ^{cd}	179 ± 6 ^{ab}	34 ± 1 ^{de}	523 ± 20 ^{c}	80 ± 3 ^{a}	581 ± 15 ^{a}
	*gid7*Δ	2.41 ± 0.14 ^{d}	4.43 ± 0.12 ^{abc}	29 ± 0 ^{cd}	167 ± 6 ^{bc}	46 ± 0 ^{d}	533 ± 19 ^{c}	60 ± 3 ^{b}	342 ± 4 ^{c}
	*gid8*Δ	2.80 ± 0.15 ^{cd}	4.07 ± 0.06 ^{abcd}	34 ± 1 ^{a}	125 ± 2 ^{de}	244 ± 2 ^{a}	1037 ± 7 ^{ab}	44 ± 1 ^{c}	221 ± 9 ^{e}
	*fyv10*Δ	4.62 ± 0.17 ^{a}	3.13 ± 0.10 ^{e}	28 ± 0 ^{d}	106 ± 2 ^{e}	215 ± 4 ^{bc}	1001 ± 9 ^{ab}	50 ± 1 ^{c}	230 ± 4 ^{de}

Significant difference among the strains ($p < 0.05$)

Table 3-6 The one-step sake brewing tests of GID gene disruptants

Parameter		Specific gravity (15°C/4°C)	Ethanol (vol %)	Glucose (g/dL)	Organic acid (mg/L)						
					Citrate	Pyruvate	Malate	Succinate	Lactate	Fumarate	Acetate
Value (mean ± SD)	BY4743	1.0096	14.92	1.57	107	227	130	575	292	7	624
	*vid30*Δ	1.0152	14.11	2.28	122	223	497	691	291	23	499
	*rmd5*Δ	1.0167	14.61	2.73	122	224	521	679	286	24	483
	*ubc8*Δ	1.0180	14.67	2.55	124	213	518	776	290	24	497
	*vid24*Δ	1.0109	13.14	2.93	122	221	501	648	272	23	540
	*vid28*Δ	1.0135	15.26	1.82	116	189	447	356	219	17	593
	*ubp14*Δ	1.0146	16.03	0.79	106	257	107	398	377	6	506
	*gid7*Δ	0.9991	15.46	2.20	109	238	173	583	274	7	594
	*gid8*Δ	1.0167	14.20	2.22	121	213	475	787	281	22	511
	*fyv10*Δ	1.0025	16.78	0.52	116	179	311	777	293	14	477

Target proteome analysis of GID disruptants The cells of nine GID disruptants and BY4743 in the preceding YM10 cultivation were collected, and target proteome analysis was conducted using the extracted proteins to determine the relationship between protein expression and the organic acid metabolism. Among the 56 target proteins described in Table 3-3, the abundance of 39 was determined (Table 3-7). The expression of Mdh2 and Pck1 was undetectable in the YM10 cultivation at 72 h. Hierarchical clustering analysis was conducted to compare the profiles of 39 intracellular proteins (Fig. 3-5a). The high malate-producing disruptants of *VID30*, *RMD5*, *UBC8*, *VID24*, *VID28*, *GID8*, and *FYV10* were found to be clustered in this analysis. Further, *vid28*Δ and *fyv10*Δ, the glucose consumption of which was considerably lower, were classified into very similar groups. These results indicate that the protein abundance profile represents the phenotypic variations of organic acids and ethanol in each disruptant. To evaluate the mechanisms of the distinct characteristics of organic acid production in the GID disruptants, the protein abundance profiles were compared between the two groups; one contained high malate-producing strains of *VID30*, *RMD5*, *UBC8*, *VID24*, and *GID8*, while the other was composed of low malate-producing strains BY4743, *ubp14*Δ, and *gid7*Δ. Since *vid28*Δ and *fyv10*Δ exhibited lower levels of malate production and glucose consumption compared to other high malate-producing disruptants (except for *fyv10*Δ vs *rmd5*Δ in malate), which were likely to be involved in the protein expression profile, these two disruptants were excluded from subsequent analysis. The volcano plot (Fig. 3-5b)

shows that the abundances of 13 proteins in low malate-producing strains were higher than those of the high malate-producing strains (low malate > high malate), whereas 13 proteins were found to have a higher abundance in the high malate-producing strains (high malate > low malate). Many of the 13 proteins that were more abundant in the low malate-producing strains appeared to be associated with ethanol fermentation. On the other hand, most of the 13 proteins that were more abundant in the high malate-producing strains tended to belong to the glycolytic pathway (Fig. 3-5c). These results suggest that high malate-producing strains adopt the metabolism to an excess of malate production by the activation of glycolysis rather than ethanol fermentation.

Table 3-7 The relative expression levels of intracellular proteins of nine GID disruptants and BY4743 in YM10 cultivation test were determined using the ^{15}N-labeled peptides as the internal standards. All cultivation tests were repeated in triplicate.

Protein	Quantification peptide	BY4743	*vid30*Δ	*rmd5*Δ	*ubc*8Δ	*vid24*Δ	*vid28*Δ	*ubp14*Δ	*gid7*Δ	*gid8*Δ	*fyv10*Δ
Ach1	AFANWENFK	0.15	0.24	0.21	0.19	0.25	0.13	0.22	0.14	0.18	0.15
Aco1	TIFTVTPGSEQIR	1.05	3.07	2.77	2.22	2.75	2.09	1.76	1.23	2.47	1.92
Adh1	ANELLINVK	8.74	3.02	3.07	3.82	8.57	0.45	15.01	8.52	2.59	4.42
Adh3	GVIFYENK	4.28	0.47	0.83	0.76	3.23	0.49	7.19	2.65	0.45	0.86
Adh6	AMGAETYVISR	3.80	8.22	8.94	7.30	8.11	10.60	9.53	4.34	6.00	7.84
Ald3	GYFIPPTIFTDVPETSK	1.46	2.58	2.08	1.54	2.40	0.21	2.90	1.62	1.70	1.71
Ald4	VAFTGSTATGR	0.48	0.22	0.19	0.24	0.35	0.01	0.70	0.43	0.08	0.12
Ald5	ALFNLADLVEK	0.80	1.02	1.03	1.28	2.11	0.18	2.27	1.10	0.72	1.32
Ald6	VGIPAGVVNIVPGPGR	0.37	0.26	0.31	0.33	0.53	0.03	0.90	0.36	0.14	0.26
Fba1	GISNEGQNASIK	5.54	1.62	2.35	2.66	4.45	0.36	13.37	4.87	1.14	1.74
Cit1	AIGVLPQLIIDR	0.23	0.15	0.15	0.16	0.22	0.02	0.40	0.20	0.08	0.10
Lpd1	LVIDDQFNSK	1.42	5.80	4.76	3.61	4.16	4.76	2.56	1.68	4.20	2.57
Eno1	NVNDVIAPAFVK	9.68	24.03	22.41	17.98	21.06	8.19	14.63	10.19	16.58	12.06
Eno2	TAGIQIVADDLTVTNPAR	117.35	32.96	35.00	26.73	81.73	24.97	200.57	101.02	17.20	5.73
Fum1	AIQQAADEVASGK	0.90	0.12	0.16	0.21	0.80	0.01	1.41	0.76	0.08	0.03
Tdh1	IDVAVDSTGVFK	35.85	110.12	99.40	73.90	87.00	60.76	53.14	37.05	84.20	51.46
Tdh2	IATFQER	9.76	30.29	24.89	20.66	23.52	28.84	17.59	11.63	22.89	17.30
Tdh3	DPANLPWGSSNVDIAIDSTGVFK	2.58	6.03	4.77	4.82	5.52	4.76	4.46	3.21	5.10	4.64
Gpm1	AIQTANIALEK	14.91	50.21	43.63	35.83	39.20	42.53	28.68	16.94	36.42	29.30
Gcy1	AVGVSNFSINNLK	3.10	2.70	2.32	2.36	2.78	0.58	14.33	8.01	1.61	1.79
Hxk1	IEDDPFENLEDTDDIFQK	11.06	25.07	23.38	14.62	20.41	3.73	10.89	12.43	13.81	12.24
Glk1	GVLLAADLGGTNFR	4.12	7.03	6.29	5.83	5.80	1.06	7.06	5.59	5.08	7.50
Idh1	DYAVFEPGSR	0.93	2.65	2.23	1.89	2.32	0.84	1.50	1.16	1.89	1.53
Idh2	LADGLFVNVAK	0.87	2.37	2.11	1.66	1.94	0.92	1.41	1.11	1.83	1.46
Idp2	ATDVIVPEEGELR	0.04	0.07	0.05	0.05	0.06	0.02	0.06	0.05	0.06	0.05
Pfk1	AVLEFTPETPSPLIGILENK	1.61	1.46	1.31	1.07	0.65	1.09	1.66	1.10	1.14	0.98
Pfk2	GWSAEGGTNIGTAR	10.91	5.19	6.66	7.65	13.06	0.09	16.70	12.77	3.30	7.91
Cdc19	EPVSDWTDDVEAR	14.47	36.16	31.74	29.75	31.27	20.85	22.95	17.68	28.71	27.29
Mdh1	FISEVENTDPTQER	0.59	1.00	0.99	0.88	1.11	0.15	0.92	0.67	0.68	0.64
Kgd1	FGLEGLESVVPGIK	0.41	0.03	0.02	0.04	0.09	0.02	0.68	0.23	0.09	0.03
Pdb1	VTGADVPTPYAK	2.43	7.87	8.35	7.55	11.80	1.08	12.66	3.52	5.21	5.24
Pdc1	TPANAAVPASTPLK	3.32	3.54	3.15	2.62	4.67	3.09	7.63	2.82	2.11	2.51
Pdc6	WAGNANELNAAYAADGYAR	1.97	1.81	1.37	1.43	1.96	1.45	3.58	1.48	1.22	1.29
Pgk1	VLENTEIGDSIFDK	5.57	4.13	4.72	5.14	8.03	0.38	9.41	5.75	2.19	4.17
Pyc1	ETYGDLSVLPTR	0.18	0.12	0.13	0.07	0.18	0.10	0.36	0.17	0.07	0.11
Pgi1	LATELPAWSK	13.69	43.34	42.11	30.59	34.30	47.31	24.94	16.32	31.32	28.39
Lsc1	VIFQGFTGK	0.75	1.49	1.38	1.24	1.66	0.41	1.48	0.84	1.03	1.04
Tpi1	ASGAFTGENSVDQIK	19.07	64.11	55.10	42.14	47.89	65.90	36.23	23.13	47.98	37.60
Icl1	LDADAAEIEK	0.01	0.01	0.01	0.01	0.02	0.01	0.02	0.01	0.01	0.01

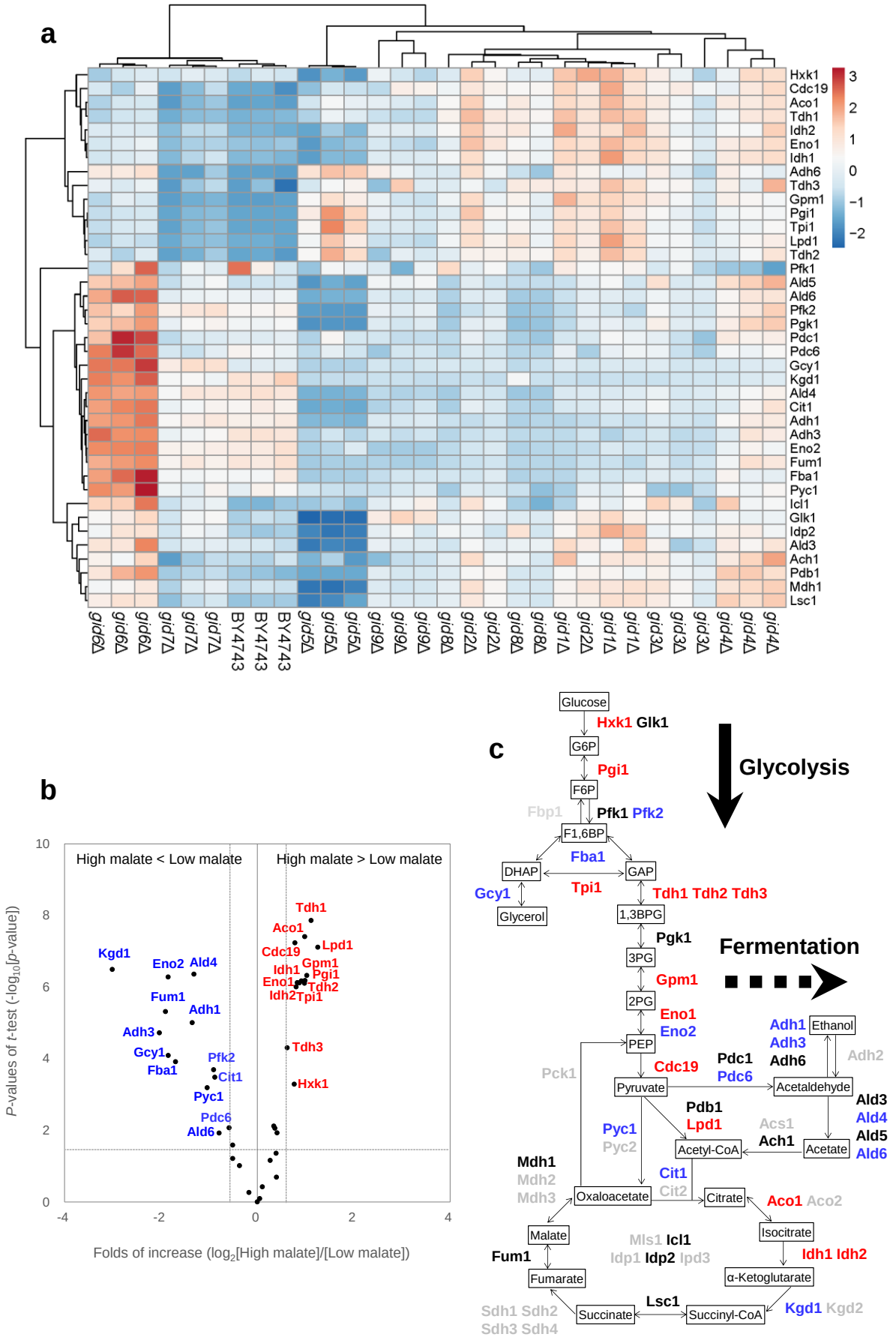
a
Hxk1
Cdc19
Aco1
Tdh1
Idh2
Eno1
Idh1
Adh6
Tdh3
Gpm1
Pgi1
Tpi1
Lpd1
Tdh2
Pfk1
Ald5
Ald6
Pfk2
Pgk1
Pdc1
Pdc6
Gcy1
Kgd1
Ald4
Cit1
Adh1
Adh3
Eno2
Fum1
Fba1
Pyc1
Icl1
Glk1
Idp2
Ald3
Ach1
Pdb1
Mdh1
Lsc1
3
2
1
0
−1
−2
gid6Δ
gid6Δ
gid6Δ
gid7Δ
gid7Δ
gid7Δ
BY4743
BY4743
BY4743
gid5Δ
gid5Δ
gid5Δ
gid9Δ
gid9Δ
gid9Δ
gid8Δ
gid2Δ
gid2Δ
gid8Δ
gid8Δ
gid1Δ
gid2Δ
gid1Δ
gid1Δ
gid3Δ
gid3Δ
gid3Δ
gid4Δ
gid4Δ
gid4Δ
b
High malate < Low malate
High malate > Low malate
Kgd1
Eno2
Ald4
Fum1
Adh1
Adh3
Gcy1
Fba1
Pfk2
Cit1
Pyc1
Pdc6
Ald6
Tdh1
Aco1
Lpd1
Cdc19
Gpm1
Idh1
Pgi1
Eno1
Tdh2
Idh2
Tpi1
Tdh3
Hxk1
P-values of t-test (-log10[p-value])
Folds of increase (log2[High malate]/[Low malate])
10
8
6
4
2
0
-4
-2
0
2
4
c
Glucose
Hxk1 Glk1
G6P
Pgi1
F6P
Fbp1
Pfk1 Pfk2
F1,6BP
Fba1
DHAP
GAP
Gcy1
Tpi1
Tdh1 Tdh2 Tdh3
Glycerol
1,3BPG
Pgk1
3PG
Gpm1
2PG
Eno1
Eno2
PEP
Pck1
Cdc19
Pyruvate
Pdc1
Pdc6
Adh1
Adh3
Adh6
Ethanol
Adh2
Acetaldehyde
Ald3
Ald4
Ald5
Ald6
Pdb1
Lpd1
Pyc1
Pyc2
Acs1
Ach1
Acetyl-CoA
Acetate
Mdh1
Mdh2
Mdh3
Cit1
Cit2
Oxaloacetate
Citrate
Aco1 Aco2
Malate
Mls1 Icl1
Idp1 Idp2 Idp3
Isocitrate
Idh1 Idh2
Fum1
Fumarate
α-Ketoglutarate
Lsc1
Sdh1 Sdh2
Sdh3 Sdh4
Succinate
Succinyl-CoA
Kgd1 Kgd2
Glycolysis
Fermentation

Fig. 3-5 Expression levels of intracellular proteins in the disruptants of GID protein-coding genes in YM10 cultivation test. The *z*-scored protein abundance data was used for analysis. All cultivation tests were repeated in triplicate. (a) Hierarchical clustering analysis of protein expression profiles. (b) Comparison of the protein abundance profiles between the five high malate-producing strains (*vid30*Δ/*gid1*Δ, *rmd5*Δ/*gid2*Δ, *ubc8*Δ/*gid3*Δ, *vid24*Δ/*gid4*Δ, and *gid8*Δ) and low malate-producing strains (*ubp14*Δ/*gid6*Δ, *gid7*Δ, and BY4743) using the volcano plot method. (c) Proteins associated with glycolysis, the TCA cycle, and ethanol biosynthesis selected for target proteome analysis. Red denotes a higher abundance of proteins, while blue denotes a lower abundance of proteins in high malate-producing strains compared with low malate-producing strains. Proteins in gray were undetectable in this analysis. Abbreviations: G6P: glucose 6-phosphate; F6P: fructose 6-phosphate; F1,6BP: fructose 1,6-bisphosphate; DHAP: dihydroxyacetone phosphate; GAP: glyceraldehyde 3-phosphate; 1,3BPG: 1,3-bisphosphoglycerate; 3PG: 3-phosphoglycerate; 2PG: 2-phosphoglycerate; PEP: phosphoenolpyruvate; acetyl-CoA: acetyl-coenzyme A; succinyl-CoA: succinyl-coenzyme A.

DISCUSSION

In yeast, the *VID24* 391G>A mutation resulted in a high production of malate during fermentation, which is known to influence the taste of sake. In this study, the author tested the hypothesis that a high malate production was attributed to the accumulation of gluconeogenesis enzymes in *VID24* mutants. As a result, the disruption of *MDH2* inhibited high malate production in the *VID24* mutant. Furthermore, the substitution of N-terminal proline, which is essential for recognition by the GID complex, for a serine (P2S) in Mdh2 resulted in a high production of malate, even in the wild-type *VID24* strain. In addition, target proteome analysis showed that the abundance of Mdh2 in *vid24*Δ cells was up-regulated in YM10 cultivated strains compared to the parent strain. Based on these data, it was concluded that a subcellular abnormal accumulation of Mdh2 in the *VID24* mutant enhanced the reduction of oxaloacetate to malate in the cytoplasm, resulting in increased malate levels. The expression of Mdh2 protein is generally facilitated by cultivation with non-fermentable carbon sources, such as ethanol, or during the diauxic

shift after glucose depletion in the culture (65, 66). Six GID proteins (Vid30, Rmd5, Vid28, Gid7, Gid8, and Fyv10) are constitutively expressed regardless of the presence of glucose, while Vid24 is only expressed upon the addition of glucose to cells growing under gluconeogenic conditions (17, 64). In current study, the *VID24* disruptant exhibited an enhancement of malate production and an accumulation of Mdh2 in YM10 cultivation, the carbon source of which was glucose (Figs. 3-3 and 3-4). These results indicate that gluconeogenic enzymes, such as Mdh2, are temporarily produced even in the presence of glucose, before being rapidly degraded via the Vid24-mediated ubiquitination pathway.

The disruptant of *vid24* produced higher amounts of malate than its parent strain BY4743 after 40 h of YM10 cultivation (Fig. 3-3). As the GID complex reportedly degrades the gluconeogenic enzymes within 2 h in the presence of glucose (16), a difference could be expected in Mdh2 abundance between the *vid24*Δ and BY4743 strains at 40 h. However, the Mdh2 accumulation in *vid24*Δ could be observed only from 136 h onwards (Fig. 3-4a). Moreover, Mdh2 was undetectable at 72 h during the YM10 cultivation test of nine GID disruptants, even though several of them showed high malate production (Table 3-5, Fig. 3-5a). There are different possible explanations for these results. First, Mdh2 could be measured inaccurately at 40 and 72 h due to its low expression in the presence of glucose. Therefore, the delay between the malate levels and Mdh2 abundance could be attributed to the detection limit of the proteome analysis employed in this study. Another possibility for the discordance between malate levels and Mdh2 abundance is the inactivation of Mdh2 via GID complex-mediated ubiquitination. The Mdh2 protein reportedly gets degraded in glucose-starved cells within 2 hours following glucose administration (16, 18). Once the Mdh2 protein gets ubiquitinated by the GID complex, enzyme activity should decline, and malate generation should reduce. However, the exact rates of synthesis and degradation following Mdh2 ubiquitination in the presence of glucose remain unknown. Hence, Mdh2 inactivation through ubiquitination may not reflect the differences in Mdh2 amounts between BY4743 and *vid24*Δ.

The author observed increased levels of succinate, pyruvate, and malate in *vid24*Δ (Fig. 3-3). The accumulated malate was presumably transported into the mitochondria

and used aerobically in the oxidative TCA cycle, leading to an increase in the level of succinate (Chapter I). The increase in pyruvate levels from 136 h to 188 h appeared to result from a decrease in the conversion of pyruvate to malate or ethanol due to a reduced yeast cell activity. This could be, in turn, an indication of reduced cell viability and the lower expression of several glycolytic enzymes in *vid24*Δ compared to BY4743 at 136 h and 188 h. The excessive organic acid production is thought to exert acid stress on yeast cells.

Vid24 recognizes the N-terminal proline residue of the degradation substrates, the gluconeogenic enzymes, in the Vid24 β-barrel as the binding pockets composed of eight β-strands and four hairpin loops (76). Inside the cavity, three amino acids of Vid24 (Gln133, Glu294, and Trp316) form hydrogen bonds with the N-terminal proline of gluconeogenic enzymes. The Vid24 Gly131 residue, whose substitution to arginine was identified as the mutation responsible for high malate production in yeast, is a component of one of the β-strands, in addition to being located in close proximity to Glu133. It is possible that the substitution of Gly131Arg prevents the entry of N-terminal proline into the Vid24 β-barrel, or at least interfered with the formation of hydrogen bonds between Glu133 of Vid24 and the N-terminal proline of substrates by a conformational change, resulting in the accumulation of intracellular Mdh2. Since the Vid24 Gly131Arg mutant and the *VID24* disruptant showed almost equal levels of organic acid production in Chapter I, the Vid24 mutation appeared to result in a complete loss of substrate recognition.

Nine GID disruptants were subjected to the YM10 cultivation test in order to evaluate the effect of the GID complex on the production of organic acids. As a result, the disruptants of *VID30*, *RMD5*, *UBC8*, *VID24*, *VID28*, *GID8*, and *FYV10* were found to produce higher levels of malate than their parent strain.

The disruption of *VID30*, *RMD5*, *VID24*, *VID28*, *GID8*, and *FYV10* has been known to result in the accumulation of intracellular Mdh2 regardless of the addition of glucose (16). Therefore, the mechanism of high malate production in these disruptants was assumed to result from the accumulation of Mdh2, similar to *vid24*Δ. Among high malate-producing disruptants, *vid28*Δ and *fyv10*Δ differed from the others in terms of the

production of ethanol and organic acids (Fig. 3-4). It has been reported that Vid28 and Fyv10 are required for the polyubiquitination of the GID-ubiquitin ligase complex, as well as other GID proteins (20, 77), however, it is unclear how they impact the growth and fermentation of yeast. It is possible that they have a biological function that differs from other GID proteins. In contrast to *vid30*Δ, *rmd5*Δ, *ubc8*Δ, *vid24*Δ, *vid28*Δ, *gid8*Δ, and *fyv10*Δ, the malate levels of *ubp14*Δ and *gid7*Δ were nearly identical to those of the parent strain. Although Ubp14 and Gid7 play important roles in the degradation of Fpb1 (20), they may not be involved in the regulation of Mdh2. A recent study indicated that Gid7 is separated from the center of GID E3 ubiquitin ligase activity, although it is essential for the degradation of Fbp1 (64). Ubp14 is a deubiquitinating enzyme (78), and not a component of the GID complex (20). In addition, the response of *upb14*Δ and *gid7*Δ to rapamycin was distinct from that of the other disruptants of the GID gene (42). Taken together, these results indicate that, although Ubp146 and Gid7 are involved in the degradation of Fbp1, they appear to contribute only partly to the degradation of gluconeogenic enzymes mediated by the GID complex.

Target proteome analysis was performed to evaluate the impact of GID-gene disruption on the intracellular metabolism. The profiles of protein expression in the GID disruptants were found to be different from one another. As a consequence of the hierarchical clustering analysis of the protein expression and metabolite profiles, the GID disruptants were classified into two groups: high malate-producing strains (*vid30*Δ, *rmd5*Δ, *ubc8*Δ, *vid24*Δ, *vid28*Δ, *gid8*Δ, and *fyv10*Δ) and low malate-producing strains (*ubp14*Δ, *gid7*Δ, and BY4743) (Table 3-5, Fig. 3-5a). Furthermore, *vid28*Δ and *fyv10*Δ, which showed lower glucose consumption and lower ethanol levels than the high malate-producing disruptants, were clustered in a similar group. The results suggested that the protein expression profiles reflected the differences in metabolites, including organic acids and ethanol. To investigate the background of the distinct organic acid productivity of GID disruptants, the protein abundance profiles were compared among five high malate-producing strains (*vid30*Δ, *rmd5*Δ, *ubc8*Δ, *vid24*Δ, and *gid8*Δ), all of which produced almost equal levels of ethanol, and three low malate-producing strains (*ubp14*Δ, *gid7*Δ, and BY4743) (Fig. 3-5b). The expression of several glycolytic enzymes was

facilitated, whereas the expression of enzymes involved in ethanol fermentation (from pyruvate to ethanol) was downregulated in the former compared to the later strains (Fig. 3-5c). Based on the assumption that a high malate production in the GID disruptants was attributed to the accumulation of Mdh2 in the cytoplasm, it was presumed that alterations to glycolytic enzymes and ethanol fermentation enzymes resulted from the increased intracellular malate levels. One possibility is that the upregulation of glycolytic enzymes may play a role in driving adenosine 5'-triphosphate (ATP) synthesis to regulate the intracellular changes in pH caused by excess malate. ATP is generally required for the regulation of cation balance in yeast cells (79). Another possibility is the need to modulate the intracellular NAD^+ and NADH levels. Increases in enzymes converting NAD^+ to NADH, such as triose-phosphate dehydrogenase (Thd1, Tdh2, and Tdh3), lipoamide dehydrogenase (Lpd1), and isocitrate dehydrogenase (Idh1 and Idh2), and decreases in enzymes converting NADH to NAD^+, such as alcohol dehydrogenase (Adh1 and Adh3), were observed (Fig. 3-5c). The fluctuations in the levels of these proteins may occur in order to regulate the NAD^+/NADH ratio, since the conversion from oxaloacetate to malate by Mdh2 consumes NADH (80). The changes in the enzymes involved in glycolysis and ethanol fermentation were predicted to result from the adjustment of the cellular metabolism to increased levels of organic acid.

In this study, the author found that the accumulation of intracellular Mdh2 by dysfunction of Vid24 resulted in a high malate-producing *VID24* mutant. Furthermore, several GID disruptants (*vid30*Δ, *rmd5*Δ, *ubc8*Δ, *vid28*Δ, *gid8*Δ, and *fyv10*Δ) exhibited high malate production, in addition to *vid24*Δ. Comparisons between the protein expression levels of the GID disruptants revealed variations in the expression profiles of glycolysis and TCA-related enzymes. These results suggested a correlation between changes in protein expression profiles and an increase in malate production. Changes in protein expression may occur during sake brewing since the production of organic acids in the sake brewing test were found to be nearly identically to that in YM10 cultivation test for all of the GID disruptants (Tables 3-5 and 3-7). Many previous studies have demonstrated that GID proteins play a key role in the regulation of gluconeogenic enzymes under a shift from gluconeogenic to glycolytic conditions by the addition of

glucose after its depletion. The data presented here confirm the important role of GID proteins in the degradation of gluconeogenic enzymes under glycolytic conditions. Gluconeogenic enzymes, such as Mdh2, are likely to be expressed regardless of the presence of glucose, and are degraded by the GID complex constitutively. Thus, the GID complex may serve to regulate gluconeogenic enzymes to determine the levels of organic acids during alcoholic fermentation, such as in sake mash, in which glucose is abundant.

SUMMARY

Vid24 is a component of the GID complex and stimulates the catabolic degradation of gluconeogenic enzymes. In this study, the mechanism by which this mutation led to high malate production in yeast cells was investigated. The evaluation of disruptants and mutants of gluconeogenic enzymes revealed that Mdh2 participated in the malate production. Furthermore, target proteome analysis indicated that an increase in malate production resulted from the accumulation of Mdh2 in *vid24* disruptant due to the loss of GID complex-mediated degradation. Next, the author investigated the effects of GID protein-coding genes (*VID30*, *RMD5*, *UBC8*, *VID24*, *VID28*, *UBP14*, *GID7*, *GID8*, and *FYV10*) on organic acid production and enzyme expression profiles in yeast. The disruptants of *VID30*, *RMD5*, *UBC8*, *VID24*, *VID28*, *GID8*, and *FYV10* exhibited high malate production. Comparison of protein abundance among the GID disruptants revealed variations in protein expression profiles, including in glycolysis and tricarboxylic acid cycle-related enzymes. The high malate-producing disruptants showed the activation of several glycolytic enzymes and a reduction in enzymes involved in the conversion of pyruvate to ethanol. These results suggest that high malate-producing disruptants adapt their metabolism to produce malate in excess via the regulation of protein expression in glucose assimilation and ethanol fermentation.

Chapter IV

Mutation in GID protein-coding genes contributing to high malate production in yeasts used for sake brewing industrially

High malate-producing strains No 28 and No. 77 were developed based on its resistance to cycloheximide and mating strategies of haploid yeast cells (Fig. 4-1) (10). These strains have been bred in the “Brewing Society of Japan”, a public interest incorporated foundation. Sake breweries can purchase these strains from the foundation. They are widely used high-malate-producing strains for sake brewing. The mechanisms contributing to the high acidity phenotype of No. 28 and No. 77 have been investigated. A suppression in the mitochondrial activity in cells of the strain No. 28 was observed to have an influence on the production malate (15). However, the gene mutations responsible for high malate production in these strains are yet to be determined.

The author reported in Chapter III that components of the GID complex were involved in high malate production in yeast. GID complex is a multisubunit E3 ubiquitin ligase that consists of seven proteins: Vid30/Gid1, Rmd5/Gid2, Vid24/Gid4, Vid28/Gid5, Gid7, Gid8, and Fyv10/Gid9 (17, 21, 22). GID complex specifically degrades gluconeogenic enzymes in the presence of glucose with the E2-conjugating enzyme Ubc8/Gid3 (16, 17). Disruption of *VID30*, *RMD5*, *UBC8*, *VID24*, *VID28*, *GID8*, and *FYV10* exhibited high malate production due to the accumulation of Mdh2 protein, which is originally degraded by GID complex in the presence of glucose (Chapter III). Furthermore, it was reported in Chapter I that sake yeast strain K-901H acquired high malate production owing to a missense mutation of *VID24*. The result demonstrated that industrial high malate-producing strains could harbor mutations in GID genes.

In this study, the author investigated the mechanism for high malate production in strain No. 28 and No. 77. Several mutations in GID genes were detected in each strain, one of them led to high malate production. The mutated GID genes affecting malate productivity differed between the No. 28 and No. 77 strains. A mutation in the *VID24* gene resulted in high malate production of No. 28, while a mutation in the *RMD5* gene led to high malate production by strain No. 77.

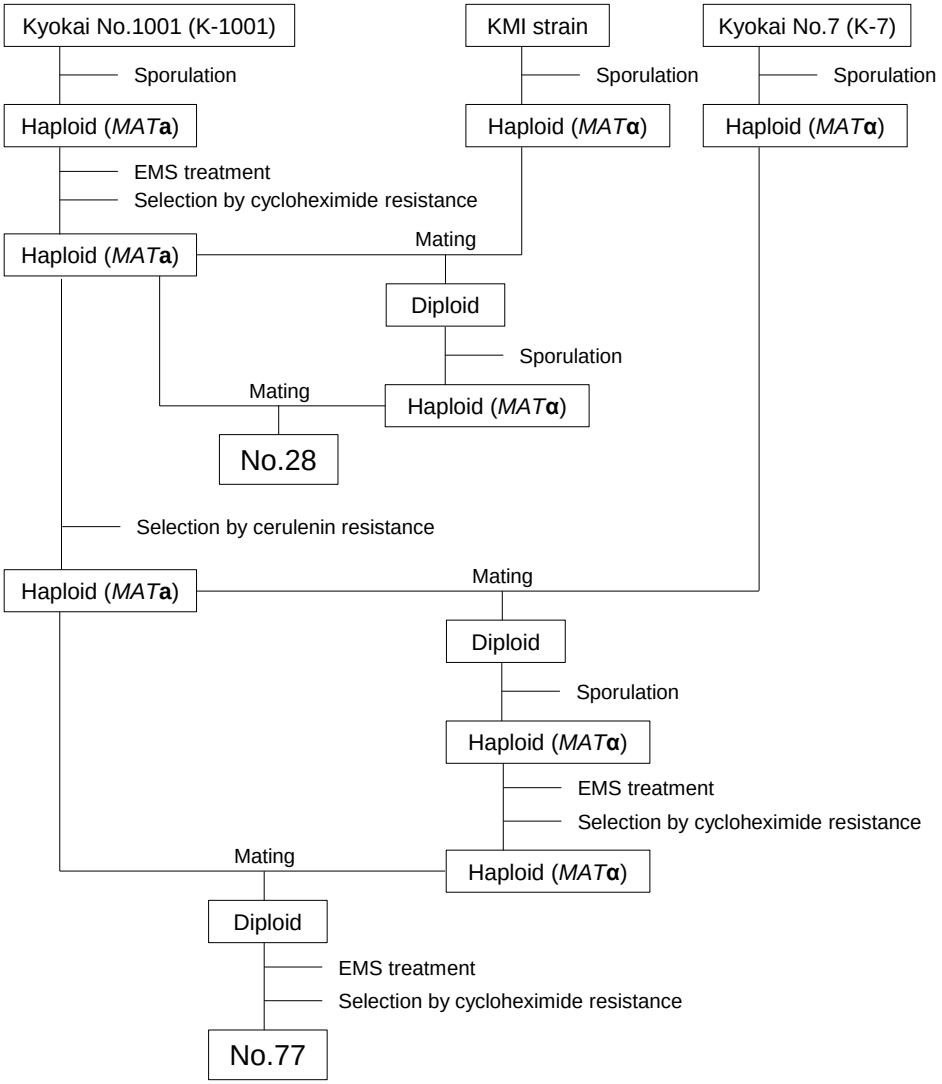

Fig. 4-1 Scheme for breeding high-malate-producing yeast strain No. 28 and No. 77 (10).

MATERIALS AND METHODS

Media and yeast strains Yeast cells were cultured in yeast extract peptone dextrose (YPD) medium consisting of yeast extract (10 g/L), polypeptone (20 g/L), or glucose (20 g/L); and in yeast malt 10 (YM10) medium consisting of yeast extract (3 g/L), malt extract (3 g/L), polypeptone (5 g/L), and glucose (100 g/L).

The sake yeast strains Kyokai No. 7 (K-7), Kyokai No. 1001 (K-1001), Kyokai No.28 and Kyokai No. 77 were obtained from Brewing Society of Japan (10) (Table 4-1).

The *MAT***a** haploid yeast strain 4011a was isolated from spores of the *MAT***a**/*MAT*α diploid yeast strain 4011 (33).

Table 4-1 Genotypes and references of *S. cerevisiae* strains used in this study

Strain	Genotype	Reference
K-7	*MAT***a**/*MAT*α	Brewing Society of Japan
K-1001	*MAT***a**/*MAT*α	Brewing Society of Japan
No.28	*MAT***a**/*MAT*α	Brewing Society of Japan
No.77	*MAT***a**/*MAT*α	Brewing Society of Japan
4011a	*MAT***a**	(33)
4011a-VID30	4011a *VID30-kanMX4*	This study
4011a-mVID30-1	4011a *VID30* 2353G>A-*kanMX4*	This study
4011a-mVID30-2	4011a *VID30* 2449G>A-*kanMX4*	This study
4011a-RMD5	4011a *RMD5-kanMX4*	This study
4011a-mRMD5	4011a *RMD5* 263G>A-*kanMX4*	This study
4011a-VID24	4011a *VID24-kanMX4*	This study
4011a-mVID24	4011a *VID24* 85G>T-*kanMX4*	This study
4011a-VID28	4011a *VID28-kanMX4*	This study
4011a-mVID28	4011a *VID28* 671T>C-*kanMX4*	This study
4011a-FYV10	4011a *FYV10-kanMX4*	This study
4011a-mFYV10-1	4011a *FYV10* 1096G>A-*kanMX4*	This study
4011a-mFYV10-2	4011a *FYV10* 1161A>G-*kanMX4*	This study
No. 28-G2/G2-mG4/mG4	No.28 *RMD5*/ *RMD5-natMX4*	This study
No. 28-mG2/G2-mG4/G4	No.28 *VID24* 85G>T/*VID24-kanMX4*	This study
No. 28-G2/G2-mG4/G4	No.28 *RMD5*/*RMD5-natMX4 VID24* 85G>T/*VID24-kanMX4*	This study
No. 28-mG2/G2-G4/G4	No.28 *VID24-kanMX4*/*VID24-kanMX4*	This study
No. 28-G2/G2-G4/G4	No.28 *RMD5*/*RMD5-natMX4 VID24-kanMX4*/*VID24-kanMX4*	This study
No. 77-mG2/G2	No.77 *RMD5* 263G>A/*RMD5-natMX4*	This study
No. 77-G2/G2	No.77 *RMD5-kanMX4*/*RMD5-natMX4*	This study

One-step sake brewing test The sake brewing test was carried out as described in Chapter I. In brief, yeast cells were cultivated aerobically in YPD medium at 30 °C for 48 h, harvested by centrifugation (5000× g, 5 min, 4 °C), and resuspended in water. Koji is a culture of *Aspergillus oryzae* that is grown on steamed rice. Polished rice was preliminarily pulverized, gelatinized, and digested with thermostable α-amylase TU20 (Amano Enzyme Co. Ltd., Nagoya, Japan). Sake mash consisted of 40 g of polished rice with a polishing ratio of 70%, 10 g of koji, 20 μl of 90% lactic acid, 80 mL of water, and 1.3×10^8 yeast cells. Fermentation was carried out at 15 °C. The loss of weight of the

mash was correlated with carbon dioxide emission levels to monitor the fermentation progress. After 20 days, the mash was centrifuged and the supernatant was analyzed. The ethanol concentration and specific gravity were measured using a Density/Specific Gravity Meter DA-650 (Kyoto Electronics Manufacturing Co. Ltd., Kyoto, Japan). Acid and amino acid levels were measured with an electric potential difference autotitration apparatus (Kyoto Electronics Manufacturing Co. Ltd.) by the National Tax Administration Agency method (40). The amount of organic acids in the supernatant was measured using a high-performance liquid chromatography-based Organic Acid Analysis System (Shimadzu Co., Ltd., Kyoto, Japan).

YM10 cultivation test Yeast cells were cultivated aerobically in YPD medium at 30 °C for 24 h and harvested by centrifugation (5000× g, 5 min, 4 °C). The cells were resuspended in YM10 medium to an optical density at 600 nm (OD_{600}) of 0.1. The culture was incubated at 30 °C for 5 d without shaking. Cell density at OD_{600} was determined using a UV spectrometer (UV-2550; Shimadzu Co., Ltd.). The organic acids in the supernatant of the culture were analyzed in the same manner as the sake brewing test.

Whole genome sequencing analysis Genomic DNA was extracted using the NucleoBond Buffer Set III and NucleoBond AXG 20 Columns (MACHEREY-NAGEL GmbH & Co. KG, Düren, Germany) from the No. 28 and No. 77 strains. Approximately 6 μg of genomic DNA was used for genome sequence analysis. Whole genome sequencing was performed by the comparative genome analysis service (Takara Bio Inc., Otsu, Japan) using the HiSeq2000 (Illumina Inc., San Diego, CA, USA). Sequence reads were assembled using the Burrows-Wheeler Aligner (BWA) v0.5.9. software. The genome sequence of the K-7 sake yeast (Brewing Society of Japan) was used as the reference genotype (2). The analysis resulted in the identification of variant positions. No. 27 or No. 77 genomes were compared with the K-7 genome using SAMtools mpileup and varFilter.

Table 4-2 Primers used in this study

Primer name	Primer Sequence (5'-3')	Description of PCR product
GID1(1001)-F	ATAACAGCTTGCAGCTATCTCAAGATGG	Partial *VID30* gene with *kanMX4* homology region
GID1+KanMX4-R	CTGCAGCGTACGTCATAAATTCAACACATC	
GID1+KanMX4-F	TTGAATTTATGACGTACGCTGCAGGTCGAC	*kanMX4* with *VID30* homology region
KanMX4+GID1ter-R	TTGTTTTATGCTTAGAAAAACTCATCGAGC	
KanMX4+GID1ter-F	AGTTTTTCTAAGCATAAAACAAGCACCTTC	3' flanking region of *VID30* with *kanMX4* homology region
GID1(3390)-R	CCTGTTTTCTAATTCATAATTACTAACAAG	
GID2(-330)-F	GAGTAACTCCAAATTTTGAAACGCTCAAG	*RMD5* gene with *kanMX4* homology region
GID2+KanMX4-R	CAGCGTACGTCAAAGCATAACAAAACGAAC	
GID2+KanMX4-F	TATGCTTTGACGTACGCTGCAGGTCGACGG	*kanMX4* with *RMD5* homology region
KanMX4+GID2ter-R	CAAAAATTTCAGTTAGAAAAACTCATCGAG	
KanMX4+GID2ter-F	GAGTTTTTCTAACTGAAATTTTTGCATAGG	3' flanking region of *RMD5* with *kanMX4* homology region
GID2(1807)-R	TTTGATGATTCTTTCTTAAATGACGATGAG	
GID2(-330)-F	GAGTAACTCCAAATTTTGAAACGCTCAAG	*RMD5* gene with *natMX4* homology region
GID2+natMX4-R(78bp)	CTGAGCTGCGCACGTCAAGACTGTCAATCAAAGCATAACAA AACGAACCTTTTTTGTACTGCTCATTGAAGTATTTAC	
GID2+natMX4-F	GTTATGCTTTGATTGACAGTCTTGACGTGC	*natMX4* with *RMD5* homology region
natMX4+GID2ter-R	GCAAAAATTTCAGTTAGGGGCAGGGCATGC	
natMX4+GID2ter-F	GCCCTGCCCCTAACTGAAATTTTTGCATAG	3' flanking region of *RMD5* with *natMX4* homology region
GID2(1807)-R	TTTGATGATTCTTTCTTAAATGACGATGAG	
GID4(-968)-F	TGTCTATTTCCTTCAAATCGTAGTCTCTG	*VID24* gene with *kanMX4* homology region
GID4+kanMX-R	GCAGCGTACGTCAAGCAAACTCAAAAGAAC	
GID4+kanMX4-F	GAGTTTGCTTGACGTACGCTGCAGGTCGAC	*kanMX4* with *VID24* homology region
kanMX4+GID4ter(70bp)-R	GTTAGTGAAGAGAAAAGGGTATGCAGGTAAAAACGAATATA TCACACATTAGAAAAACTCATCGAGCATC	
kanMX4+GID4ter-F	GTTTTTCTAATGTGTGATATATTCGTTTTT	3' flanking region of *VID24* with *kanMX4* homology region
GID4(2051)-R	TTTGCATTCTACAAAGGTGCGTTAACACC	
GID5(-492)-F	ACATTACGGAAACGTACAATTGCCCTTCTG	*VID28* gene with *kanMX4* homology region
GID5+kanMX-R	CTGCAGCGTACGTCATTTAACTTTCAAAAG	
GID5+kanMX4-F	AAAGTTAAATGACGTACGCTGCAGGTCGAC	*kanMX4* with *VID28* homology region
kanMX4+GID5ter-R	GTTCTGTGCATTTAGAAAAACTCATCGAGC	
kanMX4+GID5ter-F	GTTTTTCTAAATGCACAGAACTCGTAGTAT	3' flanking region of *VID28* with *kanMX4* homology region
GID5(3738)-R	AGATTAAGACAAGGTGCTGCCAAGTTGAG	
GID9(1)-F	ATGGCAGAGAAATCAATATTTAATGAGCC	*FYV10* gene with *kanMX4* homology region
GID9+KanMX4-R	TGCAGCGTACGTCAGGTTGGGTACATTTTG	
GID9+KanMX4-F	AACCTGACGTACGCTGCAGGTCGACGGATC	*kanMX4* with *FYV10* homology region
KanMX4+GID9ter-R	CTTGAAACTATTTTAGAAAAACTCATCGAG	
KanMX4+GID9ter-F	GTTTTTCTAAAATAGTTTCAAGCTATATGC	3' flanking region of *FYV10* with *kanMX4* homology region
GID9(2232)-R	TAATCAACAGGCTTAGCGATCATCGTTG	

Construction of the point mutants from 4011a The GID gene-point mutants were obtained by transforming the 4011a strain with the mutated GID genes and *kanMX4* module (Table 4-1) (35). Simultaneously, wild-type GID genes and *kanMX4* module were also used as controls (Table 4-1). First, using the primers listed in Table 4-2 and PrimeSTAR Max DNA polymerase (Takara Bio Inc., Japan), three DNA fragments (the mutated GID genes, *kanMX4* module, and the 3' flanking region corresponding with the GID genes) were amplified from the No. 28 or No. 77 genomic DNA, *kanMX4* module-carrying plasmid, and K-7 genomic DNA, respectively. The DNA fragment of wild-type GID genes was amplified from the K-7 genomic DNA. Next, the three DNA fragments

were used for fusion PCR, and subsequently the DNA fragment constructed by fusion PCR with the mutated or wild-type GID genes, *kanMX4* module, and the 3' flanking region of the GID genes was used for transformation. Yeast transformations were performed using the lithium acetate method (36). The genotype of the GID clones was determined by Sanger sequencing.

Construction of the complemented strain from No.28 and No.77 Complemented strains were obtained by transforming No. 28 and No. 77 strains with the wild-type *RMD5* or *VID24* genes, and *natMX4* module or *kanMX4* module (Table 4-1) (81). Similar to the 4011a-point mutants, three DNA fragments (the wild-type *RMD5* or *VID24* genes, *natMX4* or *kanMX4* module, and the 3' flanking region of the GID genes) were amplified using the primers listed in Table 4-2, and the DNA fragment for transformation was obtained by fusion PCR with the three fragments. Yeast transformations were performed repetitively to complement multiple mutation points (Fig. 4-2).

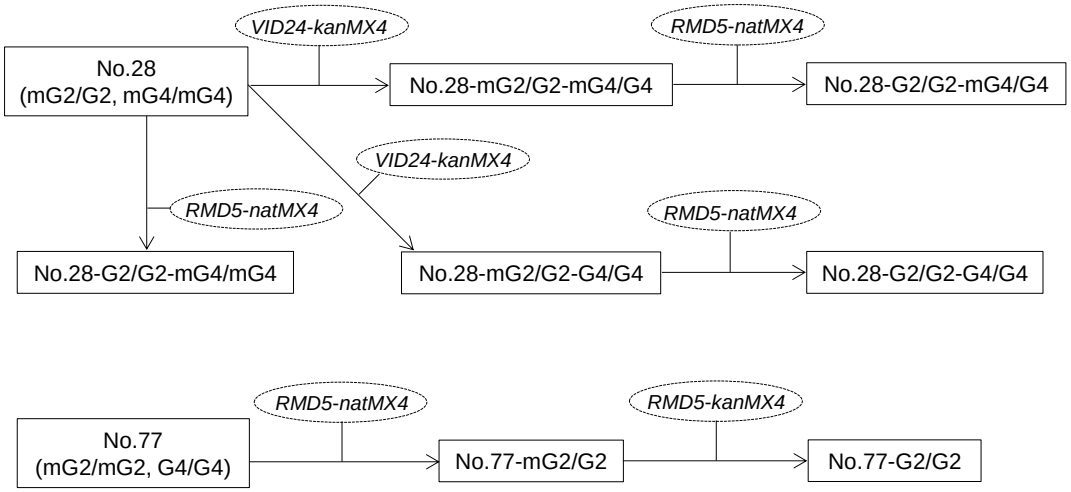

Fig. 4-2 Strategy for construction of complemented strain by replacement of mutated GID genes with wild-type GID genes. Solid square represents the strain name. Dashed ellipse represents the DNA fragment used for transformation.

RESULTS

Comparison of organic acid production between high-malate-producing strains and parent strains To evaluate the organic acid production among the strains, the one-step sake brewing test was performed using the K-7, K-1001, No. 28, and No. 77 strains. Strain No. 28 and No. 77 produced markedly higher levels of malate than K-7 and K-1001 (Table 4-3). Furthermore, the same change in the levels of malate was observed in the strains cultured in YM10 (Fig. 4-3).

Table 4-3 The concentration of ethanol, specific gravity, acid level, amino acid level, and organic acids in sake. All brewing tests were repeated in triplicate. The plus minus sign represents SD. Data were analyzed by the Tukey-Kramer test. Same letters indicate that there was no statistically significant difference among the strains ($p < 0.05$)

Parameter		Ethanol (vol %)	Specific gravity (15 °C/4 °C)	Organic acid (mg/L)					
				Malate	Succinate	Lactate	Pyruvate	Acetate	Citrate
Value (mean ± SD)	K-7	18.35 ± 0.16 [b]	0.9970 ± 0.0010 [b]	296 ± 8 [c]	575 ± 5 [b]	324 ± 3 [a]	45 ± 22 [a]	173 ± 10 [a]	73 ± 2 [c]
	K-1001	19.15 ± 0.05 [a]	0.9910 ± 0.0002 [c]	155 ± 2 [d]	512 ± 7 [c]	336 ± 5 [a]	10 ± 0 [a]	137 ± 2 [b]	85 ± 1 [b]
	No. 28	18.75 ± 0.01 [ab]	0.9940 ± 0.0004 [bc]	1374 ± 21 [a]	675 ± 5 [a]	302 ± 5 [b]	40 ± 5 [a]	113 ± 7 [b]	79 ± 0 [bc]
	No. 77	17.45 ± 0.15 [c]	1.0024 ± 0.0015 [a]	1111 ± 12 [b]	320 ± 2 [d]	239 ± 2 [c]	7 ± 6 [a]	164 ± 1 [a]	125 ± 4 [a]

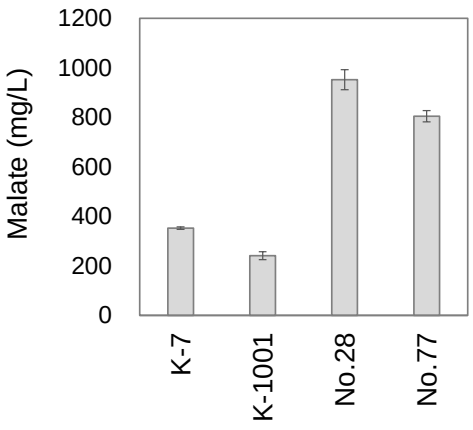

Fig. 4-3 Malate production by high-malate-producing strains and their parent strains in the YM10 cultivation test. All the cultivation tests were repeated in triplicate. Each error bar represents standard deviation. Data were analyzed by the Tukey-Kramer test. Same letters indicate that there was no statistically significant difference among the strains ($p < 0.05$).

Table 4-4 List of genes containing non-synonymous mutations in No. 28 and No. 77 genome as compared to the K-7 genome

No. 28												
00014	*ATR1*	*CWH41*	*FMP22*	*IMP1*	*MMP1b*	*PAC2*	*PSY4*	*SAY1*	*SPT21*	*TRF5*	*YDL007C-A*	*YIR003W*	*YPR015C*
00122	*AVT2*	*CYC8*	*FMP23*	*INO80*	*MMS4*	*PAH1*	*PTH2*	*SBP1*	*SPT6*	*TRK1a*	*YDL025C*	*YIR014W*	*YPR063C*
00123	*AVT4*	*CYM1*	*FMP26*	*INP1*	*MND2*	*PAM1*	*PTK2*	*SCC2*	*SPT7*	*TRK2*	*YDL027C*	*YIR016W*	*YPR071W*
00356	*AVT5*	*DAD1*	*FMP29*	*INP2*	*MNN1*	*PAM18*	*PTP3*	*SCS3*	*SQS1*	*TRM1*	*YDL063C*	*YJL068C*	*YPR078C*
00404	*AVT7*	*DAK1*	*FMP34*	*INP52*	*MNN10*	*PAT1*	*PTR2*	*SCT1*	*SRB5*	*TRM82*	*YDL109C*	*YJL070C*	*YPR084W*
00774	*AWA1*	*DAL1*	*FMP36*	*IOC3*	*MNN5*	*PAU18*	*PUB1*	*SCW10*	*SRB7*	*TRP4*	*YDR026C*	*YJL163C*	*YPR085C*
01010	*AYT1*	*DAL2*	*FMP43*	*IPL1*	*MON1*	*PAU7*	*PUF3*	*SCW11*	*SRL2*	*TRP5*	*YDR042C*	*YJL185C*	*YPR089Wb*
01104	*BAP2*	*DAL4*	*FMP50*	*IPT1*	*MON2*	*PAU8-2*	*PUF4*	*SCY1*	*SRO77*	*TRS20*	*YDR049W*	*YJL216Ca*	*YPR097W*
01105	*BAP3*	*DAL5*	*FMT1*	*IQG1*	*MOT1a*	*PBP1*	*PUF6*	*SDC25*	*SRP40*	*TRS31*	*YDR051C*	*YJR030C*	*YPR115W*
02300	*BCD1*	*DAN3-2*	*FRM2*	*IRA1*	*MOT3*	*PBP2*	*PUS1*	*SDS24*	*SSE1*	*TRS33*	*YDR061W*	*YJR079W*	*YPR148C*
02411	*BCK2*	*DAN4a*	*FUM1*	*IRS4*	*MPA43*	*PBS2*	*PUS2*	*SDS3*	*SSF2*	*tS_AGA_B*	*YDR089W*	*YJR088C*	*YPR157W*
02610	*BDP1*	*DAN4b*	*FUN14*	*ISC1*	*MPH1*	*PCA1a*	*PUT2*	*SEC12*	*SSK1*	*TSC10*	*YDR109C*	*YJR096W*	*YPR158W*
02694	*BEM3*	*DAN4c*	*FYV10*	*ISR1*	*MRC1*	*PCH2*	*PWP2*	*SEC15*	*SSK2*	*TSR1*	*YDR119W*	*YJR098C*	*YPR196W-2a*
03371	*BET5*	*DAN4d*	*FYV8*	*IST2*	*MRD1*	*PCK1*	*PXL1*	*SEC16*	*SSK22*	*tT_AGU_I1*	*YDR124W*	*YJR107W*	*YPR196W-2b*
03398	*BFR2*	*DAP2*	*FZF1*	*ISW1*	*MRF1*	*PCL10*	*QDR1*	*SEC2*	*SSL1*	*TYS1*	*YDR128W*	*YJR111C*	*YPS6*
03399	*BIM1*	*DAT1*	*FZO1*	*IXR1*	*MRM2*	*PCL8*	*QDR3a*	*SEC21*	*SSM4*	*TYW1*	*YDR161W*	*YJR116W*	*YRA1*
03404	*BIO5*	*DBF2*	*GAL3b*	*IZH3*	*MRN1*	*PCP1*	*RAD1*	*SEC26*	*SSN2*	*UBA1*	*YDR179W-A*	*YJR129C*	*YRB2*
03461	*BIR1*	*DBP6*	*GAL4a*	*JEM1*	*MRP4*	*PCT1*	*RAD14*	*SEC27*	*SSO2*	*UBP11*	*YDR186C*	*YJR136C*	*YRB30*
03725	*BIT2*	*DBP7*	*GAL83*	*JEN1*	*MRPL16*	*PDC2*	*RAD24*	*SEC28*	*SSQ1*	*UBP15*	*YDR222W*	*YJR141W*	*YSC83*
03783	*BLM10*	*DCR2*	*GAP1*	*JLP1*	*MRPL9*	*PDC6a*	*RAD30*	*SEC6*	*SSY5*	*UBP16*	*YDR262W*	*YJR142W*	*YSP2*
04474	*BNA2*	*DEM1*	*GAS1*	*KAP114*	*MRPS28*	*PDH1*	*RAD4*	*SEC61*	*SSZ1*	*UBP7*	*YDR266C*	*YJR149W*	*YTA7*
04475	*BNA4*	*DER1*	*GCD11*	*KAP122*	*MRPS9*	*PDI1*	*RAD5*	*SEC65*	*STE12*	*UBR2*	*YDR282C*	*YJR154W*	*YTP1*
04496	*BNA6*	*DIB1*	*GCD6*	*KAR3*	*MRS4*	*PDR1*	*RAD50*	*SEC7*	*STE20*	*UBS1*	*YDR307W*	*YKL033W*	*ZDS2*
04594	*BNI1*	*DIT2*	*GCN1*	*KCS1*	*MSB2*	*PDR15*	*RAD59*	*SEC9*	*STE23*	*UIP5*	*YDR333C*	*YKR015C*	*ZIP2*
05278	*BNI4*	*DMA1*	*GCN4*	*KEL1*	*MSD1*	*PDR16*	*RAD9*	*SED1*	*STE5*	*ULP2*	*YDR338C*	*YKR017C*	*ZPR1*
05502	*BNR1*	*DMA2*	*GCV1*	*KEL2*	*MSH1*	*PDR17*	*RAS2*	*SED4*	*STE50*	*UME6*	*YDR374C*	*YKR077W*	*ZRG8*
05679	*BOR1*	*DML1*	*GDH3*	*KES1*	*MSH4*	*PDR3*	*RCK1*	*SED5*	*STE6*	*UPC2*	*YDR374W-A*	*YKR078W*	*ZRT1*
06158	*BPH1*	*DNA2*	*GDT1*	*KEX1*	*MSH6*	*PDS1*	*RCR2*	*SEF1*	*STH1*	*URA8*	*YDR387C*	*YKR096W*	
06488	*BPT1a*	*DNF1*	*GET2*	*KEX2*	*MSK1*	*PDX3*	*RCY1*	*SEN1*	*STP1*	*URB2*	*YDR428C*	*YLH47*	
07260	*BPT1b*	*DNF3*	*GIC2*	*KHA1*	*MSN5*	*PEP1*	*RDN37-1*	*SEN54*	*STP2*	*URN1*	*YDR514C*	*YLL007C*	
AAD16	*BRN1*	*DNL4*	*GIS4*	*KHR1*	*MSP1*	*PEP5*	*RDS2*	*SER2*	*STP3*	*USA1*	*YEL007Wb*	*YLL054C*	
AAD6	*BRO1*	*DOG1*	*GLC3*	*KIN2*	*MSS11*	*PET100*	*REC8*	*SFB2*	*STR3*	*USO1*	*YEL025C*	*YLL055W*	
AAP1	*BRR1*	*DON1*	*GLG1*	*KIP2*	*MSS4*	*PET112*	*REF2*	*SFI1*	*STU1*	*UTP20*	*YEL047C*	*YLL056C*	
ABC1	*BRR2*	*DPB4*	*GLN4*	*KIP3*	*MSY1*	*PET130*	*REH1*	*SFP1*	*SUC2*	*UTP22*	*YEL057C*	*YLL058W*	
ABM1	*BUB1*	*DPH1*	*GLY1*	*KNH1*	*MTD1*	*PEX14*	*REV3*	*SGA1*	*SUI3*	*UTP4*	*YER071C*	*YLR001C*	
ABZ1	*BUD27*	*DPS1*	*GMH1*	*KNS1*	*MTL1*	*PEX19*	*REX2*	*SGE1*	*SUM1*	*VAM10*	*YER076C*	*YLR040C*	
ACC1	*BUD4*	*DRS1*	*GNA1*	*KOG1*	*MTO1*	*PEX22*	*RFA1*	*SGM1*	*SUN4*	*VAM6*	*YER077C*	*YLR042C*	
ACN9	*BUG1*	*DSE4*	*GND1*	*KRE1*	*MTQ1*	*PEX27a*	*RGR1*	*SGN1*	*SUP35*	*VAM7*	*YER078C*	*YLR057W*	
ACO2	*BUL2*	*DSF1a*	*GND2*	*KRE33*	*MUC1*	*PEX28*	*RHO2*	*SGS1*	*SUT2a*	*VAS1*	*YER163C*	*YLR064W*	
ADE1	*CAD1*	*DSF2*	*GPB2*	*KTR2*	*MUP3*	*PEX29*	*RIB7*	*SHE10*	*SVL3*	*VHR1*	*YER184C*	*YLR065C*	
ADE3	*CAF4*	*DSL1*	*GPI15*	*KTR3*	*MUS81*	*PEX32*	*RIC1*	*SHE9*	*SWA2*	*VID21*	*YER185W*	*YLR072W*	
ADH4	*CAM1*	*DTR1*	*GPI18*	*KTR5*	*MYO1*	*PEX5*	*RIF1*	*SHP1*	*SWI1a*	*VID24*	*YFL041W-A*	*YLR137W*	
ADO1	*CAP2*	*DUN1*	*GRR1*	*LAA1*	*NAB3*	*PFA5*	*RIM101*	*SHQ1*	*SWI1b*	*VID28*	*YFL042C*	*YLR392C*	
ADR1a	*CAX4*	*DUO1*	*GSC2*	*LAG1*	*NAB6*	*PGD1*	*RIM15*	*SIN4*	*SWP82*	*VID30*	*YFL052W*	*YLR419W*	
ADR1b	*CBP6*	*DUR1*	*GSF2*	*LAP3*	*NAF1*	*PGU1a*	*RIM4*	*SIP3*	*SWR1*	*VIP1*	*YFL054C*	*YLR422W*	
AFG1	*CCC2*	*EAF7*	*GSG1*	*LAP4*	*NAM2*	*PGU1b*	*RIX1*	*SIR1*	*SYF1*	*VMR1*	*YFR016C*	*YLR460C*	
AFG2	*CCH1*	*EBS1*	*GSH1*	*LAS1*	*NAM9*	*PHA2*	*RLP7*	*SIS1*	*SYG1*	*VPS3*	*YFR018C*	*YMC1*	
AFG3	*CCP1*	*ECM14*	*GSY1*	*LAS21*	*NAN1*	*PHO23*	*RMD5*	*SIS2*	*SYN8*	*VPS33*	*YGL007C-A*	*YML020W*	
AGA1	*CDC1*	*ECM27*	*HAA1*	*LAT1*	*NAP1*	*PHO5*	*RMD6*	*SIT1*	*SYT1*	*VPS38*	*YGL015C*	*YML053C*	
AGA2	*CDC15*	*ECM29*	*HAL5*	*LDB16*	*NBP2*	*PHO8*	*RNH201*	*SIZ1*	*tA_UGC_E*	*VPS41*	*YGL036W*	*YML081W*	
AGC1	*CDC20*	*ECM31*	*HAP2*	*LRS4*	*NCL1*	*PHO81*	*RNH202*	*SKG1*	*TAD1*	*VPS5*	*YGL081W*	*YML082W*	
AGE1	*CDC27*	*ECM32*	*HDA2*	*LSB5*	*NCR1*	*PHO87*	*RNH70*	*SKG6*	*TAF1*	*VPS70*	*YGL114W*	*YMR1*	
AGE2	*CDC2a*	*ECM5*	*HED1*	*LSC2*	*NDC1*	*PHO91*	*RNQ1*	*SKI2*	*TAF2*	*VPS72*	*YGL138C*	*YMR185W*	
AGP3	*CDC4*	*EDE1*	*HEF3a*	*LSM2*	*NEM1*	*PIB2*	*RNR1*	*SKN7*	*TAF4*	*VPS73*	*YGL176C*	*YMR196W*	
AHA1	*CDC47*	*EDS1*	*HEF3b*	*LSR1*	*NHX1*	*PIH1*	*RNR3*	*SKP2*	*TAF6*	*VPS8*	*YGL185C*	*YMR206W*	
AIR1	*CDC48*	*EEB1*	*HEH2*	*LYS2*	*NIC96*	*PIK1*	*ROG1*	*SKY1*	*TAO3*	*VTC2*	*YGL230C*	*YMR210W*	
AKL1	*CDH1*	*EGT2*	*HEM1*	*LYS4*	*NIP1*	*PIM1*	*ROK1*	*SLA1*	*TAT1*	*WAR1*	*YGL231C*	*YMR247W-A*	
AKR1	*CDS1*	*EHT1*	*HEM14*	*LYS9*	*NIS1*	*PIN3*	*ROM2*	*SLC1*	*TCB2*	*XBP1*	*YGL250W*	*YMR253C*	
ALD3	*CEF1a*	*EKI1*	*HFA1*	*MAF1*	*NMA2*	*PIN4*	*ROT2*	*SLF1*	*TCB3*	*XKS1*	*YGP1*	*YMR315W*	
ALD5	*CEF1b*	*ELP2*	*HFM1*	*MAK10*	*NMD2*	*PKH3*	*RPB4*	*SLI1*	*TCO89*	*YAL018C*	*YGR015C*	*YMR317Wa*	
ALG1	*CFD1*	*ELP6*	*HIF1*	*MAK5*	*NMD4*	*PLM2*	*RPC19*	*SLO1*	*TDP1*	*YAL061W*	*YGR021W*	*YMR317Wb*	
ALG12	*CHC1*	*EMP46*	*HIM1*	*MAL11*	*NMD5*	*PMA1*	*RPI1*	*SMA1*	*TEL1*	*YAL064W-B-1*	*YGR031W*	*YND1*	
ALG3	*CHS2*	*EMP70a*	*HIR3*	*MAL13*	*NNF2*	*PMC1*	*RPL13A*	*SMF3*	*TEL2*	*YAL064W-B-2*	*YGR035W-A*	*YNL040W*	
ALK1	*CHS3*	*EMP70b*	*HKR1*	*MAL31*	*NOP13*	*PMD1*	*RPL18B*	*SMI1*	*TEN1*	*YAP1801*	*YGR111W*	*YNL050C*	
ALR2	*CHZ1*	*END3*	*HMG1*	*MAL32*	*NOP16*	*PMR1*	*RPL1B*	*SML1*	*TEX1*	*YAP1802*	*YGR117C*	*YNL086W*	
AMA1	*CIN8*	*ENP1*	*HMS2*	*MAM33*	*NOT3*	*PMS1*	*RPM2*	*SMY2*	*TFB2*	*YAP3*	*YGR122W*	*YNL092W*	
AMD1	*CIS1*	*ENT3*	*HMT1*	*MCH2*	*NPR2*	*PMT1*	*RPN14*	*SNF1*	*TFC3*	*YAP5*	*YGR125W*	*YNL115Cb*	
AMD2	*CIS3*	*EPS1*	*HOP1*	*MCM22*	*NSE1*	*PMT4*	*RPN4*	*SNF7*	*TFC6*	*YAP6*	*YGR203W*	*YNL146C-A*	
AMN1	*CLA4*	*ERD1*	*HOR2*	*MCM6*	*NST1*	*PMT6*	*RPN7*	*SNG1*	*TFC8*	*YAR023C*	*YGR237C*	*YNL211C*	
AMS1	*CLB1*	*ERG26*	*HOS3*	*MDJ1*	*NTE1*	*PNG1*	*RPP1*	*SNM1*	*TFG1*	*YAR028W*	*YGR250C*	*YNL217W*	
ANT1	*CLB6*	*ERG9*	*HOS4*	*MDJ2*	*NTF2*	*POA1*	*RPS26B*	*snR19*	*TGL4*	*YAR029W*	*YGR266W*	*YNL247W*	
APC1	*CLN1*	*ERI1*	*HRB1*	*MDL2*	*NTH1*	*POG1*	*RPS4B*	*snR32*	*THG1*	*YAT2*	*YGR273C*	*YNL254C*	
APC4	*CMD1*	*ERR3-1*	*HRK1a*	*MDM1*	*NTH2*	*POL2*	*RPS8A*	*snR34*	*THI2*	*YBL029W*	*YGR287C-1*	*YNL305C*	
APJ1	*CNE1*	*ERV1*	*HSE1*	*MDM10*	*NTR1*	*POL32*	*RRF1*	*snR43*	*THI22*	*YBL054W*	*YHB1*	*YNL320W*	
APL3	*CNM67*	*ERV29*	*HSP26*	*MDM30*	*NUM1a*	*POL4*	*RRM3*	*snR44*	*THI3*	*YBL060W*	*YHL008C*	*YNL321W*	
APL5	*COG1*	*ERV41*	*HSP78*	*MDM36*	*NUP1*	*POL5*	*RRN6*	*snR80*	*THI74*	*YBL086C*	*YHL010C*	*YNR014W*	
APM1	*COG2*	*ESC2*	*HST2*	*MDR1*	*NUP133*	*POP1*	*RRP12a*	*SNT2*	*THO1*	*YBL095W*	*YHL029C*	*YNR036C*	
APM2	*COG5*	*ESF1*	*HTD2*	*MDS3*	*NUP145*	*POP6*	*RRP15*	*SNU71*	*THR4*	*YBP2*	*YHL039W*	*YNR062C*	
APQ12	*COG6*	*ESP1*	*HUT1*	*MEP2*	*NUP159*	*POT1*	*RRP3*	*SNX41*	*THS1*	*YBR014C*	*YHR003C*	*YNR070W*	
ARC1	*COG8*	*ETR1*	*HXT1*	*MEP3*	*NUP170*	*PPM1*	*RSA1*	*SOK1*	*tI_AAU_G*	*YBR030W*	*YHR009C*	*YOL155W-A*	
ARC15	*COS111*	*EUG1*	*HXT10*	*MET1*	*NUP49*	*PPN1*	*RSC3*	*SOK2*	*TIF35*	*YBR053C*	*YHR032W*	*YOL159C*	
ARE2	*COS7*	*FAA3*	*HXT11-1a*	*MET12*	*NUP60*	*PPS1*	*RSC30*	*SOL2*	*TIF4632*	*YBR056W*	*YHR033W*	*YOL159C-A*	
ARG4	*COX19*	*FAB1*	*HXT11-1b*	*MET18*	*NYV1*	*PPZ2*	*RSC58*	*SOM1*	*TIM44*	*YBR071W*	*YHR045W*	*YOR097C*	
ARG5	*CPA2*	*FAF1*	*HXT4*	*MET28*	*OAF1*	*PRB1*	*RSC8*	*SPA2*	*TIP20*	*YBR074W*	*YHR080C*	*YOR1*	
ARG81	*CPR8*	*FAU1*	*HXT5b*	*MET3b*	*OAF3*	*PRE6*	*RSF2*	*SPC105*	*TIR1*	*YBR085C-A*	*YHR113W*	*YOR389W-1*	
ARG82	*CRC1*	*FCY22a*	*HXT6*	*MET4*	*OCA6*	*PRM1*	*RSM26*	*SPC110*	*TIR3*	*YBR090C*	*YHR140W*	*YOR390W-1*	
ARN1	*CRM1*	*FCY22b*	*HXT7*	*MEX67*	*ODC1*	*PRM2*	*RSM28*	*SPC3*	*TKL1*	*YBR108W*	*YHR182W*	*YPL009C*	
ARO80	*CSE1*	*FET4*	*ICR1*	*MGA1*	*OLE1*	*PRM5*	*RTA1*	*SPC72*	*tL_CAA_G3*	*YBR147W*	*YHR202W*	*YPL030W*	
ARP2	*CSF1*	*FHL1*	*ICT1*	*MGR2*	*OMS1*	*PRM6*	*RTF1*	*SPG1*	*TLC1*	*YBR225W*	*YIL029C*	*YPL033C*	
ARX1	*CST6*	*FIG4*	*ICY2*	*MID1*	*OPI1*	*PRM9*	*RTN1*	*SPO1*	*TMA17*	*YBR241C*	*YIL039W*	*YPL038W-A*	
ASF1	*CTA1*	*FIR1*	*IDP1*	*MIG1*	*OPT2-1*	*PRO1*	*RTT103*	*SPO11*	*TMA64*	*YBR246W*	*YIL055C*	*YPL105C*	
ASG1	*CTF19*	*FKH2*	*IDS2*	*MIG3*	*OPT2-4a*	*PRP11*	*RTT107*	*SPO14*	*TNA1*	*YBR259W*	*YIL083C*	*YPL141C*	
ASI3a	*CTF3*	*FKS3*	*IES1*	*MIP1*	*OPY2*	*PRP16*	*RXT3*	*SPO20*	*TOM1*	*YCF1*	*YIL089W*	*YPL158C*	
ASK10	*CTF4*	*FLC3*	*IKI1*	*MKK2*	*ORC3*	*PRP21*	*SAC3*	*SPO23*	*TOM20*	*YCG1*	*YIL091C*	*YPL216W*	
ATF2	*CTL1*	*FLO19*	*IKI3*	*MKS1*	*ORC4*	*PRP22*	*SAC7*	*SPO71*	*TOM71*	*YCL045C*	*YIL102C*	*YPL230W*	
ATG2	*CTS2*	*FLO5*	*IMD2-1*	*MLF3*	*OSH2a*	*PRP43*	*SAL1*	*SPO75*	*tP_UGG_N2*	*YCL047C*	*YIL152W*	*YPL260W*	
ATG4	*CTT1*	*FLR1*	*IMD2-2*	*MLH2*	*OSH2b*	*PRP5*	*SAP4*	*SPP41*	*TPC1*	*YCR015C*	*YIL158W*	*YPL272C*	
ATO2	*CUE3*	*FMP10*	*IMD4*	*MLH3*	*OSH7*	*PRP6*	*SAS3*	*SPS1*	*TPD3*	*YCR016W*	*YIL161W*	*YPP1*	
ATP1	*CUS1*	*FMP13*	*IME4*	*MLP1*	*OSW2*	*PRP9*	*SAS4*	*SPT16*	*TPK1*	*YCR051W*	*YIL166C*	*YPR003C*	
ATP4	*CWC23*	*FMP14*	*IML1*	*MMP1a*	*PAB1*	*PSK1*	*SAT4*	*SPT2*	*TPS2*	*YDJ1*	*YIP5a*	*YPR013C*	

No. 77				
00473	*ELG1*	*MDL2*	*RPC19*	*VAM10*
00774	*ELP3*	*MDM1*	*RPL17B*	*VAM7*
02411	*ENP1*	*MED6*	*RPL1B*	*VHS3*
03371	*ERI1*	*MEI5*	*RPL28*	*VID30*
03725	*ERR3-1*	*MEP2*	*RPM2*	*VPS5*
03783	*ERS1*	*MET3a*	*RPS26B*	*WAR1*
04475	*ERV41*	*MET3b*	*RRI1*	*YAL064W-B-1*
04496	*FAA1*	*MEX67*	*RRN6*	*YAP1801*
06158	*FAA2*	*MIP1*	*RSA1*	*YAR068W-2*
06340	*FAR1*	*MKK2*	*RSC30*	*YBR025C*
06488	*FAS2*	*MLH3*	*RSC6*	*YBR147W*
AAD16	*FAT1*	*MMS1*	*RSC8*	*YBR184W*
ABP140	*FCY21*	*MMT2*	*RSF2*	*YBR225W*
ACO2	*FET3*	*MNL1*	*RSP5*	*YBR238C*
ADH4	*FMO1*	*MNN5*	*RTA1*	*YBR241C*
ADP1	*FMP26*	*MON2*	*RTG3*	*YBR246W*
ADR1a	*FRM2*	*MOT1a*	*RTT107*	*YCK1*
AGA2	*FSH2*	*MRC1*	*RUP1*	*YCL045C*
AGC1	*FUM1*	*MRD1*	*SAP190a*	*YCL047C*
AGP1	*FUS1*	*MRE11*	*SAP4*	*YCR015C*
ALD3	*FYV10*	*MRK1*	*SAT4*	*YCR016W*
ALG7	*FZF1*	*MRN1*	*SCW11*	*YCR023C*
ALK2	*FZO1*	*MSH1*	*SDA1*	*YCR051W*
ALR2	*GAL11*	*MSY1*	*SDS24*	*YDJ1*
AMD1	*GAL4a*	*NAB2*	*SEC15*	*YDR056C*
AMN1	*GAR1*	*NAB3*	*SEC26*	*YDR109C*
APC1	*GDH3*	*NAB6*	*SEC65*	*YER185W*
APL5	*GDT1*	*NAF1*	*SED4*	*YFL052W*
APM1	*GIN4*	*NAM9*	*SEO1*	*YFL054C*
ARG81	*GLN4*	*NAN1*	*SET1*	*YGL185C*
ARN2	*GSF2*	*NDC1*	*SET2*	*YGL230C*
ARO9	*GSH1*	*NDT80*	*SET6*	*YGL231C*
ARP1	*HAL5*	*NMD2*	*SGE1*	*YGL250W*
ARP2	*HAP2*	*NMD5*	*SKG6*	*YGP1*
ASF1	*HFA1*	*NOP13*	*SKI2*	*YGR053C*
ASI1	*HHO1*	*NPL4*	*SLC1*	*YGRO12W*
ATG15	*HIR3*	*NST1*	*SML1*	*YHI9a*
ATR1	*HIS2*	*NTE1*	*SMY2*	*YHR022C*
AWA1	*HIS4*	*NUP1*	*SNF5*	*YHR080C*
AYT1	*HMG1*	*NUP192*	*snR32*	*YHR113W*
BAR1	*HMI1*	*ODC1*	*snR43*	*YHR140W*
BEM3	*HOC1*	*OPT2-1*	*SNU66*	*YHR159Wa*
BET5	*HRK1a*	*OPT2-4a*	*SOL2*	*YIL091C*
BIO5	*HSM3*	*ORM1*	*SPO20*	*YIL108W*
BIR1	*HSP30*	*PAM1*	*SPO22*	*YIL152W*
BNA2	*HSP82*	*PAN2*	*SPO23*	*YIL166C*
BNI4	*HST4*	*PAT1*	*SPS100*	*YJL068C*
BNR1	*HUT1*	*PBP2*	*SPT16*	*YJL070C*
BPH1	*HXT1*	*PBS2*	*SRO77*	*YJL163C*
BTN2	*HXT11-1b*	*PCH2*	*SRP40*	*YJL185C*
BUD4	*HXT4*	*PCL8*	*SRP54*	*YJR079W*
BUD5	*HXT5a*	*PDI1*	*SSE1*	*YJR088C*
BUL2	*HXT5b*	*PDR3*	*SSK22*	*YKR077W*
CBF5	*ICY2*	*PEP5*	*SSN2*	*YLL029W*
CDC11	*IDS2*	*PES4*	*SSQ1*	*YLL054C*
CDC13	*ILS1*	*PET130*	*STE12*	*YLL055W*
CDC47	*IMD2-2*	*PEX27a*	*STE50*	*YLL056C*
CIS3	*IMD4*	*PEX28*	*STR3*	*YLR137W*
CLA4	*IME4*	*PEX32*	*STT4a*	*YLR446Wa*
CLB1	*IML1*	*PEX5*	*SUC2*	*YML020W*
CNM67	*IMP1*	*PFS1*	*SUS1*	*YML053C*
COG3	*INO80*	*PGD1*	*SWA2*	*YML081W*
COG8	*INP52*	*PHO23*	*SWI5*	*YML082W*
COQ4	*IPL1*	*PHO87*	*SWM1*	*YMR098C*
COS111	*IRA1*	*PIB2*	*SWT1*	*YMR185W*
COX23	*IRC10*	*PKH3*	*SYP1*	*YMR259C*
CRC1	*ISW1*	*PMD1*	*TAF2*	*YMR278W*
CRM1	*IWR1*	*PMR1*	*TCB2*	*YMR291W*
CSE1	*IXR1*	*PNG1*	*TCB3*	*YNL086W*
CSF1	*JEM1*	*POL4*	*TCO89*	*YNL115Cb*
CTR86	*JLP1*	*PRE6*	*TDP1*	*YNL146C-A*
CUE3	*KAP122*	*PRM6*	*TEL2*	*YNR062C*
CUS1	*KAP95*	*PRP21*	*TGL5*	*YNR070W*
CWC2	*KAR4*	*PRP5*	*THI2*	*YOL047C*
CWH43	*KAR5*	*PRP8*	*THP1*	*YOL057W*
DAK1	*KEL1*	*PSK1*	*THR4*	*YOR097C*
DAN4a	*KES1*	*PTK2*	*TIF2*	*YOR112W*
DAT1	*KEX1*	*PUS1*	*TIM11*	*YOR129C*
DBP6	*KGD1*	*PUS4*	*TMA108*	*YOR152C*
DEM1	*KHA1*	*PUS9*	*TOM71*	*YOR389W-1*
DER1	*KIP2*	*PWP2*	*TPK1*	*YOR390W-1*
DMA1	*KIP3*	*RAD27*	*TPS1*	*YPL141C*
DMA2	*KOG1*	*RAV1*	*TRA1*	*YPL158C*
DNA2	*KRE33*	*RCY1*	*TRE2*	*YPL216W*
DNL4	*KSP1*	*RDN37-1*	*TRK1a*	*YPL230W*
DON1	*KTR3*	*REF2*	*TRM11*	*YPL260W*
DOT1	*LAA1*	*RER2*	*TRP5*	*YPR089Wb*
DPB2	*LAG1*	*RHO1*	*TRS120*	*YPR097W*
DRS2	*LAP4*	*RHO2*	*TRS20*	*YSC84*
DSE4	*LAS21*	*RIB4*	*TRS33*	*ZDS2*
DSN1	*LCB1*	*RIB7*	*TYW1*	*ZIP1*
DTR1	*LDB16*	*RIF1*	*UBA1*	*ZIP2*
DUR1	*LIN1*	*RIM15*	*UBI4*	*ZRT1*
DYS1	*LSB5*	*RKR1*	*UBP14*	*ZSP1*
EAF3	*LSM2*	*RMD5*	*UBP7*	
EAF7	*LSR1*	*RNH201*	*UFD4*	
ECM14	*LTE1*	*RNQ1*	*UPC2*	
ECM31	*MAK5*	*ROK1*	*URA2*	
EEB1	*MAL11*	*ROT2*	*USA1*	
EHT1	*MCH2*	*RPB4*	*UTP22*	

Detection of GID gene mutations in strain No. 28 and No. 77 To identify the genes responsible for high malate production, genomic DNAs extracted from the cells of No. 28 and No. 77 strains were subjected to whole genome sequencing analysis. In this analysis, 2495 non-synonymous substitutions in 1327 genes were observed in the genome of strain No. 28, as compared to the K-7 genome. In the No. 77 genome, 689 non-synonymous substitutions in 494 genes were detected (Table 4-4). Since these strains had an enormous number of mutations, we started with evaluation of mutations in GID genes, which caused high malate production in case of a functional deficiency. As a result, we observed that strain No. 28 had nonsense substitution each in *RMD5* and *VID24*, and missense substitution each in *VID30*, *VID28*, and *FYV10*. Strain No. 77 harbored nonsense substitution in *GID2*, and missense substitution each in *VID30* and *FYV10* (Table 4-5). The mutations of *VID30* and *RMD5* were common in strain No. 28 and No. 77. The zygosity of the *RMD5* mutation was different between these strains.

Table 4-5 Mutations of GID protein-coding genes in strain No. 28 and No. 77 genomes as compared to the K-7 genome

Gene name	Systematic gene name	Base substitution	Amino acid change	Zygosity	
				No.28	No.77
VID30/*GID1*	*YGL227W*	2353G>A	V785I	Homozygous	Homozygous
		2449G>A	V817M	Homozygous	Homozygous
RMD5/*GID2*	*YDR255C*	263G>A	W88^{amber}	Heterozygous	Homozygous
VID24/*GID4*	*YBR105C*	85G>T	E29^{ochre}	Homozygous	-
VID28/*GID5*	*YIL017C*	671T>C	L224P	Homozygous	-
FYV10/*GID9*	*YIL097W*	1096G>A	D366N	-	Heterozygous
		1161A>G	I387M	Homozygous	-

A mutation in the GID gene responsible for high malate production Individual haploid mutants with GID gene substitutions were constructed (Table 4-1). In addition, strains in which only *kanMX4* module was induced were also prepared, to assess the effect of the insertion of the marker gene immediately after the stop codon of GID genes. The YM10 cultivation test was performed using point mutants. The amount of malate produced by 4011a-mRMD5 and 4011a-mVID24 was higher than that produced by the

respective control strain (Fig. 4-4). This result suggested that the heterozygous mutation in *RMD5* and/or homozygous mutation in *VID24* led to the high-malate-producing phenotype in strain No. 28, and the homozygous nonsense substitution in *RMD5* resulted in the phenotype in strain No. 77. The insertion of the marker gene had no effect on malate production.

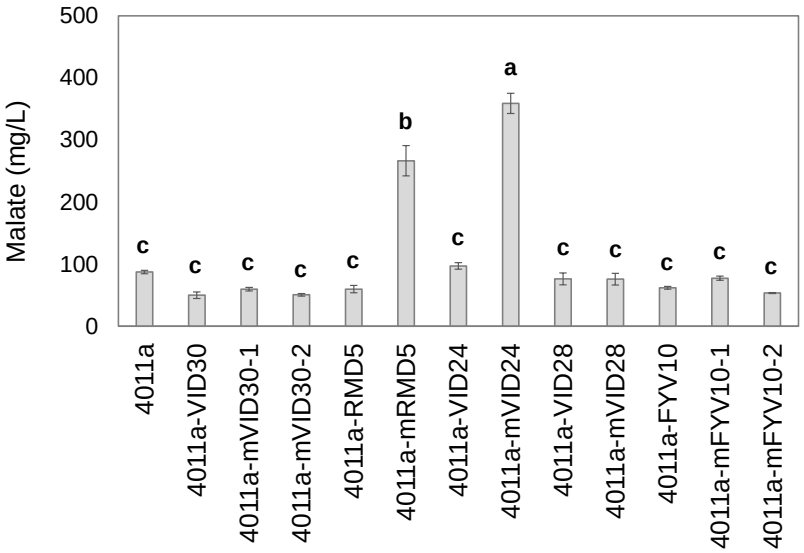

Fig. 4-4 Malate production by the GID gene-point mutants and their control strains in the YM10 cultivation test. All the cultivation tests were repeated in triplicate. Each error bar represents standard deviation. Data were analyzed by the Tukey-Kramer test. Same letters indicate that there was no statistically significant difference among the strains ($p < 0.05$).

Complementation tests of GID genes in strain No. 28 and No. 77 It was not certain that the high malate production by strain No. 28 and No. 77 was attributed to the substitutions in *RMD5* and *VID24* genes, since the strains possessed numerous mutations in addition to GID gene mutations (Table 4-4). To confirm whether the mutations in *RMD5* and *VID24* genes are responsible for the high malate production in these strains, *RMD5* gene containing the 263 G>A mutation and *VID24* gene containing the 85 G>T mutation in the No. 28 and No. 77 genomes were replaced with the wild-type *RMD5* and *VID24*, respectively, derived from the K-7 genome. To evaluate the genotype of the GID

gene mutation, heterozygous mutants and homozygous complementary strains were constructed (Table 4-1). For instance, the wild-type *VID24* was introduced into strain No. 28, and *VID24*-heterozygous mutant No. 28-mG2/G2-mG4/G4 and *VID24*-homozygous wild-type strain No. 28-mG2/G2-G4/G4 were obtained. Further, the wild-type *RMD5* was introduced into strain No. 77, and heterozygous mutant No. 77-mG2/G2 and homozygous wild-type strain No. 77-G2/G2 were obtained (Fig. 4-2). The complementary strains were cultivated in YM10, during which the concentration of malate was measured (Fig. 4-5). The amount of malate produced by *VID24*-heterozygous mutants No. 28-mG2/G2-mG4/G4 and No. 28-G2/G2-mG4/G4 was lower than that produced by strain No. 28. In addition, the malate level appeared to decrease in the *VID24* wild-type strains No. 28-mG2/G2-G4/G4 and No. 28-G2/G2-G4/G4 as compared to the malate level in the *VID24*-heterozygous mutants. This result showed that the nonsense mutation in *VID24* was the single cause for high malate production in strain No. 28, and was semi-dominant as seen in Chapter II. On the other hand, the level of malate observed in *RMD5* wild-type strain No. 77-G2/G2 was lower than that in strain No. 77, and was identical to that in *RMD5*-heterozygous mutant No. 77-mG2/G2. This data indicated that the nonsense mutation in *RMD5* was responsible for high malate production in strain No. 77, and the heterozygous mutation of the *RMD5* gene was recessive.

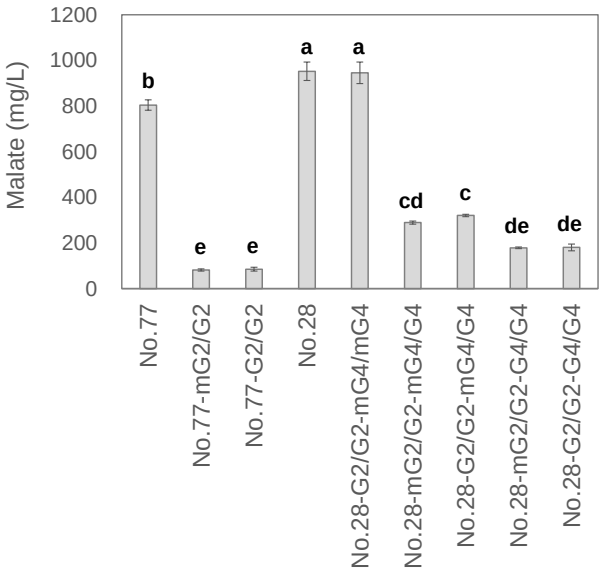

Fig. 4-5 Malate production by *GID* gene-complemented strains and their control strains in the YM10 cultivation test. All the cultivation tests were repeated in triplicate. Each error bar represents standard deviation. Data were analyzed by the Tukey-Kramer test. Same letters indicate that there was no statistically significant difference among the strains ($p < 0.05$).

DISCUSSION

The mechanisms for increasing malate production in two sake yeast strains distributed by the Brewing Society of Japan were investigated. The nonsense mutations of *VID24* and *RMD5* genes in strains No. 28 and No. 77, respectively, were identified as being responsible for the increase in malate production. These genes encoded the subunits of GID complex, which plays a role in the degradation of gluconeogenic enzymes such as fructose-1,6-bisphosphatase (Fbp1), phosphoenolpyruvate carboxykinase, and Mdh2 (16, 17). The author reported that the disruptants of *VID30*, *RMD5*, *UBC8*, *VID24*, *VID28*, *GID8*, and *FYV10* produced high quantities of malate, and the high malate production in the strain *vid24*Δ was attributed to facilitation of the conversion of oxaloacetate to malate by the accumulation of intracellular Mdh2 protein (Chapter III). Furthermore, the disruption of *VID30*, *RMD5*, *VID24*, *VID28*, *GID8*, and *FYV10* was known to result in the accumulation of Mdh2, regardless of the addition of glucose (16). These data indicated that high malate production in strain No. 28 and No. 77 results from the accumulation of Mdh2 due to dysfunction of Vid24 and Rmd5 proteins, respectively. Previous studies suggested that mitochondrial activity was suppressed in strain No. 28, resulting in high malate production (15). Based on the assumption that a high malate production in strain No. 28 was attributed to the dysfunction of Vid24, it was presumed that the reduction of mitochondrial activity in strain No. 28 resulted from increased intracellular malate levels. Mitochondrial function is diminished under acidic conditions in the cytoplasm by the generation of reactive oxygen species (82).

The homozygous nonsense mutation of *RMD5* in strain No. 77 led to high malate production. In contrast, the heterozygous mutation of *RMD5* in strain No. 28 brought no change to malate production levels (Fig. 4-5). These results indicated that the heterozygous *RMD5* 263G>A mutation was recessive. On the other hand, the *VID24* mutation was considerd to be semi-dominant for malate production (Chapter II), and the present data supported this notion (Fig. 4-5). The distinction was considered to be derived from different expression patterns between Rmd5 and Vid24 proteins. Rmd5 protein is constitutively expressed regardless of the presence of glucose, while Vid24 protein is only

expressed upon the addition of glucose to cells living under glucose depleted conditions (22). Vid24 is tightly regulated on the transcriptional and protein level by the carbon source, in order to control proper functioning of the GID complex (64). Therefore, the ploidy of the functional *VID24* gene might affect the expression level. These features of expression could determine whether the heterozygous mutations are semi-dominant or recessive.

Strain No. 28 and No. 77 possessed a large number of substitutions in their genomes as compared to the K-7 genome. According to complementation tests, *VID24* and *RMD5* gene mutations were the sole cause for high malate production in strain No. 28 and No. 77, respectively (Fig. 4-5). Strain No. 77 showed lower malate production than strain No. 28 (Table 4-3). Furthermore, the malate productivity of 4011a-mRMD5 was lower as compared to that of 4011a-mVID24 (Fig. 4-4), although the disruptant of *RMD5* exhibited similar malate production levels as the disruptant of *VID24* in Chapter III. These data suggested that the nonsense substitution of $W88^{amber}$ did not completely impair the function of Rmd5 protein. Rmd5 protein has a RING domain at amino acid residues 361 to 404, which is essential for the polyubiquitination of Fbp1 (17). The nonsense substitution appeared to result in a complete loss of Rmd5 function, but the truncated Rmd5 might partly retain its ability to degrade gluconeogenic enzymes.

In the present study, the author revealed that high malate production in both industrial sake yeast strains No. 28 and No. 77 was acquired due to mutation of GID protein-coding genes. A mutation in *VID24* was identified in Chapter I as being responsible for the high malate phenotype in another sake yeast strain, K-901H. K-901H, and the strain No. 28 and No. 77, differed in the procedures of isolation (10, Chapter I). Nevertheless, the mechanisms for high malate production were nearly identical in these strains. It is assumed that mutations of GID genes occur frequently as a result of high malate productivity in industrial sake yeast. One possibility is that the process of breeding high-malate-producing yeast, in which the candidate strains are generally selected based on their superior growth, ethanol fermentation, and malate production, may bring about the assumed phenomena. Suppression of mitochondrial activity or deficiency of peroxisome homeostasis, which are known to be involved in high malate production (4,

14, Chapter V), could give rise to a reduction in various stress tolerances of yeast under brewing conditions, resulting in reduced ethanol production. The functions of mitochondria and peroxisome are known to be necessary for adaptation to various stresses (82-84). On the other hand, GID mutations are likely not to affect growth as compared to mitochondrial dysfunction or peroxisomal defect, since gluconeogenesis proteins appear to have no negative impact on growth and ethanol production in yeast during fermentation. A detailed analysis of the production capacity of ethanol and other compounds in yeast that affect the taste of sake, as well as understanding organic acid production, is important for sake brewing. Since identification of the mutated gene responsible for malate production leads to suggestions for the brewing characteristics in strains No. 28 and No. 77, the finding will be useful for the process of sake brewing using these industrial strains.

SUMMARY

High-malate-producing yeast strain No. 28 and No. 77 have been developed by the Brewing Society of Japan. In this study, the genes responsible for the high malate phenotype in these strains were investigated. The author had found in Chapter III that the deletion of components of the GID complex led to high malate production in yeast. Upon examining GID protein-coding genes in yeast strain No. 28 and No. 77, a nonsense homozygous mutation of *VID24* in strain No. 28, and of *RMD5* in strain No. 77, were identified as the cause of high malate production. Furthermore, complementary tests of these mutations indicated that the heterozygous nonsense mutation in *RMD5* was recessive. In contrast, the heterozygous nonsense mutation in *VID24* was considered semi-dominant.

Chapter V

Mutation in the peroxin-coding gene *PEX22* contributing to high malate production in *Saccharomyces cerevisiae*

Most organic acids present in sake, such as malate, succinate, and acetate, are produced by the yeast *Saccharomyces cerevisiae* during fermentation. Among them, malate is synthesized from glucose via three metabolic pathways in yeast: an oxidative pathway in the TCA cycle for aerobic metabolism, an alternate oxidative pathway via the glyoxylate cycle, and a reductive pathway in the cytosol for anaerobic metabolism (5-7, 27). A large proportion of malate in sake mash is known to be generated by the reduction of oxaloacetate due to anaerobic conditions during alcoholic fermentation (4). This reaction is catalyzed by the cytosolic malate dehydrogenase (Mdh2) (41). Two isozymes for malate dehydrogenase isozymes (Mdh1 and Mdh3) are also present in *S. cerevisiae*. Mdh1p is localized in the mitochondria and is involved in the oxidative TCA cycle, while Mdh3p is localized in peroxisomes and is involved in the glyoxylate cycle (85). Much attention has been focused on the effect of malate dehydrogenase present in the cytosol on malate production under anaerobic conditions during sake brewing (4, 5, 11, 12).

Since malate has a desirable sour taste (8), various methods have been developed for breeding high malate-producing yeast strains (9, 12, 13, 56). Additionally, many studies have reported the mechanisms resulting in the high malate phenotype using several mutants. For example, a decrease in the mitochondrial activity in yeast was observed to have an immense influence on the production of malate (4, 14, 15). Other studies reported that the up-regulation of transcription of *MDH2* gene resulted in high malate production (12, 13). Furthermore, the down-regulation of genes of the thiamine biosynthesis pathway was also responsible for high malate production (86). The gene mutations responsible for high malate production in these strains are yet to be determined. In Chapter I, the author isolated a high-malate-producing strain based on its sensitivity towards DMS, and then revealed that a missense mutation in the *VID24* was responsible for the high-malate-producing phenotype. The primary traits responsible for the ability of above-mentioned strains to yield high levels of malate are expected to be different from those of the *VID24*

mutant. Thus, there are various mechanisms for increasing the production of malate in yeast, each of which is characterized by different gene mutations.

In the current study, the author isolated another high-malate-producing yeast strain F-701H. Interestingly, F-701H harbored no mutations in *VID24*, despite being isolated on the basis of DMS sensitivity. To elucidate the mechanisms underlying enhanced malate production in the industrial sake yeast strains, other than those mediated by *VID24* mutation, gene mutations present in the high-malate phenotypes were investigated in strain F-701H. As a result, the author observed a mutation in the *PEX22* gene, which is classified as a peroxin gene involved in the regulation of peroxisome biogenesis (87, 88), resulting in high malate production. The research indicated that the deficiency of Pex22 prevented Mdh3, a peroxisomal matrix protein, from localizing to the peroxisomes, thereby promoting the production of malate in the yeast cytoplasm.

MATERIALS AND METHODS

Media and yeast strains Yeast cells were cultured in yeast extract peptone dextrose (YPD) medium [yeast extract (10 g/L), polypeptone (20 g/l), and glucose (20 g/L], yeast malt (YM) medium [YM10; yeast extract (3 g/L), malt extract (3 g/L), polypeptone (5 g/L), and glucose (100 g/L)], synthetic defined medium lacking uracil [SD – ura; yeast nitrogen base without amino acids (YNB w/o AA, 6.7 g/L; Becton Dickinson and Company, Franklin Lakes, NJ, USA), complete supplement mixture – ura (0.77 g/L; MP Biomedicals, Solon, OH, USA) and glucose (20 g/L)], 5-fluoroorotic acid (5-FOA) medium [5-FOA (1 g/L), uracil (20 mg/L), YNB w/o AA (6.7 g/L), and glucose (20 g/L)], or synthetic defined complete medium lacking uracil [SDC – ura; YNB w/o AA (6.7 g/L), complete supplement mixture – ura (0.77 g/L), casamino acids (20 g/L), and glucose (20g/L)].

The media used for evaluating DMS sensitivity included Dropout Base (DOB) medium [YNB w/o AA (6.7 g/L) and glucose (20 g/L)] or DMS medium [YNB w/o AA (6.7 g/L), glucose (20 g/L), and DMS (15 g/L)].

The sake yeast strain F-701 was isolated from the strain Kyokai no. 701 (K-701) by

examining its tolerance towards 5, 5, 5-trifluoro-DL-leucine as described previously (89). The high-malate-producing strain F-701H was obtained from the strain F-701 using ethyl methyl sulfonate and DMS (9).

Disruptants derived from the strain BY4743 were obtained from the Yeast Knock Out Homozygous Diploid Collection (YSC1056; Thermo Fisher Scientific Inc., Waltham, MA, USA) (Table 5-1).

Disruption of the *PEX22*, *MDH1*, *MDH2*, *MDH3*, *MLS1*, *MLS2*, or *CIT2* genes in the *MAT***a** uracil auxotroph strain GX-11 was performed by a PCR-based method using the primers listed in Table 5-2, a *kanMX4* module-carrying plasmid (35), and PrimeSTAR Max DNA Polymerase (Takara Bio Inc., Otsu, Japan). Yeast transformations were performed using the lithium acetate method (36). The disruptants are listed in Table 5-1.

Comparison of growth in DMS medium Yeast strains were cultivated aerobically in YPD medium at 30 °C for 24 h. For comparing DMS sensitivity of the sake yeast strains derived from K-701, the cells were collected and resuspended in DOB or DMS medium, to an optical density (at 660 nm) of 0.01. Cell suspension cultures were incubated aerobically at 30°C, and their cell densities were measured with a Bio-Photorecorder (Advantec Toyo Co. Ltd., Tokyo, Japan).

YM10 cultivation test Yeast cells were cultivated aerobically in YPD medium at 30 °C for 24 h and harvested by centrifugation (4000 × *g*, 5 min, 4 °C). The cells were resuspended in YM10 medium to an optical density (at 660 nm) of 0.1. The culture was incubated at 30 °C for 4 days without shaking. The amount of organic acids was measured using the high-performance liquid chromatography-based Organic Acid Analysis System (Shimadzu Co. Ltd., Kyoto, Japan).

One-step sake brewing test The sake brewing test and analysis of the supernatant from the sake mash were carried out as described in Chapter I.

Table 5-1 Genotypes and references of *S. cerevisiae* strains used in this study

Strain	Genotype	Reference
K-701	*MAT***a**/*MAT*α	Brewing Society of Japan
F-701	K-701 *PEX22* 374G>A/*PEX22*	This study
F-701H	K-701 *PEX22* 374G>A/*PEX22* 374G>A	This study
F-701H-PEX22	K-701 *PEX22* 374G>A/*PEX22-kanMX4*	This study
BY4743	*MAT***a**/*MAT*α *his3Δ1/his3Δ1 leu2Δ0/leu2Δ0 LYS2/lys2Δ0 met15Δ0/MET15 ura3Δ0/ura3Δ0*	Thermo Fisher Scientific Inc.
BY4743 *pex22*Δ	BY4743 *pex22*::*kanMX4*/*pex22*::*kanMX4*	Thermo Fisher Scientific Inc.
BY4743 *cdc19*Δhetero	BY4743 *cdc19*::*kanMX4*/*CDC19*	Thermo Fisher Scientific Inc.
BY4743 *fun12*Δ	BY4743 *fun12*::*kanMX4*/*fun12*::*kanMX4*	Thermo Fisher Scientific Inc.
BY4743 *dse1*Δ	BY4743 *dse1*::*kanMX4*/*dse1*::*kanMX4*	Thermo Fisher Scientific Inc.
BY4743 *oye2*Δ	BY4743 *oye2*::*kanMX4*/*oye2*::*kanMX4*	Thermo Fisher Scientific Inc.
BY4743 *ayr1*Δ	BY4743 *ayr1*::*kanMX4*/*ayr1*::*kanMX4*	Thermo Fisher Scientific Inc.
BY4743 *nup100*Δ	BY4743 *nup100*::*kanMX4*/*nup100*::*kanMX4*	Thermo Fisher Scientific Inc.
BY4743 *coq9*Δ	BY4743 *coq9*::*kanMX4*/*coq9*::*kanMX4*	Thermo Fisher Scientific Inc.
BY4743 *pex1*Δ	BY4743 *pex1*::*kanMX4*/*pex1*::*kanMX4*	Thermo Fisher Scientific Inc.
BY4743 *pex2*Δ	BY4743 *pex2*::*kanMX4*/*pex2*::*kanMX4*	Thermo Fisher Scientific Inc.
BY4743 *pex3*Δ	BY4743 *pex3*::*kanMX4*/*pex3*::*kanMX4*	Thermo Fisher Scientific Inc.
BY4743 *pex4*Δ	BY4743 *pex1*::*kanMX4*/*pex4*::*kanMX4*	Thermo Fisher Scientific Inc.
BY4743 *pex5*Δ	BY4743 *pex5*::*kanMX4*/*pex5*::*kanMX4*	Thermo Fisher Scientific Inc.
BY4743 *pex6*Δ	BY4743 *pex6*::*kanMX4*/*pex6*::*kanMX4*	Thermo Fisher Scientific Inc.
BY4743 *pex7*Δ	BY4743 *pex7*::*kanMX4*/*pex7*::*kanMX4*	Thermo Fisher Scientific Inc.
BY4743 *pex8*Δ	BY4743 *pex8*::*kanMX4*/*pex8*::*kanMX4*	Thermo Fisher Scientific Inc.
BY4743 *pex9*Δ	BY4743 *pex9*::*kanMX4*/*pex9*::*kanMX4*	Thermo Fisher Scientific Inc.
BY4743 *pex10*Δ	BY4743 *pex10*::*kanMX4*/*pex10*::*kanMX4*	Thermo Fisher Scientific Inc.
BY4743 *pex11*Δ	BY4743 *pex11*::*kanMX4*/*pex11*::*kanMX4*	Thermo Fisher Scientific Inc.
BY4743 *pex12*Δ	BY4743 *pex12*::*kanMX4*/*pex12*::*kanMX4*	Thermo Fisher Scientific Inc.
BY4743 *pex13*Δ	BY4743 *pex13*::*kanMX4*/*pex13*::*kanMX4*	Thermo Fisher Scientific Inc.
BY4743 *pex14*Δ	BY4743 *pex14*::*kanMX4*/*pex14*::*kanMX4*	Thermo Fisher Scientific Inc.
BY4743 *pex15*Δ	BY4743 *pex15*::*kanMX4*/*pex15*::*kanMX4*	Thermo Fisher Scientific Inc.
BY4743 *pex17*Δ	BY4743 *pex17*::*kanMX4*/*pex17*::*kanMX4*	Thermo Fisher Scientific Inc.
BY4743 *pex18*Δ	BY4743 *pex18*::*kanMX4 pex18*::*kanMX4*	Thermo Fisher Scientific Inc.
BY4743 *pex19*Δ	BY4743 *pex19*::*kanMX4 pex19*::*kanMX4*	Thermo Fisher Scientific Inc.
BY4743 *pex21*Δ	BY4743 *pex21*::*kanMX4*/*pex21*::*kanMX4*	Thermo Fisher Scientific Inc.
BY4743 *pex25*Δ	BY4743 *pex25*::*kanMX4*/*pex25*::*kanMX4*	Thermo Fisher Scientific Inc.
BY4743 *pex27*Δ	BY4743 *pex27*::*kanMX4*/*pex27*::*kanMX4*	Thermo Fisher Scientific Inc.
BY4743 *pex28*Δ	BY4743 *pex28*::*kanMX4*/*pex28*::*kanMX4*	Thermo Fisher Scientific Inc.
BY4743 *pex29*Δ	BY4743 *pex29*::*kanMX4*/*pex29*::*kanMX4*	Thermo Fisher Scientific Inc.
BY4743 *pex30*Δ	BY4743 *pex30*::*kanMX4*/*pex30*::*kanMX4*	Thermo Fisher Scientific Inc.
BY4743 *pex31*Δ	BY4743 *pex31*::*kanMX4*/*pex31*::*kanMX4*	Thermo Fisher Scientific Inc.
BY4743 *pex32*Δ	BY4743 *pex32*::*kanMX4*/*pex32*::*kanMX4*	Thermo Fisher Scientific Inc.
BY4743 *pex33*Δ	BY4743 *pex33*::*kanMX4*/*pex33*::*kanMX4*	Thermo Fisher Scientific Inc.
BY4743 *pex35*Δ	BY4743 *pex35*::*kanMX4*/*pex35*::*kanMX4*	Thermo Fisher Scientific Inc.

Table 5-1 Genotypes and references of *S. cerevisiae* strains used in this study (continued)

Strain	Genotype	Reference
GX-11	*MAT***a** *ura3*	Chapter I
GX-11 *pex22*Δ	GX-11 *pex22*::*kanMX4*	This study
GX-11 *mdh1*Δ	GX-11 *mdh1*::*kanMX4*	Chapter I
GX-11 *mdh2*Δ	GX-11 *mdh2*::*kanMX4*	Chapter I
GX-11 *mdh3*Δ	GX-11 *mdh3*::*kanMX4*	Chapter I
GX-11 *mls1*Δ	GX-11 *mls1*::*kanMX4*	This study
GX-11 *mls2*Δ	GX-11 *mls2*::*kanMX4*	This study
GX-11 *cit2*Δ	GX-11 *cit2*::*kanMX4*	This study
GX-mPEX22	GX-11 *PEX22* 374G>A	This study
GX-mPEX22 *mdh1*Δ	GX-mPEX22 *mdh1*::*kanMX4*	This study
GX-mPEX22 *mdh2*Δ	GX-mPEX22 *mdh2*::*kanMX4*	This study
GX-mPEX22 *mdh3*Δ	GX-mPEX22 *mdh3*::*kanMX4*	This study
GX-mPEX22 *mls1*Δ	GX-mPEX22 *mls1*::*kanMX4*	This study
GX-mPEX22 *mls2*Δ	GX-mPEX22 *mls2*::*kanMX4*	This study
GX-mPEX22 *cit2*Δ	GX-mPEX22 *cit2*::*kanMX4*	This study
GX-11 *mdh3*Δ [pMDH3]	GX-11 *mdh3*::*kanMX4* [pMDH3]	This study
GX-11 *mdh3*Δ [pMDH3SKLΔ]	GX-11 *mdh3*::*kanMX4* [pMDH3SKLΔ]	This study
GX-mPEX22 *mdh3*Δ [pMDH3]	GX-mPEX22 *mdh3*::*kanMX4* [pMDH3]	This study
GX-mPEX22 *mdh3*Δ [pMDH3SKLΔ]	GX-mPEX22 *mdh3*::*kanMX4* [pMDH3SKLΔ]	This study

Whole genome sequencing: Genomic DNA was extracted using the NucleoBond Buffer Set III and NucleoBond AXG 20 Columns (MACHEREY-NAGEL GmbH & Co. KG, Düren, Germany) from the F-701 and F-701H strains. Approximately 6 μg of genomic DNA was used for genome sequence analysis. Whole genome sequencing was performed by the comparative genome analysis service (Takara Bio Inc., Otsu, Japan) using the HiSeq2000 (Illumina Inc., San Diego, CA, USA). Sequence reads were assembled using the Burrows-Wheeler Aligner (BWA) v0.5.9. software. Using the genome sequence of the Kyokai no. 7 (K-7) sake yeast (Brewing Society of Japan) as the reference genotype (2), the analysis resulted in the identification of variant positions. Comparison of the F-701 or F-701H genomes with the K-7 genome was performed using SAMtools mpileup and varFilter.

Construction of the *PEX22* point mutant GX-mPEX22: Mutation in *PEX22* was introduced in the strain GX-11 using a two-step gene replacement method (37). The

plasmid pRS406-PEX22 was constructed using the In-Fusion HD Cloning Kit (Takara Bio Inc., Otsu, Japan) with the pRS406 and *PEX22* fragments. The pRS406 fragment was amplified from the pRS406 plasmid (Stratagene, La Jolla, CA, USA) using the pRS406_InFusion-F and pRS406_InFusion-R primers. The *PEX22* fragment, corresponding to the mutated fragment of *PEX22* from F-701H, was amplified by PCR using the PEX22(1)InFusion-F and PEX22(743)InFusion-R primers (Table **5-2**) and the F-701H genomic DNA as the template. After the plasmid pRS406-mPEX22 (containing *URA3* and mutated *PEX22*) was digested with *Kpn*I (the open reading frame (ORF) of *PEX22* contains the *Kpn*I restriction site endogenously), the linearized DNA was used to transform GX-11. Transformants were selected by growing the cells on SD - ura medium. Next, they were cultivated in YPD medium for 24 h and plated onto 5-FOA medium. The colonies appearing on the 5-FOA medium, resulting from the loss of extraneous plasmid sequences containing *URA3*, were selected as the *PEX22* 374G>A mutant progeny, namely GX-mPEX22. The genotype of the *PEX22* clones was determined by DNA sequencing.

Construction of the complemented strain F-701H-PEX22 by replacement of the mutated *PEX22* with wild-type *PEX22* A complemented strain F-701H-PEX22 was obtained by transforming F-701H with the wild type (K-701) *PEX22* and kanMX4 module. First, using the primers listed in Table 5-2 and PrimeSTAR Max DNA polymerase, three DNA fragments (the wild-type *PEX22*, *kanMX4* module, and the 3' flanking region of *PEX22*) were amplified from K-7 genomic DNA, *kanMX4* module-carrying plasmid, and F-701H genomic DNA, respectively. Next, the three DNA fragments were used for fusion PCR with the PEX22(-71)-F and PEX22(1023)-R primers, and subsequently, the DNA fragment constructed using the wild-type *PEX22*, *kanMX4* module, and the 3' flanking region of *PEX22* was used for transformation..

Construction of *PEX22* mutants and their parent strains with EGFP-MDH3 or -MDH3SKLΔ The plasmid pMDH3 contained the ORF coding for Ura3p and enhanced green fluorescent protein (EGFP)-tagged Mdh3p. pMDH3 was constructed with the

pRS416-SED1pro and EGFP-MDH3 fragments using the In-Fusion HD Cloning Kit (Takara Bio Inc., Otsu, Japan). The pRS416-SED1pro fragment was amplified from the pYCUE-BGL1 plasmid (90) using the primers pRS416-SED1pro-InFusion-F and pRS416-SED1pro-InFusion-R (90). The EGFP-MDH3 fragment was obtained by performing fusion PCR with EGFP and MDH3 fragments. The EGFP fragment was amplified using the primers EGFP(1)InFusion-F and EGFP+MDH3-R and using pEGFP as the template (91). The MDH3 fragment was amplified using the primers EGFP+MDH3-F and MDH3(1443)InFusion-R and the K-7 genomic DNA as the template. The plasmid pMDH3SKLΔ contained the ORF coding for Ura3p and EGFP-tagged Mdh3p in which the carboxy-terminal tripeptide, serine, lysine, and leucine (SKL), was eliminated. pMDH3SKLΔ was constructed using the pRS416-SED1pro and EGFP-MDH3SKLΔ fragments by the same procedure as that of pMDH3. The EGFP-MDH3SKLΔ fragment was generated using the EGFP, MDH3SKLΔ-5', and MDH3SKLΔ-3' fragments. MDH3SKLΔ-5' and MDH3SKLΔ-3' fragments were amplified using the K-7 genomic DNA as the template and the primer pairs EGFP+MDH3-F/Mdh3SKLdelta-R and Mdh3SKLdelta-F/MDH3(1443)InFusion-R, respectively (Table 5-2). The strains GX-11 *mdh3*Δ [pMDH3] and GX-11 *mdh3*Δ [pMDH3SKLΔ] were obtained by the transforming the strain GX-11 *mdh3*Δ with pMDH3 and pMDH3SKLΔ, respectively. The strains GX-mPEX22 *mdh3*Δ [pMDH3] and GX-mPEX22 *mdh*3Δ [pMDH3SKLΔ] were obtained using the same method as that for the strain GX-mPEX22 *mdh3*Δ (Table 5-1).

Fluorescence microscopy Analysis of live cells for EGFP fluorescence was performed using the BX51 microscope equipped with the NIBA filter sets (Olympus Corporation, Tokyo, Japan). Prior to inspection, yeast cells were grown aerobically in SDC - ura medium at 30 °C for 2 days. In case of uracil auxotrophic strains, uracil (20 mg/L) was added. After cultivation, yeast cells were harvested by centrifugation, and resuspended in phosphate-buffered saline.

Table 5-2 Primers used in this study

Primer name	Primer sequence (5'-3')
PEX22_kanMX4-up	ATGAAACAATAATGAAGAATAAAGAAGAAGAAGATATAAAACCGTACGCTGCAGGTCGACGG
PEX22_kanMX4-down	TATTTATTCTTTACATACTGTTACAAGAAACTCTTTTCTACATTATTAGAAAAACTCATCGAGCA
MDH1_kanMX4-up	GGAAGAAAAAAAACAAAAGGAAAAGGAAGGATACCATATACACGTACGCTGCAGGTCGACGG
MDH1_kanMX4-down	TTTTTTTCCCTATTTTTCACTCTATTTCTGATCTTGAACAATCTATTAGAAAAACTCATCGAGCA
MDH2_kanMX4-up	TATAAAGATAAAGATTTATCGATATGAGATAAAGATTGCTGCCGTACGCTGCAGGTCGACGG
MDH2_kanMX4-down	ATTATCAATTTGCTGCATTCTTATGCTTCGGTCCGATGCTCATTATTAGAAAAACTCATCGAGCA
MDH3_kanMX4-up	GTCAGTGCAAAAGAAAATAAAAAGAGACAAACAATCATAAACCGTACGCTGCAGGTCGACGG
MDH3_kanMX4-down	AAAGGAGTATAGAGTTAAGAAAAATATAAAAATTGAAGTAGCTCATTAGAAAAACTCATCGAGCA
MLS1_kanMX4-up	GAACTAAACAAAGTAGTAAAAGCACATAAAAGAATTAAGAAACGTACGCTGCAGGTCGACGG
MLS1_kanMX4-down	ATGAATATATTTTTATATATGTGTACACTGGGGCAAGGGAGATCATTAGAAAAACTCATCGAGCA
MLS2_kanMX4-up	ACTTAGAGTATGTGTCATAGGCACGGTAAAGAGCACTGAACACGTACGCTGCAGGTCGACGG
MLS2_kanMX4-down	TAAAATTCTTCGAATATTCGTCAGGTTATGTACGTATACATTCTATTAGAAAAACTCATCGAGCA
CIT2_kanMX4-up	TTCTCAAAACTTTTTGTTTTAATAATACTAGTAACAAGAAAACGTACGCTGCAGGTCGACGG
CIT2_kanMX4-down	AGAAAAATATGCAGAGGGGTGTAAAAGTAGGATGTAATCCAACTATTAGAAAAACTCATCGAGCA
pRS406_InFusion-F	CAGCTTTTGTTCCCTTTAGTGAGGG
pRS406_InFusion-R	CAATTCGCCCTATAGTGAGTCGTATTAC
PEX22(1)InFusion-F	CTATAGGGCGAATTGATGCCACCACCATCAAGAAGTAGAATAAACAAAACAAGAACATTAGGAATAG
PEX22(743)InFusion-R	AGGGAACAAAAGCTGGGCATTGTTAGACATCTAATTGATTCGGTCAAGTTGTAATGATGATTTC
PEX22(-71)-F	TAAGGGAAGATTGTGCTGATGAAATAGAC
PEX22+kanMX4-R	CTGCAGCGTACGTTATTATTTCACCTTCTC
PEX22+kanMX4-F	GTGAAATAATAACGTACGCTGCAGGTCGAC
kanMX4+PEX22terminator-R	GCTGCTTACTTATTAGAAAAACTCATCGAG
kanMX4+PEX22terminator-F	GAGTTTTTCTAATAAGTAAGCAGCTCGGTT
PEX22(1023)-R	ATTCAACGATGACTTGACTGGTCAAGCAG
pRS416-SED1pro-InFusion-F	GGTACCCAATTCGCCCTATAGTGAGTCG
pRS416-SED1pro-InFusion-R	CTTAATAGAGCGAACGTATTTTATTTTGC
EGFP(1)InFusion-F	GTTCGCTCTATTAAGATGGTGAGCAAGGGCGAGGAGCTGTTCACCGGGGTGGTGCCCATCCTGGTCGAG
EGFP+MDH3-R	GACTTTGACCATCGAGCCATGGAGATCTGC
EGFP+MDH3-F	TCCATGGCTCGATGGTCAAAGTCGCAATTC
MDH3(1443)InFusion-R	GGCGAATTGGGTACCAGCTCTCCGGTAGATCCTAACGGATAATGCTGCCCCTGGTTAGTTCCTCATCGG
Mdh3SKLdelta-R	TTGAAGTAGCTCAAGAGTCTAGGATGAAAC
Mdh3SKLdelta-F	TCCTAGACTCTTGAGCTACTTCAATTTTTA

RESULTS

Isolation of high malate-producing strain The high malate-producing strain F-701H was isolated based on its sensitivity towards DMS from F-701. F-701H was isolated by ethyl methyl sulfonate-induced mutagenesis and negative selection based on DMS sensitivity. First, 88 DMS-sensitive colonies were isolated from the 8,000 mutated F-701 colonies. Of these 88 colonies, 4 colonies exhibited higher malate production than the F-701 colonies in the YM10 cultivation test. One out of these 4 colonies was selected as F-701H, based on its ethanol productivity (data not shown). The one-step sake brewing test was performed using F-701 and F-701H strains. The amount of malate produced in the F-701H was 3.2-fold higher than that produced by the F-701 (Table 5-3). In addition, in YM10 cultivation test, high amount of malate was produced by the F-701H cells (Fig. 5-1). Automatic measurement of cell densities showed a delay in the onset of logarithmic phase in the F-701H cells as compared with that of F-701 in the DMS medium (Fig. 5-2a).

Table. 5-3 The sake brewing tests of F-701and F-701H

Parameter		Value (mean ± SD)	
		F-701	F-701H
Ethanol (vol %)		18.24 ± 0.03	17.23 ± 0.02 [a]
Specific gravity (15°C/4°C)		0.9918 ± 0.0001	0.9981 ± 0.0001 [b]
Acid level		3.81 ± 0.05	6.53 ± 0.05 [b]
Amino acid level		2.30 ± 0.01	2.19 ± 0.01
Organic acid (mg/L)	Malate	833 ± 6	2626 ± 15 [b]
	Succinate	678 ± 2	661 ± 1 [a]
	Lactate	575 ± 2	448 ± 2 [a]
	Pyrvate	134 ± 5	168 ± 1 [b]
	Acetate	17 ± 1	4 ± 0 [b]

The brewing tests were repeated thrice. Plus or minus represents the respective standard deviation.

[a] Significantly lower than F-701 (*t*-test; $p < 0.01$)

[b] Significantly higher than F-701 (*t*-test; $p < 0.01$)

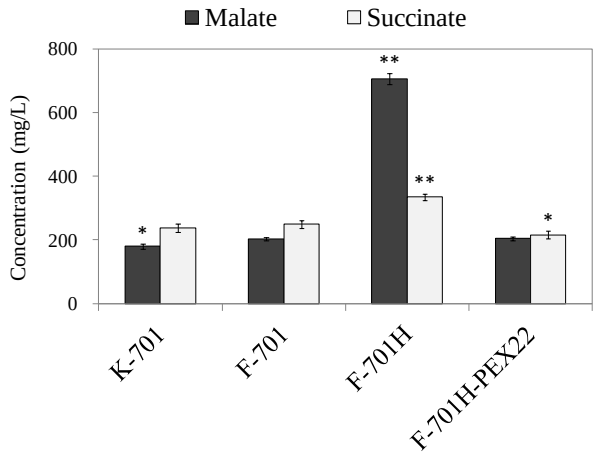

Fig. 5-1 Malate and succinate production by K-701, F-701, F-701H, and F-701H-PEX22 in the YM10 cultivation test. All cultivation tests were repeated thrice. Each error bar represents the respective standard deviation. The significance of the difference in malate and succinate production between K-701, F-701H and F-701-PEX22 versus F-701 was analyzed by student *t* test (*$p < 0.05$, **$p < 0.01$).

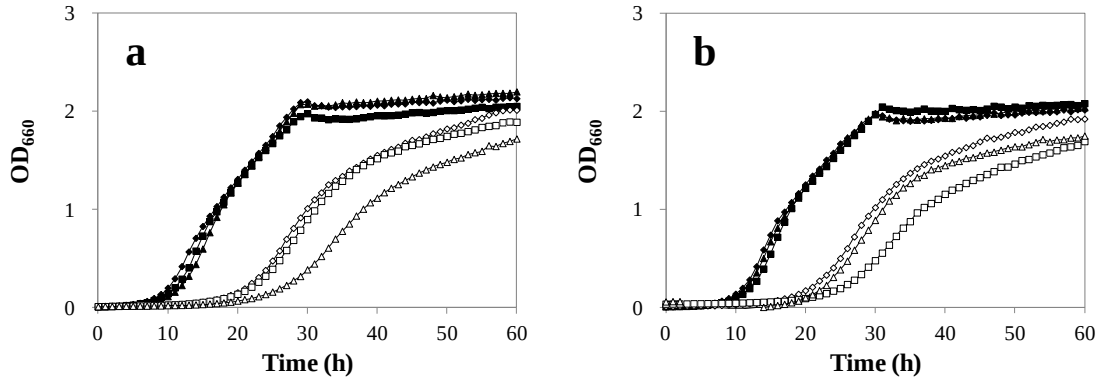

Fig. 5-2 Growth rates of different yeast strains in medium containing DMS. Plots represent the mean values of two independent experiments. (a) Growth curves of K-701, F-701, and F-701H in DOB or DMS medium. (Symbols: closed diamonds, K-701 in DOB; closed squares, F-701 in DOB; closed triangles, F-701H in DOB; open diamonds, K-701 in DMS; open squares, F-701 in DMS; open triangles, F-701H in DMS). (b) Growth curves of F-701, F-701H, and F-701H-PEX22 in DOB or DMS medium. (Symbols: closed diamonds, F-701 in DOB; closed squares, F-701H in DOB; closed triangles, F-701H-PEX22 in DOB; open diamonds, F-701 in DMS; open squares, F-701H in DMS; open triangles, F-701H-PEX22 in DMS).

A mutation in the *PEX22* gene responsible for high malate production Genomic DNAs extracted from F-701 and F-701H were subjected to whole genome sequencing analysis for identifying the genes responsible for high malate production in F-701H. In this analysis, 1 nonsense substitution, 14 missense substitutions, 7 synonymous substitutions, and 33 intergenic mutations were observed between the genomes of F-701 and F-701H (Table 5-4). Among the 15 genes encompassing the nonsense and missense substitutions in the F-701H genome, we focused on 8 genes involved in carbon and energy metabolism. Eight disruptants derived from the strain BY4743 were subjected to the one-step sake brewing test (Table 5-1). The concentration of malate in the strain BY4743 *pex22*Δ was higher than that in the parental strain BY4743 (Fig. 5-3). *PEX22* was selected as the candidate gene potentially responsible for high malate production. A homozygous guanine to adenine substitution at nucleotide position 374 in *PEX22* was observed, which resulted in the substitution of tryptophan at residue 125 with a homozygous stop codon in F-701H. The *PEX22* 374G>A strain, namely GX-mPEX22, was constructed. The one-step sake brewing test was performed using GX-mPEX22 and the parental strain GX-11. The amount of malate produced by GX-mPEX22 was 2.1-fold higher than that produced by GX-11 (Table 5-5). This result indicated that the high-malete-producing phenotype of F-701H was attributed to the homozygous mutation in *PEX22* (374G>A).

Table. 5-4 Genes containing missense or nonsense mutations between F-701 and F-701H

Gene name	Systematic Name	Base substitution	Amino acid change	Zygosity	
				in F-701H	in F-701
PEX22	*YAL055W*	374G>A	Trp125^{amber}	Homozygous	Heterozygous
CDC19	*YAL038W*	823G>A	Glu275Lys	Homozygous	Heterozygous
FUN12	*YAL035W*	283G>A	Glu95Lys	Homozygous	Heterozygous
ARO1	*YDR127W*	4610G>A	Ser1537Asn	Heterozygous	Wild type
DSE1	*YER124C*	1995G>A	Val399Ile	Heterozygous	Wild type
ZUO1	*YGR285C*	605C>T	Thr202Ile	Heterozygous	Wild type
YAP3	*YHL009C*	131C>A	Pro44Gln	Heterozygous	Wild type
ORC6	*YHR118C*	34G>A	Glu12Lys	Heterozygous	Wild type
OYE2	*YHR179W*	843G>T	Lys281Asn	Heterozygous	Wild type
AYR1	*YIL124W*	742G>A	Val248Ile	Heterozygous	Wild type
NUP100	*YKL068W*	359A>G	Asn120Ser	Heterozygous	Wild type
SRP40	*YKR092C*	113T>C	Phe38Ser	Homozygous	Heterozygous
FLO10	*YKR102W*	307G>A	Glu103Lys	Homozygous	Heterozygous
COQ9	*YLR201C*	29G>A	Arg15His	Heterozygous	Wild type
SSU1	*YPL092W*	1162G>A	Val388Ile	Heterozygous	Wild type

Wild type represents the genotype of K-7 genome.

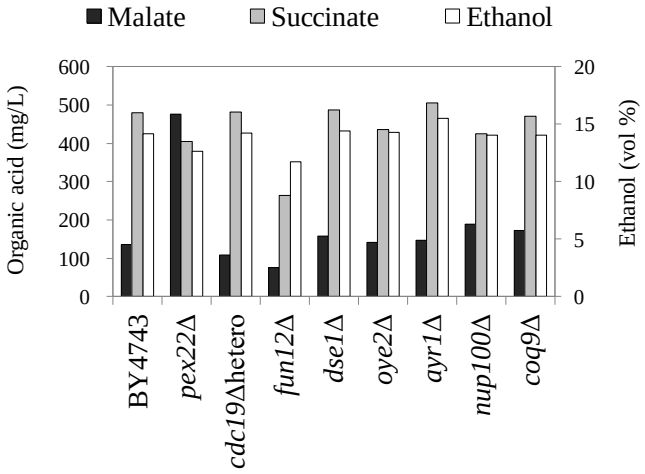

Fig. 5-3 Malate, succinate, and ethanol production by the BY4743 parental strain and the gene disruptants in sake brewing tests.

Parameter		Value (mean ± SD)	
		GX-11	GX-mPEX22
Ethanol (vol %)		16.92 ± 0.01	15.97 ± 0.01
Specific gravity (15°C/4°C)		1.0060 ± 0.0002	1.0127 ± 0.0000
Acid level		4.34 ± 0.02	5.99 ± 0.07
Amino acid level		2.50 ± 0.03	2.25 ± 0.01
Organic acid (mg/L)	Malate	517 ± 21	1062 ± 9
	Succinate	957 ± 1	1519 ± 15
	Lactate	336 ± 1	284 ± 13
	Pyrvate	379 ± 3	266 ± 10
	Acetate	32 ± 7	7 ± 0

Table 5-5 The sake brewing tests of GX-11 and GX-mPEX22.
The brewing tests were repeated twice. Plus or minus represents the respective standard deviations.

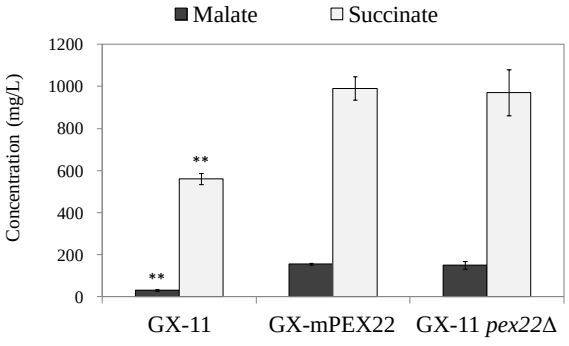

Fig. 5-4 Malate and succinate production by GX-11, GX-PEX22, and GX-11 *pex22*Δ in the YM10 cultivation test. The cultivation tests were repeated thrice. Each error bar represents the respective standard deviation. The significance of the difference in malate and succinate production between GX-11 and GX-11 *pex22*Δ versus GX-PEX22 was analyzed by student *t* test (**$p < 0.01$)

Similarity between the *PEX22* 374G>A mutant and the *PEX22* disruptant in terms of acid production Pex22 interacts with Pex4p, which is ubiquitin-conjugating enzyme required for ubiquitination of the peroxisomal import receptor Pex5 (92), at the peroxisomal membrane (87). This interaction requires the amino acid residues 54-180 present in the carboxy-terminus of Pex22 (92). Since the carboxy-terminus was missing in mutated Pex22, it was assumed that the W125 amber mutation resulted in a loss of function of this protein. In order to evaluate the effect of *PEX22* 374G>A mutation on the function of Pex22p, the disruptant GX-11 *pex22*Δ was generated. GX-11, GX-mPEX22, and GX-11 *pex22*Δ were subjected to the YM10 cultivation test. The levels of organic acids were almost equal in GX-mPEX22 and GX-11 *pex22*Δ (Fig. 5-4). These results suggested that the *PEX22* 374G>A mutation resulted in a functional deficiency in Pex22.

Complementation test of *PEX22* in F-701H In order to confirm whether the 374G>A mutation in *PEX22* was actually responsible for high malate production and the sensitivity towards DMS in F-701H, *PEX22* containing the 374G>A mutation was replaced with the wild-type *PEX22* derived from K-7 genome in the F-701H genome. The complemented strain F-701H-PEX22, F-701H, and F-701 were subjected to the YM10 cultivation test. The amount of malate produced by F-701H-PEX22 was the same as that produced by F-701; however, it was lower than that produced by F-701H (Fig. 5-1). Furthermore, the growth characteristics of F-701H-PEX22 were almost identical to those of F-701 in DMS medium (Fig. 5-2b). These data demonstrated that *PEX22* containing the nonsense mutation was responsible for high malate production and DMS sensitivity in F-701H.

Enhanced malate production in peroxin-coding gene disruptants Pex22 is a protein localized in peroxisomal membrane in yeast cells. The proteins required for peroxisome assembly and division are called peroxins (93, 94). To evaluate the role of peroxins in organic acid production in yeast cells, 29 disruptants of the peroxin-coding genes were subjected to the YM10 cultivation test, in which the amount of organic acids produced by each disruptant was measured. As a result, it was observed that the

disruptants of *PEX1*, *3*, *4*, *5*, *6*, *8*, *10*, *12*, *13*, *14*, *15*, *17*, *19*, and *22* produced higher levels of malate than that produced by BY4743 (Fig. 5-5). Among these peroxins, Pex1, 4, 6, 8, 10, 12, 13, 14, 15, 17, and 22 are known to be involved in peroxisomal matrix protein import mediated by Pex5 (94). Pex3 and Pex19 are required for peroxisomal membrane biogenesis and proper localization of the peroxisomal membrane proteins (95). These data suggest that a deficiency in peroxins affects the import of peroxisomal matrix proteins, thereby resulting in high malate production in yeast.

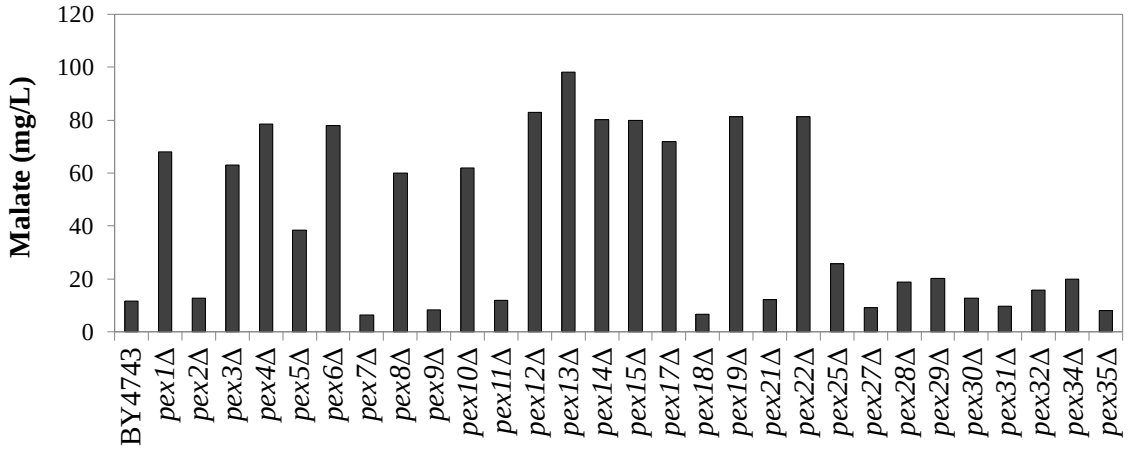

Fig. 5-5 Malate production in the BY4743 parental strain and the disruptants of the peroxin-coding gene

Increase in malate production in *PEX22* mutants attributed to the presence of Mdh3 Pex5 serves as the import receptor for the peroxisomal matrix proteins that are sorted via the peroxisomal targeting signal 1 (PTS1) protein import pathway (96). The author observed that the loss of PTS1 protein import resulted in high malate production in the *PEX22* mutants of F-701H. The PTS1 sequence recognized by the Pex5 receptor is located at the carboxy-terminus of the peroxisomal matrix proteins, and typically consists of the SKL sequence (97). The peroxisomal matrix proteins containing the SKL motif include Mdh3, malate synthase (Mls1, Mls2), and peroxisomal citrate synthase (Cit2). The enzymes regulating the glyoxylate cycle in peroxisomes appeared to affect the production of organic acids in the *PEX*22 mutants. To investigate the effects of the glyoxylate cycle enzymes on malate production, *MDH3*, *MLS1*, MLS2, and *CIT2* disruptants were generated in the GX-11 and GX-mPEX22 strains. In addition to these

disruptants, the disruption of mitochondrial malate dehydrogenase (*MDH1*) and cytoplasmic malate dehydrogenase (*MDH2*), encoding isozymes of Mdh3, were also constructed. These isozymes of Mdh3 were presumed to be related to malate production, since Mdh2p played an important role in malate production during fermentation (4, 11, 12). The one-step sake brewing test was performed using the *MDH1*, *MDH2*, *MDH3*, *MLS1*, *MLS2*, and *CIT2* disruptants of the GX-11 and GX-mPEX22 strains (Table 5-6). The profile of organic acids observed in GX-mPEX22 *mdh3*Δ was almost similar to those observed in GX-11 and GX-11 *mdh3*Δ. Thus, disruption of *MDH3* inhibited high malate production in the *PEX22* mutant. These results implied that the loss of Mdh3p import into the peroxisomes mediated by the peroxins in the *PEX22* mutant facilitated the conversion of oxaloacetate to malate in the cytosol, thereby enhancing malate production.

Table 5-6 The sake brewing tests of disrutants derived from GX-11 and GX-mPEX22

	Ethanol (vol %)	Specific gravity (15°C/4°C)	Acid level	Amino acid level	Organic acid (mg/L)				
					Malate	Succinate	Lactate	Pyrvate	Acetate
GX-11	12.57	1.0368	4.28	3.80	58	539	225	n.d.	1167
GX-11 *mdh1*Δ	13.16	1.0323	4.31	3.85	164	394	215	n.d.	1457
GX-11 *mdh2*Δ	13.14	1.0322	3.90	3.82	30	425	234	n.d.	1251
GX-11 *mdh3*Δ	13.01	1.0337	4.15	3.84	71	594	229	6	1078
GX-11 *mls1*Δ	12.32	1.0384	4.25	3.82	54	546	221	11	1214
GX-11 *mls2*Δ	12.86	1.0338	4.43	3.97	55	578	223	8	1272
GX-11 *cit2*Δ	12.70	1.0349	4.28	3.95	54	466	225	n.d.	1328
GX-mPEX22	12.61	1.0358	5.38	3.80	235	1292	216	10	820
GX-mPEX22 *mdh1*Δ	11.32	1.0447	5.67	3.97	829	433	183	22	1564
GX-mPEX22 *mdh2*Δ	12.01	1.0401	5.05	3.75	214	1205	204	10	779
GX-mPEX22 *mdh3*Δ	11.67	1.0420	4.27	3.93	56	511	216	9	1303
GX-mPEX22 *mls1*Δ	11.69	1.0418	5.20	3.79	209	1245	208	10	868
GX-mPEX22 *mls2*Δ	12.39	1.0365	5.43	3.72	231	1335	215	16	850
GX-mPEX22 *cit2*Δ	11.83	1.0424	4.94	3.88	226	1114	213	8	844

n.d. means not detected

Localization of Mdh3p to the cytoplasm in the *PEX22* mutant To corroborate the hypothesis that Mdh3 mislocalization led to high malate production, the localization of Mdh3 in the *PEX22* mutant and its parental strain was investigated. Four transformants were constructed, namely GX-11 *mdh3*Δ [pMDH3], GX-11 *mdh3*Δ [pMDH3SKLΔ], GX-mPEX22 *mdh*3Δ [pMDH3], and GX-mPEX22 *mdh3*Δ [pMDH3SKLΔ]. The amino-terminal EGFP fusion of Mdh3 in GX-11 *mdh3*Δ [pMDH3] strain exhibited a punctate

fluorescent pattern that was assumed to represent its localization to the peroxisomes. In contrast, EGFP-tagged Mdh3p showed a diffuse fluorescent pattern typical for cytosolic localization in GX-mPEX22 *mdh3*Δ. EGFP-Mdh3p-SKLΔ, which contained the PTS1-truncated Mdh3, was similarly localized to the cytosol in both GX-11 *mdh3*Δ and GX-mPEX22 *mdh3*Δ (Fig. 5-6a). These results showed that in the wild-type strain, Mdh3 was localized to the peroxisomes due to the presence of the carboxy-terminal region PTS1; however, in the *PEX22* mutant, Mdh3 was mislocalized to the cytosol. In addition, in the YM10 cultivation test, the malate level observed in GX-11 *mdh3*Δ [pMDH3] was lower than those observed in GX-11 *mdh3*Δ [pMDH3SKLΔ], GX-mPEX22 *mdh3*Δ [pMDH3], and GX-mPEX22 *mdh3*Δ [pMDH3SKLΔ] (Fig 5-6b). Taken together, these results supported the hypothesis that the mislocalization of Mdh3p to the cytosol resulted in high malate production in the *PEX22* mutant.

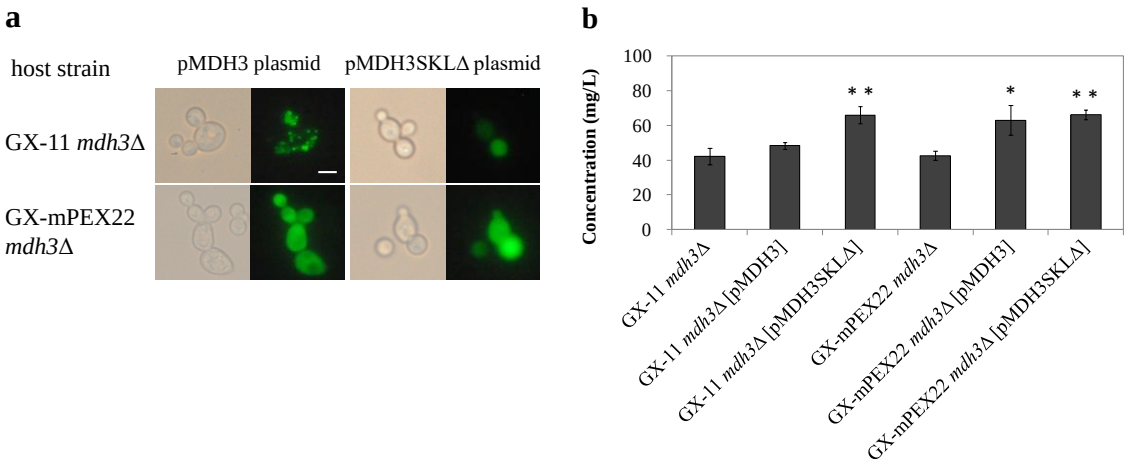

Fig. 5-6 Expression of EGFP-tagged Mdh3 or PTS1-truncated Mdh3 in *mdh3* disruptants of GX-11 or GX-mPEX22. (a) Pictures on the right-hand panel were obtained using bright-field microscopy. Pictures on the left-hand panel represent the intracellular localization of EGFP constructs visualized using fluorescence microscopy (Bar, 5 μm). (b) Malate and succinate production by different yeast strains in the YM10 cultivation test. All cultivation tests were repeated thrice. Each error bar represents the respective standard deviation. The significance of the difference in malate production between GX-11 *mdh3*Δ [pMDH3] and GX-11 *mdh3*Δ [pMDH3SKLΔ] versus GX-11 *mdh3*Δ, and between GX-mPEX22 *mdh3*Δ [pMDH3] and GX-mPEX22 *mdh3*Δ [pMDH3SKLΔ] versus GX-mPEX22 *mdh3*Δ was analyzed by student *t* test (*$p < 0.05$, **$p < 0.01$).Malate production in the BY4743 parental strain and the disruptants of the peroxin-coding gene

DISCUSSION

The author isolated a high malate-producing sake yeast strain F-701H, on the basis of its sensitivity towards DMS, and revealed that a nonsense mutation in *PEX22* was responsible for high malate production in this strain. *PEX22* encodes a peroxin, which regulates peroxisomal biogenesis. *S. cerevisiae* has been reported to have 29 peroxins (Pex1-15, 17-19, 21, 22, 25, 27-32, 34 and 35p) (95, 98). Some peroxins including Pex22 play an important role in the transportation of peroxisomal matrix proteins. The transportation of peroxisomal matrix proteins depends on two peroxisomal targeting signals, namely PTS1 and PTS2. PTS1, present at the carboxy-terminus, contains the tripeptide SKL or its variants (99). PTS1 is recognized by its receptor Pex5p present in the cytosol, and the proteins containing PTS1 are translocated across the peroxisomal membrane and released into the peroxisome (92, 93). Proteins such as Mdh3, Mls1, Mls2, Cit2, catalase (Cta1), and peroxisomal 2,4-dienoyl-CoA reductase (Sps19) are classified as PTS1-proteins. On the other hand, PTS2 is a nonapeptide present near the amino-terminal region (100). PTS2 is recognized by the receptor Pex7, along with its co-receptors Pex18 and Pex20 (101). The proteins containing PTS2 were also imported into the peroxisomes, similar to the PTS1-containing proteins. After the translocation of PTS1- and PTS2-containing proteins, Pex5 and Pex7 were recycled to the cytosol (102). Translocation of the PTS-containing proteins and the recycling of its receptors are regulated by peroxins, such as Pex1, 2, 4, 6, 8, 10, 12, 13, 14, 15, 17, and 22. It has been reported that defects in these peroxins cause mislocalization of the PTS1-containing-proteins to the cytosol, thereby resulting in the dysfunction of peroxisomal homeostasis (95). Additionally, Pex3 and Pex19 are known to be involved in the formation of peroxisomal membrane and the insertion of membrane proteins, such as peroxins, in the peroxisomal membrane (93). The mutants for two peroxins have demonstrated defects in the peroxisomal membrane structures (95). We demonstrated that the disruptants of *PEX1, 3, 4, 5, 6, 8, 10, 12, 13, 14, 15, 17, 19,* and *22* produced higher levels of malate than their parent strain (Fig. 5-5). Additionally, the deletion of *MDH3* in the *PEX22* mutant inhibited high malate production (Table 5-6). These results suggested that in the peroxin

disruptants, Mdh3, which was routinely present in the peroxisomal matrix, was mislocalized to the cytosol where it enhanced the process of reduction of oxaloacetate to malate (Fig. 5-6). This hypothesis is supported by previous studies, which revealed that the mislocalization of Mdh3 to the cytosol resulted in an increase in malate level (6).

Pex22, a peroxisomal integral membrane protein, interacts with the ubiquitin-conjugating enzyme Pex4 (88, 92). The Pex22-Pex4 complex is required for recycling of the PTS1-protein receptor Pex5. The carboxy-terminal cytosolic domain of Pex22, comprising the amino acid residues 54-180, interacts with the carboxy-terminus of Pex4 (92). In addition, the amino-terminus of Pex22, comprising the amino acid residues 1-35, contains the peroxsomal membrane-targeting signal (87, 103). Therefore, both the carboxy- and amino-terminal domains of Pex22 are considered to be essential for its function. Pex22 present in the high-malate-producing strain F-701H lacked its carboxy-terminal residues 125-180 due to a homozygous missense mutation (Table 5-4). F-701H appeared to lack the functionally active Pex22. Indeed, the Pex22 mutant and the *PEX22* disruptant showed almost equal production of organic acids (Fig. 5-4). High malate production observed in the *PEX22* 374G>A mutant was attributed to the presence of Pex22, which was dysfunctional due to the loss of its carboxy terminus. F-701H represents a diploid yeast strain with a homozygous *PEX22* mutation. On the other hand, F-701 that was a heterozygous carrier of the *PEX22* mutation did not show high malate production (data not shown). This suggested that the *PEX22* mutation was recessive in diploid yeast.

Peroxins also participate in the peroxisomal translocation of Cta1, and the β-oxidation enzymes (Sps19 and acetyl-CoA acyltransferase (Pot1)) (104, 105). The localization of these enzymes, as well as the glyoxylate cycle enzymes, is altered in the peroxin mutants (104, 105). Although mislocalization of these enzymes appeared to occur in *PEX22* mutants, little effect on the level of metabolites or growth of cells were observed in the sake brewing and YM10 cultivation tests (Table 5-5, Fig. 5-4). It is likely that phenotypic plasticity may be observed under different nutrient conditions. For instance, the growth of *PEX22* mutants may decrease when cultivated in a medium containing oleic acid as the sole carbon source, due to its reduced capacity to metabolize the long-chain

fatty acid (106). Since the *PEX22* mutants exhibited altered phenotypic characteristic, it is possible to develop a novel method for breeding high malate-producing yeast strains harboring peroxin mutations, without the use of DMS sensitivity.

F-701H was isolated based on its sensitivity towards DMS. It was observed that the *PEX22* mutation was also sufficient to confer sensitivity towards DMS (Fig. 5-2b). On the other hand, the author has reported in Chapter I that a mutation in *VID24* conferred high malate productivity and DMS sensitivity upon *S. cerevisiae*. The putative mechanisms responsible for increasing the production of malate were observed to be different between the *PEX22* and *VID24* mutants. While the former was associated with mislocalization of Mdh3 (Fig. 5-6), the later was associated with increased accumulation of Mdh2p in the cytoplasm. Nevertheless, the phenotype of DMS sensitivity was common between them. This observation suggests that DMS sensitivity was not directly affected by the functions of Pex22 and Vid24, but was elicited by the intracellular accumulation of malate. Malate was converted to succinate via the TCA cycle under aerobic conditions. High-malate-producing strains appeared to be susceptible towards excess accumulation of succinate, which could not be metabolized in the presence of DMS (a succinate dehydrogenase-specific inhibitor). This hypothesis upholds the possibility that high malate production could be induced by DMS sensitivity via various mechanisms. Furthermore, considering the different mechanisms responsible for increasing malate production in the *PEX22* and *VID24* mutants, a *PEX22-VID24* double mutant might exhibit higher production of malate than the strains harboring single gene mutation.

There are numerous reports related to the regulation of malate production in several high malate-producing sake yeast strains (4, 12-15, 86). These reports mainly revealed the activity of mitochondria or the expression of genes involved in the TCA cycle in the high malate-producing yeast strains. Relatively little attention has been paid to the impact of peroxisomal function on organic acid production during sake brewing. In the present study, the author identified the mutation in *PEX22* gene that was responsible for high production of malate in yeast. These findings shall be considerably useful in controlling malate production in yeast, which could be used for improving the taste of sake.

SUMMARY

A high-malate-producing yeast strain F-701H was isolated. This mutant was sensitive to DMS and harbored a nonsense mutation in the peroxin gene *PEX22*, which was identified as the cause of high malate production by comparative genome analysis. This mutation, which appeared to cause Pex22 dysfunction, was sufficient to confer increased malate productivity and DMS sensitivity to yeast cells. Next, the author investigated the mechanism by which this mutation led to high malate production in yeast cells. Peroxins, such as Pex22, maintain peroxisomal biogenesis. Analysis of 29 *PEX* disruptants revealed an increased malate production by deletion of the genes encoding peroxins responsible for importing proteins (containing peroxisomal targeting signal 1, PTS1) into the peroxisomal matrix, and those responsible for the assembly of peroxins themselves in the peroxisomal membrane. A defect in peroxisomal malate dehydrogenase (Mdh3), harboring endogenous PTS1, inhibited the high malate-producing phenotype in the *PEX22* mutant. Moreover, Mdh3, which was normally sorted to the peroxisomal matrix, was potentially mislocalized to the cytosol in the *PEX22* mutant. This suggested that an increase in malate production resulted from the mislocalization of Mdh3 from the peroxisome to the cytoplasm due to the loss of peroxin-mediated transportation. Thus, the present study revealed a novel mechanism for organic acid productions in yeast during sake brewing.

CONCLUSION

Since malate contributes to the pleasant taste of sake, various methods for breeding high-malate-producing yeast strains have been developed. The present study has been carried out to identify the gene involved in the high malate production of sake yeast strains, and elucidate the mechanisms underlying enhanced malate production.

The author isolated a high-malate-producing strain K-901H and revealed that the heterozygous mutation of *VID24* resulted in enhancement of malate productivity. Vid24 is known as a component of the multisubunit ubiquitin ligase and participates in the degradation of gluconeogenic enzymes such as Mdh2. A subcellular abnormal accumulation of Mdh2 in the *VID24* mutant enhanced the reduction of oxaloacetate to malate in the cytoplasm, resulting in increased malate levels (Fig. 6-1a). Furthermore, the heterozygous mutation in *VID24* exhibited semi-dominant in diploid yeast. The author developed a method for selecting a homozygous *VID24* mutant from the heterozygous mutant K-901H without employing a genetic engineering approach. The homozygous *VID24* mutant showed a higher level of malate production than K-901H.

The author investigated the effects of GID protein–coding genes (*VID30*/*GID1*, *RMD5*/*GID2*, *UBC8*/*GID3*, *VID24*/*GID4*, *VID28*/*GID5*, *UBP14*/*GID6 GID7*, *GID8*, *FYV10*/*GID9*) on organic acid production and enzyme expression profiles in yeast. The disruptants of *vid30*, *rmd5*, *ubc8*, *vid24*, *vid28*, *gid8*, and *fyv10* exhibited high malate production. Comparison of protein abundance indicated that the high-malate-producing disruptants showed the activation of several glycolytic enzymes and a reduction in enzymes involved in the conversion of pyruvate to ethanol.

The genes responsible for the high malate phenotype in yeast strain No. 28 and No. 77 were investigated. Upon examining GID protein–coding genes in these strains, a nonsense homozygous mutation of GID4 in strain No. 28 and of GID2 in strain No. 77 were identified as the cause of high malate production.

Next, a high-malate-producing strain F-701H was isolated and the heterozygous mutation of *PEX22* was identified as the cause of enhancement of malate productivity. Pex22 is a protein, called peroxin, required for peroxisome assembly and division. An

increase in malate production in *PEX22* mutant resulted from the mislocalization of Mdh3 from the peroxisome to the cytoplasm due to the loss of peroxin-mediated transportation (Fig. 6-1b).

The author demonstrated that high malate production in industrial sake yeast strain K-901H, No. 28 and No. 77 was acquired due to mutation of GID protein–coding genes, and the genotype of the *VID24* mutation influenced the level of malate production in diploid yeasts. These findings provided useful information to selection of a high malate-producing yeast strain. Furthermore, it was shown that a nonsense mutation in *PEX22* was responsible for high malate production in the strain F-701H. Additionally, the mechanisms contributing to the high acidity phenotype of these strains were elucidated. Since identification of the mutated gene responsible for malate production leads to suggestions for the brewing characteristics in these strains, the findings will be useful for the process development for sake brewing.

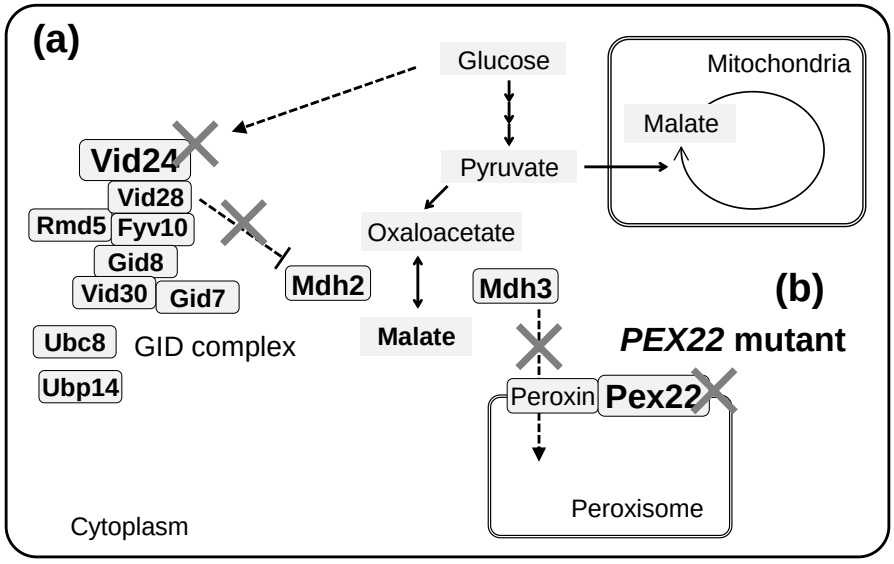

Fig. 6-1 The mechanism for the increased malate production of the *VID24* mutant and the *PEX22* mutant. (a) The loss of gluconeogenesis protein degradation mediated by the GID complex leads to the accumulation of intracellular Mdh2 in the *VID24* mutant, which facilitates the conversion of oxaloacetate to malate. (b) The mislocalization of Mdh3 from the peroxisome to the cytoplasm due to the loss of peroxin-mediated transportation in the *PEX22* mutant results in enhancement of the reduction of oxaloacetate to malate in the cytoplasm.

REFERENCES

1. **Goffeau, A., Barrell, B. G., Bussey, H., Davis, R. W., Dujon, B., Feldmann, H., Galibert, F., Hoheisel, J. D., Jacq, C., Johnston, M., Louis, E. J., Mewes, H. W., Murakami, Y., Philippsen, P., Tettelin, H., and Oliver, S. G.:** Life with 6000 genes, Science, **274**, 563-567 (1996)
2. **Akao, T., Yashiro, I., Hosoyama, A., Kitagaki, H., Horikawa, H., Watanabe, D., Akada, R., Ando, Y., Harashima, S., Inoue, T., and other 25 authors Inoue, Y., Kajiwara, S., Kitamoto, K., Kitamoto, N., Kobayashi, O., Kuhara, S., Masubuchi, T., Mizoguchi, H., Nakao, Y., Nakazato, A., Namise, M., Oba, T., Ogata, T., Ohta, A., Sato, M., Shibasaki, S., Takatsume, Y., Tanimoto, S., Tsuboi, H., Nishimura, A., Yoda, K., Ishikawa, T., Iwashita, K., Fujita, N., and Shimoi, H.:** Whole-genome sequencing of sake yeast *Saccharomyces cerevisiae* Kyokai no. 7, DNA Res., **18,** 423-434 (2011).
3. **Tadenuma, M.:** Organic acids in sake, J. Brew. Soc. Japan, **61**, 1092-1097 (1966) (in Japanese)
4. **Motomura, S., Horie, K., and Kitagaki, H.:** Mitochondrial activity of sake brewery yeast affects malic and succinic acid production during alcoholic fermentation, J. Inst. Brew., **118**, 22-26 (2012)
5. **Arikawa, Y., Kobayashi, M., Kodaira, R., Shimosaka, M., Muratsubaki, H., Enomoto, K., and Okazaki, M.:** Isolation of sake yeast strains possessing various levels of succinate- and/or malate-producing abilities by gene disruption or mutation, J. Biosci. Bioeng., **87**, 333-339 (1999)
6. **Zelle, R. M., de Hulster, E., van Winden, W. A., de Waard, P., Dijkema, C., Winkler, A. A., Geertman, J. M., van Dijken, J. P., Pronk, J. T., and van Maris, A. J.:** Malic acid production by *Saccharomyces cerevisiae*: engineering of pyruvate carboxylation, oxaloacetate reduction, and malate export, Appl. Environ. Microbiol., **74**, 2766-2777 (2008)
7. **Chi, Z., Wang, Z. P., Wang, G. Y., Khan, I., Chi, Z. M.:** Microbial biosynthesis and secretion of L-malic acid and its applications, Crit. Rev. Biotechnol., **36**, 99-107,

(2016)

8. **Sato, S., Oba, T., Takahashi, K., Kokubu, K., Kobayashi, M., and Kobayashi, K.:** Studies on taste of sake (part 7), J. Brew. Soc. Japan, **72**, 801-805 (1977) (in Japanese)
9. **Aikawa, M., Suizu, T., Ichikawa, E., Kawato, A., Abe, Y., and Imayasu, S.:** Breeding of higher malic acid-productive mutants from *Saccharomyces cerevisiae* Kyokai No.7, Hakko-kogaku, **70**, 473-477 (1992) (in Japanese)
10. **Yoshida, K.:** Breeding of sake yeasts with high and low acid-producing abilities. J Brew Soc Japan, **90**, 751-758 (1995) (in Japanese)
11. **Kosugi, S., Kiyoshi, K., Oba, T., Kusumoto, K., Kadokura, T., Nakazato, A., and Nakayama, S.**: Isolation of a high malic and low acetic acid-producing sake yeast *Saccharomyces cerevisiae* strain screened from respiratory inhibitor 2,4-dinitrophenol (DNP)-resistant strains, J. Biosci. Bioeng., **117**, 39-44 (2014)
12. **Asano, T., Kurose, N., and Tarumi, S.:** Isolation of high-malate-producing sake yeasts from low-maltose-assimilating mutants, J. Biosci. Bioeng., **92**, 429-433 (2001)
13. **Koganemaru, K.**, **Kanda, K., Yasuda, M., Kato, F., Tasiro, K., and Kuhara, S.:** Gene expression concerning malate production of a cycloheximide-resistant mutant and industrial scale sake brewing, J. Brew. Soc. Japan, **98**, 303-309 (2003) (in Japanese)
14. **Oba, T., Kusumoto, K., Kichise, Y., Izumoto, E., Nakayama, S., Tashiro, K., Kuhara, S., and Kitagaki, H.**: Variations in mitochondrial membrane potential correlate with malic acid production by natural isolates of *Saccharomyces cerevisiae* sake strains, FEMS Yeast Res., **14**, 789-796 (2014)
15. **Nakayama, S., Tabata, K., Oba, T., Kusumoto, K., Mitsuiki, S., Kadokura, T., and Nakazato, A.:** Characteristics of the high malic acid production mechanism in *Saccharomyces cerevisiae* sake yeast strain No. 28, J. Biosci. Bioeng., **114**, 281-285 (2012)
16. **Hung, G. C., Brown, C. R., Wolfe, A. B., Liu, J., and Chiang, H. L.:** Degradation of the gluconeogenic enzymes fructose-1,6-bisphosphatase and malate dehydrogenase is mediated by distinct proteolytic pathways and signaling events, J. Biol. Chem., **279**, 49138-49150 (2004)

17. **Santt, O., Pfirrmann, T., Braun, B., Juretschke, J., Kimmig, P., Scheel, H., Hofmann, K., Thumm, M., and Wolf, D. H.:** The yeast GID complex, a novel ubiquitin ligase (E3) involved in the regulation of carbohydrate metabolism, Mol. Biol. Cell., **19**, 3323-3333 (2008)

18. **Chen, S. J., Wu, X., Wadas, B., Oh, J. H., Varshavsky, A.:** An N-end rule pathway that recognizes proline and destroys gluconeogenic enzymes. Science 355:eaal6323 (2017)

19. **Hino, A**.: Safety assessment and public concerns for genetically modified food products; the Japanese experience, Toxicol. Pathol. 30, 126-128 (2002)

20. **Regelmann, J., Schüle, T., Josupeit, F. S., Horak, J., Rose, M., Entian, K. D., Thumm, M., and Wolf, D. H.:** Catabolite degradation of fructose-1,6-bisphosphatase in the yeast *Saccharomyces cerevisiae*: a genome-wide screen identifies eight novel GID genes and indicates the existence of two degradation pathways, Mol. Biol. Cell., **14**, 1652-1663 (2003)

21. **Menssen, R., Schweiggert, J., Schreiner, J., Kusevic, D., Reuther, J., Braun, B., and Wolf, D. H.:** Exploring the topology of the Gid complex, the E3 ubiquitin ligase involved in catabolite-induced degradation of gluconeogenic enzymes, J. Biol. Chem., **287**, 25602-25614 (2012)

22. **Liu, H., and Pfirrmann, T.:** The Gid-complex: an emerging player in the ubiquitin ligase league, Biol. Chem., **400**, 1429-1441 (2019)

23. **Kim, P. K., and Hettema, E. H.:** Multiple pathways for protein transport to peroxisomes, J. Mol. Biol., **427**, 1176-1190 (2015)

24. **Yuan, W., Veenhuis, M., and van der Klei, I. J.:** The birth of yeast peroxisomes, Biochim. Biophys. Acta., **1863**, 902-910 (2016)

25. **Oba, T., Suenaga, H., Ichimatsu, T., Hatano, Y., Mitsuiki, S., and Suzuki, M.:** Isolation and characterization of a high acid-producing yeast strain from *sake*-mash obtained from *sake* breweries, J. Brew. Soc. Japan, **103**, 949-953 (2008) (in Japanese)

26. **Arikawa, Y., Kuroyanagi, T., Shimosaka, M., Muratsubaki, H., Enomoto, K., Kodaira, R., and Okazaki, M.:** Effect of gene disruptions of the TCA cycle on production of succinic acid in *Saccharomyces cerevisiae*, J. Biosci. Bioeng., **87**, 28-36

(1999)

27. **Asano, T., Kurose, N., Hiraoka, N., and Kawakita, S.:** Effect of NAD+-dependent isocitrate dehydrogenase gene (*IDH1*, *IDH2*) disruption of sake yeast on organic acid composition in sake mash, J. Biosci. Bioeng., **88**, 258-263 (1999)

28. **Arikawa, Y., Kobayashi, M., Kodaira, R., Shimosaka, M., Muratsubaki, H., Enomoto, K., and Okazaki, M.:** Isolation of sake yeast strains possessing various levels of succinate- and/or malate-producing abilities by gene disruption or mutation, J. Biosci. Bioeng., **87**, 333-339 (1999)

29. **Kubo, Y., Takagi, H., and Nakamori, S.:** Effect of gene disruption of succinate dehydrogenase on succinate production in a sake yeast strain, J. Biosci. Bioeng., **90**, 619-624 (2000)

30. **Enomoto, K., Arikawa, Y., and Muratsubaki, H.:** Physiological role of soluble fumarate reductase in redox balancing during anaerobiosis in *Saccharomyces cerevisiae*, FEMS Microbiol. Lett., **215**, 103-108 (2002)

31. **Kitagaki, H., Kato, T., Isogai, A., Mikami, S., and Shimoi, H.:** Inhibition of mitochondrial fragmentation during sake brewing causes high malate production in sake yeast, J. Biosci. Bioeng., **105**, 675-678 (2008)

32. **Shigematsu, T., Kimura, A., and Murata, K.:** Function of glycolytic bypass and *S*-lactoylglutathione in sporulation of yeast cells, J. Ferment. Bioeng., **73**, 408-411 (1992)

33. **Suizu, T., Tsutsumi, H., Kawato, A., Murata, K., Suginami, K., and Imayasu, S.**: Methods for sporulation of industrially used sake yeasts, J. Ferment. Bioeng., **81**, 93-97 (1996)

34. **Boeke, J. D., LaCroute, F., and Fink, G. R:** A positive selection for mutants lacking orotidine-5'-phosphate decarboxylase activity in yeast: 5-fluoro-orotic acid resistance, Mol. Gen. Genet., **197**, 345-346 (1984)

35. **Wach, A., Brachat, A., Pöhlmann, R., and Philippsen, P.:** New heterologous modules for classical or PCR-based gene disruptions in *Saccharomyces cerevisiae*, Yeast, **10**, 1793-1808 (1994)

36. **Ito, H., Fukuda, Y., Murata, K., and Kimura, A.:** Transformation of intact yeast cells treated with alkali cations, J. Bacteriol., **153**, 163-168 (1983)

37. **Akada, R., Matsuo, K., Aritomi, K., and Nishizawa, Y.:** Construction of recombinant sake yeast containing a dominant *FAS2* mutation without extraneous sequences by a two-step gene replacement protocol, J. Biosci. Bioeng., **87**, 43-48 (1999)

38. **Imayasu, S., Hata, Y., Oishi, K., Kawato, A., and Suginami, K.:** Sake brewing using the liquefied product of rice slurry as raw, Nippon Nogeikagaku Kaishi, **63**, 971-979 (1989) (in Japanese)

39. **Iwano, K., Mikami, S., Fukuda, K., Shiinoki, S., and Shimada, T.:** The properties of various enzymes of shochu koji (*Aspergillus kawachii*), J. Brew. Soc. Japan, **81**, 490-494 (1986) (in Japanese)

40. **Okazaki, N.:** Seishu, gousei-seishu, pp. 7-33, In The Annotation of Official Methods of Analysis of the National Tax Administration Agency, Japan, 4th edn, Nishiya N (ed.) The Brewing Society of Japan: Tokyo (1993) (in Japanese)

41. **Minard, K. I. and McAlister-Henn, L.:** Isolation, nucleotide sequence analysis, and disruption of the *MDH2* gene from *Saccharomyces cerevisiae*: evidence for three isozymes of yeast malate dehydrogenase, Mol. Cell. Biol., **11**, 370-380 (1991)

42. **Snowdon, C., Hlynialuk, C., and van der Merwe, G.:** Components of the Vid30c are needed for the rapamycin-induced degradation of the high-affinity hexose transporter Hxt7p in *Saccharomyces cerevisiae*, FEMS Yeast Res., **8**, 204-216 (2008)

43. **Thompson, L. M. and McAlister-Henn, L.:** Dispensable presequence for cellular localization and function of mitochondrial malate dehydrogenase from *Saccharomyces cerevisiae*, J. Biol. Chem., **264**, 12091-12096 (1989)

44. **van Roermund, C. W., Elgersma, Y., Singh, N., Wanders, R. J., and Tabak, H. F.:** The membrane of peroxisomes in *Saccharomyces cerevisiae* is impermeable to NAD(H) and acetyl-CoA under *in vivo* conditions, EMBO J., **14**, 3480-3486 (1995)

45. **Pines, O., Shemesh, S., Battat, E., and Goldberg, I.:** Overexpression of cytosolic malate dehydrogenase (MDH2) causes overproduction of specific organic acids in *Saccharomyces cerevisiae*, Appl. Microbiol. Biotechnol., **48**, 248-255 (1997)

46. **Minard, K. I. and McAlister-Henn, L.:** Glucose-induced degradation of the MDH2 isozyme of malate dehydrogenase in yeast, J. Biol. Chem., **267**, 17458-17464 (1992)

47. **Chiang, H. L. and Schekman, R.:** Regulated import and degradation of a cytosolic protein in the yeast vacuole, Nature, **350**, 313-318 (1991)

48. **Schork, S. M., Thumm, M., and Wolf, D. H.:** Catabolite inactivation of fructose-1,6-bisphosphatase of *Saccharomyces cerevisiae*. Degradation occurs via the ubiquitin pathway, J. Biol. Chem., **270**, 26446-26450 (1995)

49. **Hoffman, M. and Chiang, H. L.:** Isolation of degradation-deficient mutants defective in the targeting of fructose-1,6-bisphosphatase into the vacuole for degradation in *Saccharomyces cerevisiae*, Genetics, **143**, 1555-1566 (1996)

50. **Chiang, M. C. and Chiang, H. L.:** Vid24p, a novel protein localized to the fructose-1,6-bisphosphatase-containing vesicles, regulates targeting of fructose-1,6-bisphosphatase from the vesicles to the vacuole for degradation, J. Cell. Biol., **140**, 1347-1356 (1998)

51. **Brown, C. R., Wolfe, A. B., Cui, D., and Chiang, H. L.:** The vacuolar import and degradation pathway merges with the endocytic pathway to deliver fructose-1,6-bisphosphatase to the vacuole for degradation, J. Biol. Chem., **283**, 26116-26127 (2008)

52. **McAlister-Henn, L. and Thompson, L. M.:** Isolation and expression of the gene encoding yeast mitochondrial malate dehydrogenase, J. Bacteriol., **169**, 5157-5166 (1987)

53. **Ichikawa, E., Hosokawa, N., Hata, Y., Abe, Y., Suginami, K., and Imayasu, S.:** Breeding of a sake yeast with improved ethyl caproate productivity, Agric. Biol. Chem., **55**, 2153-2154 (1991)

54. **Kotaka, A., Sahara, H., and Hata, Y.:** The construction and application of diploid sake yeast with a homozygous mutation in the *FAS2* gene, J. Biosci. Bioeng., **110**, 675-678 (2010)

55. **Kotaka, A., Sahara, H., Kondo, A., Ueda, M., and Hata, Y.**: Efficient generation of recessive traits in diploid sake yeast by targeted gene disruption and loss of heterozygosity, Appl. Microbiol. Biotechnol., **82**, 387-395 (2009)

56. **Yoshida, K., Inahashi, M., Nakamura, K., and Nojiro, K.**: Strains with high malate acid-producing ability obtained from a cycloheximide-resistant yeast, J. Brew. Soc.

Japan, **88**, 645-647 (1992) (in Japanese)

57. **Hashimoto, S., Ogura, M., Aritomi, K., Hoshida, H., Nishizawa, Y., and Akada, R.:** Isolation of auxotrophic mutants of diploid industrial yeast strains after UV mutagenesis, Appl. Environ. Microbiol. **71**, 312-319 (2005)
58. **Daigaku, Y., Endo, K., Watanabe, E., Ono, T., Yamamoto, K.**: Loss of heterozygosity and DNA damage repair in *Saccharomyces cerevisiae*, Mutat. Res. **556**, 183-191 (2004)
59. **Takagi, Y., Akada, R., Kumagai, H., Yamamoto, K., and Tamaki, H.:** Loss of heterozygosity is induced in *Candida albicans* by ultraviolet irradiation, Appl. Microbiol. Biotechnol. **77**, 1073-1082 (2008)
60. **Brown, C. R., Hung, G. C., Dunton, D., and Chiang, H. L.**: The TOR complex 1 is distributed in endosomes and in retrograde vesicles that form from the vacuole membrane and plays an important role in the vacuole import and degradation pathway, J. Biol. Chem., 285, 23359-23370 (2010)
61. **Hiraoka, M., Watanabe, K., Umezu, K., and Maki, H.:** Spontaneous loss of heterozygosity in diploid *Saccharomyces cerevisiae* cells, Genetics, 156, 1531-1548 (2000)
62. **Akada, R.**: Genetically modified industrial yeast ready for application, J. Biosci. Bioeng., **94**, 536-544 (2002)
63. **Ando, A., Suzuki, C., and Shima, J.**: Survival of genetically modified and self-cloned strains of commercial baker's yeast in simulated natural environments: environmental risk assessment, Appl. Environ. Microbiol. **71**, 7075-7082 (2005)
64. **Menssen, R., Bui, K., and Wolf, D. H.:** Regulation of the Gid ubiquitin ligase recognition subunit Gid4, FEBS Lett., **592**, 3286-3294 (2018)
65. **Picotti, P., Bodenmiller, B., Mueller, L. N., Domon, B., and Aebersold, R.:** Full dynamic range proteome analysis of *S. cerevisiae* by targeted proteomics, Cell, **138**, 795-806 (2009)
66. **Costenoble, R., Picotti, P., Reiter, L., Stallmach, R., Heinemann, M., Sauer, U., and Aebersold, R.:** Comprehensive quantitative analysis of central carbon and amino-acid metabolism in *Saccharomyces cerevisiae* under multiple conditions by targeted

proteomics, Mol. Syst. Biol., **7**, 464 (2011)

67. **Uebayashi, K., Shimizu, H., and Matsuda, F.:** Comparative analysis of fermentation and enzyme expression profiles among industrial *Saccharomyces cerevisiae* strains, Appl. Microbiol. Biotechnol., **102**, 7071-7081 (2018)
68. **Bradford, M. M.:** A rapid and sensitive method for the quantitation of microgram quantities of protein utilizing the principle of protein-dye binding, Anal. Biochem., **72**, 248-254 (1976)
69. **Kamiie, J., Ohtsuki, S., Iwase, R., Ohmine, K., Katsukura, Y., Yanai, K., Sekine, Y., Uchida, Y., Ito, S., and Terasaki, T.:** Quantitative atlas of membrane transporter proteins: development and application of a highly sensitive simultaneous LC/MS/MS method combined with novel in-silico peptide selection criteria, Pharm. Res., **25**, 1469-1483 (2008)
70. **Rappsilber, J., Mann, M., and Ishihama, Y.:** Protocol for micro-purification, enrichment, pre-fractionation and storage of peptides for proteomics using StageTips, Nat. Protoc., **2**, 1896-1906 (2007)
71. **Matsuda, F., Ogura, T., Tomita, A., Hirano, I., and Shimizu, H.:** Nano-scale liquid chromatography coupled to tandem mass spectrometry using the multiple reaction monitoring mode based quantitative platform for analyzing multiple enzymes associated with central metabolic pathways of *Saccharomyces cerevisiae* using ultra fast mass spectrometry, J. Biosci. Bioeng., **119**, 117-120 (2015)
72. **Matsuda, F., Kinoshita, S., Nishino, S., Tomita, A., and Shimizu, H.:** Targeted proteome analysis of single-gene deletion strains of *Saccharomyces cerevisiae* lacking enzymes in the central carbon metabolism, PLoS One, **12**, e0172742 (2017)
73. **MacLean, B., Tomazela, D. M., Shulman, N., Chambers, M., Finney, G. L., Frewen, B., Kern, R., Tabb, D. L., Liebler, D. C., MacCoss, M. J.:** Skyline: an open source document editor for creating and analyzing targeted proteomics experiments, Bioinformatics, **26**, 966-968 (2010)
74. **Bereman, M. S., MacLean, B., Tomazela, D. M., Liebler, D. C., MacCoss, M. J.:** The development of selected reaction monitoring methods for targeted proteomics via empirical refinement, Proteomics, **12**, 1134-1141 (2012)

75. **Metsalu, T., and Vilo, J.:** ClustVis: a web tool for visualizing clustering of multivariate data using Principal Component Analysis and heatmap, Nucleic Acids Res., **43**, W566-570 (2015)

76. **Dong, C., Zhang, H., Li, L., Tempel, W., Loppnau, P., and Min, J.:** Molecular basis of GID4-mediated recognition of degrons for the Pro/N-end rule pathway, Nat. Chem. Biol., **14**, 466-473 (2018)

77. **Braun, B., Pfirrmann, T., Menssen, R., Hofmann, K., Scheel, H., Wolf, D. H.:** Gid9, a second RING finger protein contributes to the ubiquitin ligase activity of the Gid complex required for catabolite degradation, FEBS Lett., **585**, 3856-3861 (2011)

78. **Amerik, A., Swaminathan, S., Krantz, B. A., Wilkinson, K. D., Hochstrasser, M.**: In vivo disassembly of free polyubiquitin chains by yeast Ubp14 modulates rates of protein degradation by the proteasome, EMBO J., **16**, 4826-4838 (1997)

79. **Eskes, E., Deprez, M. A., Wilms, T., and Winderickx, J.:** pH homeostasis in yeast; the phosphate perspective, Curr. Genet., **64**, 155-161 (2018)

80. **Bakker, B. M., Overkamp, K. M., van Maris, A. J., Kötter, P., Luttik, M. A., van Dijken, J. P., and Pronk, J. T.:** Stoichiometry and compartmentation of NADH metabolism in *Saccharomyces cerevisiae*, FEMS Microbiol. Rev., **25**, 15-37 (2001)

81. **Goldstein, A. L., McCusker, J. H.:** Three new dominant drug resistance cassettes for gene disruption in *Saccharomyces cerevisiae*, Yeast, **15**, 1541-1553 (1999)

82. **Guaragnella, N., Ždralević, M., Antonacci, L. Passarella, S., Marra, E., and Giannattasio, S.:** The role of mitochondria in yeast programmed cell death, Front Oncol., **2**, 70 (2012)

83. **Zdralević, M., Guaragnella, N., Antonacci, L., Marra, E., and Giannattasio, S.:** Yeast as a tool to study signaling pathways in mitochondrial stress response and cytoprotection, Sci. World J., 912147 (2012)

84. **Gonzalez, R., Morales, P., Tronchoni, J., Bueso, G. C., Vaudano, E., Quirós, M., Novo, M., Pérez, R. T., and Valero, E.:** New genes involved in osmotic stress tolerance in *Saccharomyces cerevisiae*, Front Microbiol., **7**, 1545 (2016)

85. **Gibson, N. and McAlister-Henn, L.:** Physical and genetic interactions of cytosolic malate dehydrogenase with other gluconeogenic enzymes, J. Biol. Chem., **278**, 25628-

25636 (2003)

86. **Oba, T., Suenaga, H., Nakayama, S., Mitsuiki, S., Kitagaki, H., Tashiro, K., and Kuhara, S.:** Properties of a high malic acid-producing strains of *Saccharomyces cerevisiae* isolated from sake mash, Biosci. Biotechnol. Bichem., **75**, 2025-2029 (2011)

87. **Koller, A., Snyder, W. B., Faber, K. N., Wenzel, T. J., Rangell, L., Keller, G. A., and Subramani, S.:** Pex22p of *Pichia pastoris*, essential for peroxisomal matrix protein import, anchors the ubiquitin-conjugating enzyme, Pex4p, on the peroxisomal membrane, J. Cell Biol., **146**, 99-112 (1999)

88. **El Magraoui, F., Schrötter, A., Brinkmeier, R., Kunst, L., Mastalski, T., Müller, T., Marcus, K., Meyer, H. E., Girzalsky, W., Erdmann, R., Platta, H. W.:** The cytosolic domain of Pex22p stimulates the Pex4p-dependent ubiquitination of the PTS1-receptor, PLoS One., **9**, e105894 (2014)

89. **Ashida, S., Ichikawa, E., Suginami, K., and Imayasu, S.:** Isolation and Application of Mutants Producing Sufficient Isoamyl Acetate, a Sake Flavor Component, Agric. Biol. Chem., **51**, 2061-2065 (1987)

90. **Kotaka, A., Sahara, H., Kuroda, K., Kondo, A., Ueda, M., and Hata, Y.:** Enhancement of beta-glucosidase activity on the cell-surface of sake yeast by disruption of *SED1*, J. Biosci. Bioeng., **109**, 442-6 (2010)

91. **Shibasaki, S., Tanaka, A., and Ueda, M.:** Development of combinatorial bioengineering using yeast cell surface display--order-made design of cell and protein for bio-monitoring, Biosens, Bioelectron., **19**, 123-130 (2003)

92. **Williams, C., van den Berg, M., Panjikar, S., Stanley, W. A., Distel, B., and Wilmanns, M.:** Insights into ubiquitin-conjugating enzyme/ co-activator interactions from the structure of the Pex4p:Pex22p complex, EMBO J., **31**, 391-402 (2012)

93. **Ma, C., Agrawal, G., Subramani, S.:** Peroxisome assembly: matrix and membrane protein biogenesis, J. Cell Biol., **193**, 7-16 (2011)

94. **Kim, P. K., and Hettema, E. H.:** Multiple pathways for protein transport to peroxisomes, J. Mol. Biol., **427**, 1176-1190 (2015)

95. **Yuan, W., Veenhuis, M., and van der Klei, I. J.:** The birth of yeast peroxisomes, Biochim. Biophys. Acta., **1863**, 902-910 (2016)

96. **Girzalsky, W., Saffian, D., and Erdmann, R.:** Peroxisomal protein translocation, Biochim. Biophys. Acta., **1803**, 724-731 (2010)

97. **Elgersma, Y., Vos, A., van den Berg, M., van Roermund, C. W., van der Sluijs, P., Distel, B., and Tabak, H. F.:** Analysis of the carboxyl-terminal peroxisomal targeting signal 1 in a homologous context in *Saccharomyces cerevisiae*, J. Biol. Chem., **271**, 26375-26382 (1996)

98. **Yofe, I., Soliman, K., Chuartzman, S. G., Morgan, B., Weill, U., Yifrach, E., Dick, T. P., Cooper, S. J., Ejsing, C. S., Schuldiner, M., Zalckvar, E., and Thoms, S.:** Pex35 is a regulator of peroxisome abundance, J. Cell Sci., **130**, 791-804 (2017)

99. **Gould, S. J., Keller, G. A., Hosken, N., Wilkinson, J., and Subramani, S.:** A conserved tripeptide sorts proteins to peroxisomes, J. Cell Biol., **108**, 1657-1664 (1989)

100. **Petriv, O. I., Tang, L., Titorenko, V. I., and Rachubinski, R. A.**: A new definition for the consensus sequence of the peroxisome targeting signal type 2, J. Mol. Biol., **341**, 119-134 (2004)

101. **Purdue, P. E., Yang, X., and Lazarow, P. B.:** Pex18p and Pex21p, a novel pair of related peroxins essential for peroxisomal targeting by the PTS2 pathway, J. Cell Biol., **143**, 1859-1869 (1998)

102. **Platta, H. W., Brinkmeier, R., Reidick, C., Galiani, S., Clausen, M. P., and Eggeling, C.:** Regulation of peroxisomal matrix protein import by ubiquitination,, Biochim. Biophys. Acta., **1863**, 838-849 (2016)

103. **Halbach, A., Rucktäschel, R., Rottensteiner, H., Erdmann, R.:** The N-domain of Pex22p can functionally replace the Pex3p N-domain in targeting and peroxisome formation, J. Biol. Chem., **284**, 3906-3916 (2009)

104. **van der Klei, I. J., and Veenhuis, M.:** PTS1-independent sorting of peroxisomal matrix proteins by Pex5p, Biochim. Biophys. Acta., **1763**, 1794-800 (2006)

105. **Klein, A. T., van den Berg, M., Bottger, G., Tabak, H. F., and Distel, B.:** *Saccharomyces cerevisiae* acyl-CoA oxidase follows a novel, non-PTS1, import pathway into peroxisomes that is dependent on Pex5p, J. Biol. Chem., **277**, 25011-25019 (2002)

106. **Lockshon, D., Surface, L. E., Kerr, E. O., Kaeberlein, M., and Kennedy, B. K.:**

The sensitivity of yeast mutants to oleic acid implicates the peroxisome and other processes in membrane function, Genetics, **175**, 77-91 (2007).

ACKNOWLEDGMENTS

The author would like to express his sincere gratitude to Dr. Jun Ogawa, Professor of Kyoto University, for his best guidance and encouragements.

The author expresses special thanks to Mr. Haruhiko Okura, President of Gekkeikan Sake Co. Ltd., for their encouragements and support throughout this work.

The author is very grateful to Dr. Yoji Hata, Executive Managing Director of Gekkeikan Sake Co. Ltd., and Dr. Hiroki Ishida, Research Manager of Gekkeikan Sake Co. Ltd., for the management of this work and valuable advices.

The author greatly thanks to Dr. Hiroshi Shimizu, Professor of Osaka University, and Dr. Fumio Matsuda, Professor of Osaka University, for their collaboration on the analysis of protein expression profiles in yeast.

The author express his superior thanks to Dr. Kengo Matsumura, President of Gekkeikan Sake (USA), Inc., and Dr. Atsushi Kotaka, Chief Market Researcher of Gekkeikan Sake Co. Ltd., for their kind guidance and valuable advices.

The author is very grateful to Dr. Akinori Ando, Assistant Professor of Kyoto University, for his helpful discussion.

The author wishes to thanks to Ms. Hiroko Tsutsumi, Mr. Hiroshi Sahara, and Mr. Mitsuru Sakamoto for their good support and nice collaborations, and to all members of Gekkeikan Sake Co. Ltd. who provided an optimal environment for carrying out this work.

Finally, the author greatly thanks to his family, Masayuki Negoro, Fumiko Negoro, Kanji Fukui, Shigeko Fukui, Sayaka, Naoki, and Takumi for their warm supports.

Hiroaki Negoro

PUBLICATIONS

Negoro H, Kotaka A, Matsumura K, Hata Y.: Enhancement of malate-production and increase in sensitivity to dimethyl succinate by mutation of the *VID24* gene in *Saccharomyces cerevisiae*. *J. Biosci. Bioeng.*, 121(6), 665-671 (2016)

Negoro H, Kotaka A, Matsumura K, Tsutsumi H, Sahara H, Hata Y.: Breeding of high malate-producing diploid sake yeast with a homozygous mutation in the *VID24* gene. *J. Inst. Brew.*, 122(4), 605-611 (2016)

Negoro H, Sakamoto M, Kotaka A, Matsumura K, Hata Y.: Mutation in the peroxin-coding gene *PEX22* contributing to high malate production in *Saccharomyces cerevisiae*. *J. Biosci. Bioeng.*, 125(2), 211-217 (2018)

Negoro H, Matsumura K, Matsuda F, Shimizu H, Hata Y, Ishida H.: Effects of mutations of GID protein-coding genes on malate production and enzyme expression profiles in *Saccharomyces cerevisiae*. *Appl. Microbiol. Biotechnol.*, 104(11), 4971-4983 (2020)

Negoro H, Kotaka A, Ishida H.: Mutation in genes coding for glucose-induced degradation-deficient protein contribute to high malate production in yeast strains No. 28 and No. 77 used for industrial brewing of sake. *Biosci. Biotechnol. Biochem.*, 85(5), 1283-1289 (2021)